Multicomponent Aerosol Formation Model

MAFOR Model version 2.2

User's Guide

2024

Author:
Dr. Matthias Karl

Table of Contents

MAFOR v2.2 – User's Guide

1 Intro to MAFOR

The MAFOR (**M**ulticomponent **A**erosol **FOR**mation) model is a zero-dimensional Lagrangian type sectional aerosol box model which includes gas phase and aqueous phase chemistry in addition to aerosol dynamics. MAFOR consistently solves the time evolution of the particle number and mass concentration distribution of a multicomponent aerosol using the fixed sectional method and simultaneously the time-dependent concentrations of chemical compounds in the gas phase and also in the aqueous phase of supermicron droplets. The basic gas phase chemistry and aqueous phase chemistry is based on the "Module Efficient Calculating the Chemistry of the Atmosphere (MECCA)" developed by Rolf Sander at the Max-Planck Institute of Chemistry . With MAFOR version 2.0, the multiphase chemistry is based on CAABA/MECCA v4.0 (Sander et al., 2019).

The kinetic pre-processor KPP version 2.2.3 (Sandu and Sander, 2006) is used to generate Fortran 90 code for the chemistry module. The Rosenbrock ROS3 solver with automatic time step control is used to integrate the differential equation system of gas phase and aqueous phase reactions. In short, MAFOR is the coupling of the (dynamically generated) chemistry module from MECCA and a new aerosol dynamics module. The treatment of aerosol dynamics is based on the concepts by M. Z. Jacobson described in his book "Fundamentals of Atmospheric Modeling" (Jacobson, 2005a). The MAFOR model offers great flexibility to the user who may decide about the included aerosol processes, the included chemistry, the size resolution of the model aerosol and many other parameters of the simulation.

MAFOR version 1.4 was the first version of the model that was distributed as binary executable on http://mafor.nilu.no in June 2012. Version 1.5 fixed a bug for reading tab-delimited input files and improves the calculation of aerosol water content. Version 1.9.5 is the last version of the model that was distributed under a commercial license.

With version 2.0, the source code of the model is released as open source under the GNU General Public License (GPL) as the new community aerosol dynamics box model MAFOR.

The use of MAFOR on a personnel computer (Linux) is quite simple if the instructions and test examples in this User's Guide are followed. The user should have some experience with running computer models because there are many options in the input files and there is little built-in error checking on the input.

The main intention of distributing the executable of the MAFOR model is the usage for educational purposes. If you should plan to use the model in a research project it is strongly recommended to contact the author (mattkar 'at' googlemail.com) to clarify for example if all necessary processes are implemented in the model.

1.1 History

The code development for MAFOR started in autumn 2008 using the first released version of MECCA, version 0.9.1 (Sander et al., 2005), KPP version 1.1-f90-alpha12 (Sandu et al., 1997), the code of MONO32 by L. Pirjola, and an aerosol model code freely distributed by K. E. J. Lehtinen at the CESAR Summer School (Research Centre Jülich, Germany, Aug. 21st – Sept. 1st, 2006). The aerosol code was then completely transformed to be in accordance with the treatment by M. Z. Jacobson using the fixed sectional method. The first stable version of the MAFOR model was used in a Lagrangian type scenario simulation for the Arctic Ocean. The model code of MAFOR version 1.0 was finally revised to be in full accordance with theory of aerosol dynamics as published by Karl et al. (2011). In the model versions 1.1, 1.2, and 1.3 mainly the gas phase chemistry of the model was extended and the aerosol dynamic processes were made modular. In version 1.3 the photolysis calculation routine was revised and now data on absorption coefficients and quantum yields recommended by the Jet Propulsion Laboratory (JPL) Evaluation no. 15 is used. In MAFOR version 1.4 the aqueous phase chemistry was comprehensively tested and extended. In version 1.5 the calculation of aerosol water content was improved. In version 1.6 the condensation of ammonium as ammonium bisulfate, ammonium sulfate or ammonium nitrate was included. In version 1.7 the gas phase chemistry was extended and the aqueous phase chemistry was restricted to the droplet mode. In version 1.8 three alternative options for plume dispersion and three alternative options for dry deposition of particles became available. In version 1.9 the Multicomponent Equilibrium Solver for Aerosols (MESA) was coupled to MAFOR to solve the growth of particles by dissolution of nitric acid. MESA is part of the MOSAIC code (Zaveri et al., 2008) distributed with the community developed model WRF-Chem. In version 2.0, the 2-D volatility basis set (VBS) developed by Donahue et al. (2011) was introduced together with nine lumped organic vapor species. In version 2.2, the activation of aerosol particles to form cloud droplets following the rate of change of the supersaturation and of the droplet growth described by Leaitch et al. (1986) was implemented, enabling droplet microphysics in addition to aqueous phase chemistry in a closed volume of air in which a fog or a cloud is formed and dissipated.

1.2 Model features and applications

The Multicomponent Aerosol FORmation model MAFOR is a 0-D Lagrangian type sectional aerosol process model, which includes multiphase chemistry in addition to aerosol dynamics.

Novel aspects of the coupled gas phase / aerosol model MAFOR are 1) the full flexibility of gas phase chemistry and the degree of detail specifically in the chemistry of dimethyl sulphide (DMS), isoprene, and amines, 2) the detailed treatment of liquid phase chemistry (gas/liquid equilibrium partitioning, dissociation equilibrium reactions, aqueous phase chemical reactions) in the droplet mode, which can be extended according to needs, 3) simultaneous solution of the time evolution of the particle number and mass distribution of a multicomponent aerosol using a sectional approach.

Why is MAFOR initialized with modal mass concentrations?

A major advantage of the model is the consistent treatment of particle number concentrations and mass concentrations of each aerosol component through the simultaneous solution of aerosol dynamics processes in terms of number and mass. This procedure allows the changes in the average density of particles to affect the predicted number and mass size distributions.

The aerosol is initialised based on the modal mass composition, which is then distributed over the size bins of the model and converted to number based in the material density of the different aerosol components, assuming spherical particles. This procedure assures that the initial aerosol is consistent in terms of mass and number. The model also computes the aerosol water content based on the initial (dry) mass composition and relative humidity. The output of the modelled particle number size distribution and mass concentration size distribution can be directly compared to observed number and mass conentration size distributions, respectively. The model user needs to give an estimate of the chemical composition, mean (mass-based) diameter and bandwidth of the initial aerosol for each mode. Ideally, such an estimate can be derived from an observed mass concentration size distribution. In most cases, the typical chemical composition of atmospheric PM1 or PM2.5 is used to match observed initial particle number size distribution.

The initialization with a modal mass composition sometimes does not well match with the initial particle number size distribution. In a future version of MAFOR, it will be possible to initialise the simulation with the observed particle number size distribution.

For which applications is MAFOR useful?

The high flexibility of the chemistry part of MAFOR makes it an ideal tool for studies on multiphase chemistry of DMS, amines, and other water-soluble organics relevant to the marine atmosphere. The MAFOR model is increasingly used for simplified plume simulations to study the temporal evolution of traffic-generated aerosols, such as vehicle exhaust particles and ship emissions.

The aerosol model MAFOR is very versatile and meanwhile has been adapted to address various research questions: 1) new particle formation over the Arctic Ocean, 2) gas phase chemistry and particle formation in environmental chambers, 3) aqueous phase chemistry of amines in fog/cloud, and 4) ultrafine exhaust particles emitted by road traffic and ship traffic in cities.

1.3 Model documentation

A detailed model description of MAFOR (version 1.0) is provided in the following article:

Karl, M., Gross, A., Pirjola, L., and C. Leck, A new flexible multicomponent model for the study of aerosol dynamics in the marine boundary layer, Tellus B, 63(5), 1001-1025, doi: 10.1111/j.1600-0889.2011.00562.x, 2011.

Applications of the model using later sub versions of MAFOR v1 are presented in the following articles:

Karl, M., Leck, C., Gross, A. and L. Pirjola, A study of new particle formation in the marine boundary layer over the central Arctic Ocean using a flexible multicomponent aerosol dynamic model, Tellus B, 64, 17158, doi: 10.3402/ tellusb.v64i0.17158, 2012a.

Karl, M., Dye, C., Schmidbauer, N., Wisthaler, A., Mikoviny, T., D'Anna, B., Müller, M., Clemente, E., Muñoz, A., Porras, R., Ródenas, M., Vázquez, M. and T. Brauers, Study of OH-initiated degradation of 2-aminoethanol, Atmos. Chem. Phys., 12, 1881-1901, 2012b.

Keuken, M., Henzing, J. S., Zandveld, P., van den Elshout, S., and M. Karl, Dispersion of particle numbers and elemental carbon from road traffic, a harbor and an airstrip in the Netherlands, Atmos. Environ., 54, 320-327, 2012.

Karl, M., Leck, C., Coz, E., and J. Heintzenberg, Marine nanogels as a source of atmospheric nanoparticles in the high Arctic, Geophysical Research Letters, 40 (14), 3738-3743, doi: 10.1002/grl.50661, 2013.

Pirjola, L., Karl, M., Rönkkö, T., and F. Arnold, Model studies of volatile diesel exhaust particle formation: Organic vapours involved in nucleation and growth?, Atmos. Chem. Phys., 16, 4817-4835, doi:10.5194/acp-16-4817-2016, 2016.

Karl. M., Kukkonen, J., Keuken, M. P., Lützenkirchen, S., Pirjola, L., and T. Hussein, Modeling and measurements of urban aerosol processes on the neighborhood scale in Rotterdam, Oslo and Helsinki, Atmos. Chem. Phys., 16, 4817-4835, doi:10.5194/acp-16-4817-2016, 2016.

Karl, M., Pirjola, L., Karppinen, A., Jalkanen, J.-P., and Ramacher, M. O. P., and J. Kukkonen, Modeling of the concentrations of ultrafine particles in the plumes of ships in the vicinity of major harbors, J. Environ. Res. Public Health, 17, 777, 1-24, doi:10.3390/ijerph17030777, 2020.

Zhang, X., Karl, M., Zhang, L., and J. Wang, Influence of aviation emission on the particle number concentration near Zurich Airport, Environ. Sci. Technol., 54(22), 14161-14171, doi:10.1021/acs.est.0c02249, 2020.

Fink, L., Karl, M., Matthias, V., Weigelt, A., Irjala, M., and Simonen, P., Using the Multicomponent Aerosol FORmation Model (MAFOR) to determine improved VOC emission factors in ship plumes, Toxics, 12, 432, 1-26, https://doi.org/10.3390/toxics12060432, 2024.

A detailed model description of MAFOR (version 2.0) is provided in the following article:

Karl, M., Pirjola, L., Grönholm, T., Kurppa, M., Anand, S., Zhang, X., Held, A., Sander, R., Dal Maso, M., Topping, D., Jiang, S., Kangas, L., and J. Kukkonen, Description and evaluation of the community aerosol dynamics model MAFOR v2.0, Geosci. Model Dev., 15, 3969-4026, doi:10.5194/gmd-15-3969-2022, 2022.

1.4 Changes in version 2.2

Compared to MAFOR version 2.0 the following items were changed or added:

Size distribution representation:

- The initial particle size distribution is now represented by five modes. An additional mode (NA) was added between nucelation mode (NU) and Aitken mode (AI). Mode-wise output was changed to five modes.

Particle emission flux:

- Sea-salt particle emission flux multiplied by open water fraction (owf). Sea-salt particle flux parametrization from Spada et al. (2013) was replaced by the the sea spray function of Salter et al. (2015).
- Additional option for particle emissions (option 3 in sensitiv.dat): combined emission of sea-salt particles and continuous primary particles after dissipation of clouds, designed for simulation of arctic marine cases.

Emission and entrainment of gases:

- Marine emissions of molecular iodine, I_2, (given in inchem.dat) are activated when owf is below 0.3 (30% of surface cell area).
- Marine emissions of Isoprene and SOA-1 (BLOV) during sunlight, depending on owf (Bruggemann et al., 2017).
- New option for (continuous) entrainment of SOA-1 from the free troposphere (FT): entrainment velocity is 0.6 cm/s and assumed SOA-1 concentration in the FT is $2x10^7$ molec/cm^3.

Coupling with MOSAIC:

- Call of MESA interface every 90 s (instead of 120 s).
- Increased robustness of chlorine depletion.

Nucleation:

- Nucleation of sulfuric acid/iodic acid clusters (nucleation option 14) assuming sulfuric acid induced activation, according to a parameterization for OIO nucleation in Vuollekoski et al. (2009). The nucleated particles are inserted at 1.5 nm diameter.
- Neutral and ion-induced nulceation of iod acid (nucleation option 15) according a parameterization for J1.7 given by Zhao et al. (2024) for global models. The nucleated particles are inserted at 1.5 nm diameter.

Condensation:

- Condensation of iodic acid (HIO_3) as extremely low volatility compound.
- Condensation of MSA as ELVOC when air temperature is below a certain transition temperature (Hodshire et al., 2019).
- Correction of condensation of SOA-5 (ALOV).

Coagulation:

Collection kernel for collision/coalescence of droplets and/or aerosol particles in fog/cloud (if coagulation option is 1 in sensitiv.dat).

Deposition:

- Size-dependent wet scavenging of particles (new option in sensitiv.dat) based on raindrop-aerosol collection efficiency E, for a fix raindrop diameter of 1 mm. Based on the correlation for E that fits experiments presented by Slinn (1983).

- New routine for gravitational settling of droplets during cloud processing (if deposition option is 1 in sensitiv.dat).

Plume dispersion:

Write output to soadis.res and aerconc.res during plume dispersion runs.

Fog cycle chemistry:

If cloud option 1 in ingeod.dat is selected, a prescribed fog/cloud is activated for the selected hour, with aqueous phase chemistry in the CS mode (if aqueous phase partitioning and chemistry is on). After the end of a fog or cloud cycle, the in-cloud produced particle mass of sulfate, MSAp, ammonium, oxalate and succhinate is added to the reconstructed coarse mode. Interstitial aerosol scavenging of small particles by collision with the droplets in CS mode happens if coagulation option is 1. The total number of droplets in prescribed CS mode was reduced by a factor of 10 compared to earlier versions.

Aerosol activation and cloud processes:

- If cloud option 2 in ingeod.dat is selected, cloud formation occurs in a smog-fog-smog cycle for the selected hour is activated along a temperature profile similar to that in Pandis et al. (1990a, Fig. 1 therein).
- If the aqueous phase partitioning and chemistry option is 1 in sensitiv.dat, then the partitioning of gases to the droplets of AI, AS and CS modes and aqueous phase chemistry in the three bulk modes is considered, given that LWC is higher than $1x10^{-10}$ m^3/m^3.
- The condensation and evaporation of water vapor follows the description of Pruppacher and Klett (1997), with the kinetic factor, the modified diffusion coefficient for water vapor and the modified diffusion coefficient of air calculated according to Abdul-Razzak et al. (1998) and Seinfeld and Pandis (2006).
- The fraction of activated particles in terms of total number and mass concentration is given in the output (total_n.res).
- Equilibrium supersaturation is modeled using Köhler theory, with the Kelvin effect and the Raoult effect calculated according to Abdul-Razzak and Ghan (2000). However, instead of the hygroscopicity parameter, the dynamically calculated concentrations in the liquid droplet are used.
- The Raoult effect considers partly dissociated soluble gases and slightly soluble matter due to the explicit computation of aqueous phase concentrations in the droplet modes. The Kelvin effect considers organic surfactants.
- Gravitational settling of droplets during cloud processing.
- Collision/coalescence of particles during cloud processing by Brownian diffusion.
- In-cloud condensation: mass increase of activated aerosols by uptake of water-soluble gases to droplets and by chemical reactions within the cloud droplets.

Utilities:

ingeod_prep.xls: new colum for open water fraction (position 22).
inaero_prep.xls: configuration with 5 modes

Changed input files:

ingeot.dat (new column: open water fraction)
sensitiv.dat (new options)
inaero.dat, inbgair.dat (5 modes)
organic.dat (organic fractions in 5 modes)

1.5 Known issues

The model is initialized with mass concentrations in five log-normal modes. The initialization with a bin-wise input of a given number size distribution is not possible. Before the implementation of a bin-wise reading of observed particle number concentrations, we would need to know if dN/dlogDp is always measured at ambient relative humidity.

1.6 Computer information

The Linux executable was compiled with **gfortran-9** on Linux Ubuntu with 64bit. Testing was only done with the Linux 64bit executable. For Windows 10, two versions of Ubuntu are available to download from the Microsoft Store: adding to the existing Ubuntu 18.04, Ubuntu 20.04 has also now arrived. Ubuntu 20.04 requires the Windows Subsystem for Linux, WSL 2. The Ubuntu emulation on Windows 10 provides access to the Ubuntu Terminal, as well as the latest version of command line utilities such as bash, ssh, git, apt and so on. In order to install the software, you'll need to enable Windows' Subsystem for Linux. Windows 10 users are encouraged to test the Linux executable on Ubuntu 20.04 and report any issues to the author.

1.7 Graphical display

Several MATLAB scripts for plotting of the model's output are available together with the test examples (see chapter 5) for download. The scripts can be used with MathWorks® MATLAB and with the free open source software GNU Octave (https://www.gnu.org/software/octave/). The scripts can be easily modified to plot additional chemical species (see Appendix A) or components of the aerosol (section 3.2).

1.8 Download

Link to the github repository: https://github.com/mafor2/mafor.git

Documentation:

Users_Guide_MAFOR-v2.2.pdf
meccanism_mafor_v2.2.0.pdf
gas+aqueous_species-v2.2.0.pdf
chemprop-v2.2.0.pdf
README_caaba_mafor
maforv2.2.0specno.xls

README_caaba_mafor explains how to add new chemical species and reactions to the chemistry mechanism of MAFOR.

1.9 Problems

First you should try to run the provided Test examples on your computer. If a problem occurs while running the Test examples, please post a description of the problem including information about your computer system and the error message to the github Forum (https://github.com/mafor2/mafor/issues). If you experience problems with running MAFOR on a self created set of input files, contact the author (mattkar ' at' googlemail.com) by email with a description of the problem and the error message, including the input files as attachment.
A list of MAFOR error messages and instructions how to avoid the error can be found in the new Appendix C.

2 Input Files

This chapter provides an overview of the necessary input files to run the MAFOR model. Complete sets of input files are provided together with the test examples (see chapter 5). All input files are in ASCII format.

A minimum set of input files consists of:

Gas phase:	inchem.dat
Aerosol:	inaero.dat
Organic:	organic.dat
Dispersion	dispers.dat
General:	ingeod.dat
Configuration:	sensitiv.dat

Until now the program does little checking of the input. The program will stop if a required input file does not reside in the same folder. There is however no detailed check on the format and validity of the input data.

2.1 Configuration

The configuration of the MAFOR model run is controlled with the input file sensitiv.dat. With 0|1 switches it is possible to disable/enable certain processes during the model simulation.

Documentation for input file sensitiv.dat is given by the list on the next two pages.

Entries in first line:

1. dry particle deposition	**0 |1 |2 |3 |4**	**(1=water surface; Schack et al. (1985); 2= forest canopy; Kouznetsov and Sofiev (2012) 3= any rough surface; Hussein et al. (2012) 4 = any surface; Zhang et al. (2001)**
2. wet scavenging of particles	**0 |1 |2**	**(1=bulk, 2=size-resolved)**
3. coagulation of particles	**0 |1 |2 |3 |4 |5**	**(1=Brownian coagulation, 2=Brownian with fractal geometry of soot, 3=Brownian corrected for van der Waals forces, 4=Brownian with explicit kernel for van derWaals forces, 5=Brownian with fractal geometry and van der Waals forces)**
4. condensation of vapors	**0|1**	
5. nucleation	**0|1**	
6. nucleation mechanism	**1 |2 |3 |4 |5 |6 |7 |8 |9 |10 |11 |12 |13 |14 |15**	**(explanation of the different nucleation options see section 2.74.5).**
7. chamber experiment	**0 |1 |2**	**(2=wall loss aging chamber)**

Entries in second line:

1. condensation of H2SO4, MSA, and HIO3	**1|2**	**(1=accomm. coeff. see Table 4.2, 2= unity**
2. condensation of Organics	**0|1**	**(1=condensation of organic vapors)**
3. condensation of Amines	**0|1**	**(if set to 1, AMMO in inaero.dat is treated as aminium)**
4. condensation of Ammonium	**0|1**	**(if set to 1, formation of ammonium nitrate is enabled and condensation of amines is disabled)**
5. emission of particles	**0 |1 |2**	**(1=continuous particle emission, 2=sea-air particle flux, 3=sea-air particle flux and continuous particle emission)**
6. chemistry integration	**0|1**	
7. Kelvin effect considered	**0|1**	

Entries in third line:

1. prescribe DMS and NH3 from input	**0|1**	**(read from ingeod.dat)**
2. prescribe O3 from input	**0|1**	**(read from ingeod.dat)**
3. prescribe SOA-1 concentration	**0 |1 |2**	**(1=read from ingeod.dat, 2=entrainment from FT)**
4. debugging information	**0|1**	**(write to debug.res)**
5. dilution with bg particles	**0 |1 |2 |3 |4 |5 |6 |7**	**(for plume simulation: 1=type 1, 2=type 2, 3=type 3, 4=type 4, 5=type 5, 6=type 6, 7=type 7)**
6. SOA partitioning 2-D VBS	**0 |1 |2**	**(1=absorptive partitioning, 2=absorptive partitioning + physical adsorption)**
7. use nano-koehler	**0|1**	

Entries in the fourth line:

1. condensation of water	**0 |1 |2**	**(1= condensation of H2O, 2 = condensation of H2O and MESA thermodynamic module activated)**
2. partitioning to aqueous phase	**0|1**	
3. aqueous phase chemistry	**0|1**	

In the first line of sensitiv.dat any of the aerosol dynamic processes can be switched off, by setting the flag to 0.

Deposition of particles:
For dry deposition to water surface (ocean) it is recommended to use the option **1** (Schack et al. (1985). For dry deposition to a (vegetation) canopy of height ZCAP with rough surface (e.g. forest) it is recommended to use the option **2** (Kouznetsov and Sovief (2012). Option **4** (Zhang et al., 2001) can also be used for vegetation. For any rough surface it is recommended to use the option **3** (Hussein et al. (2012). The control parameters of the two dry deposition schemes are entered in in dispers.dat (section 2.7).

Wet scavenging of particles:
For wet scavenging of particles, two options are possible. Option **1** activates the bulk precipitation scavenging for particles. Nucleation mode particles are not scavenged. Option **2** activates the size-dependent precipitation scavenging of particles based on raindrop-aerosol collection efficiency E for a fix raindrop diameter of 1 mm. The wet scavenging bases on the correlation for E that fits experiments presented by Slinn (1983). The cloud volume for precipitation is assumed to be 10% of the box volume. Wet scavenging of particles uses the rainfall rate (rain) given in ingeod.dat.

Coagulation of particles:
Brownian coagulation is activated if the coagulation option is set to **1**. By setting the coagulation option to **2**, the effect of fractal geometry on coagulation is taken into account by considering the effect on radius, diffusion coefficient and the Knudsen number in the Brownian collision kernel. The radius of primary spherules is assumed to be 13.5 nm and the fractal dimension is assumed to be 1.7. These parameters can be changed in organic.dat. By setting the coagulation option to **3**, an empirical correction factor accounting for van der Waals and viscous forces is applied to the Brownian collision kernel (Karl et al., 2016). With the coagulation option **4**, an exact correction for van der Waals and viscous forces is done. With coagulation option **5**, both fractal geometry and van der Waals forces (exact correction) are used. Details in section **4.8**.

Nucleation:
It can be chosen among 14 different nucleation mechanisms. Details on the nucleation option are given in section 4.5.

Condensation:
The condensation of organic vapors is explained in section 4.6. The condensation of sulfuric acid (H_2SO_4), methane sulfonic acid (MSA), and iodic acid (HIO_3) is explained in section 4.7. Condensation of ammonium occurs either as ammonium bisulfate, ammonium sulfate or ammonium nitrate. By setting “Kelvin effect considered” to 1 the condensation of H2SO4, MSA, HIO3, organics, amines, and ammonium will be corrected by the Kelvin effect. By setting “SOA partitioning” to 1 the condensation of organics is corrected by allowing partitioning to the organic liquid mixture following the description in Kerminen et al. (2000). This option makes use of the two-dimensional volatility basis set (2-D VBS) developed by Donahue et al. (2011) that employs saturation mass concentration C_0 and the oxygen content (O:C ratio) to describe volatility and mixing thermodynamics of organic aerosol. By setting “SOA partitioning” to 2 in addition considers physical adsorption (Pankow, 1994) to ECBC and DUST primary particles. By setting “use nano-koehler” to 1 the Nano-Köhler theory as outlined by Kulmala et al. (2004) is used. The implementation of Nano-Köhler theory is experimental and its use is not recommended.

Emission of particles:
There are two options for emissions of particles, either as continuous flux of particles with a prescribed chemical composition or as sea-salt particle flux controlled by wind speed, sea surface

temperature and salinity. In addition, option **3** allows for the combination of emission of sea-salt particles and continuous release of primary particles occurring after the dissipation of clouds, designed for simulation of arctic marine cases. For the continuous flux of particles, it is is required to set the switch for particle emission to **1**. In this case, the input file emitpar.dat with constant emission rate for each aerosol component in each mode has to be provided, see section 2.3.5. For the sea-salt particle emission flux, the switch for particle emission is **2**. Sea-salt particle emissions will depend on wind speed (hourly changing), sea surface temperature (constant value) and salinity (constant value) using the parameterization of Salter et al. (2015). Sea-salt particle emissions are scaled with the open water fraction (owf) that is provided in the input file ingeod.dat. More details are given in section 4.9.

Uptake of water and dissolutional growth:
By setting "condensation of water" to **1** the aerosol water content is calculated according to the Zdanovskii-Stokes-Robinson (ZSR) relationship. This option provides the wet diameter of the aerosol based on water content of each size bin. If the option is set to **0**, aerosol water will not be considered and only dry diameter is used. Debugging information (debug flag = 1), e.g. on mass and number conservation during condensation and coagulation is written to debug.res.
Setting "condensation of water" to **2** activates the coupling between MAFOR and the MESA model (Zaveri et al., 2005b). MESA solver for solid, liquid and mixed phase aerosols enables the calculation of aerosol water content and activity coefficients of electrolytes in droplets within all size sections using the MTEM (Multicomponent Taylor Expansion Method; Zaveri et al., 2005a). MESA considers the aqueous solution system SO_4^{2-}, NH_3/NH_4^+, HNO_3/NO_3^-, and typical crustal elements such as K^+, Mg^{2+}, Ca^{2+} of sea-salt and dust aerosols. Every two minutes, MAFOR aerosol components are mapped onto MESA species and the electrolyte composition in each size bin is re-calculated. Finally, the MESA model calculates the parameters required for using the Analytical Predictor of Nonequilibrium Growth (PNG; Jacobson, 2002, 2005b) to solve growth by dissolution. PNG was implemented and coupled with MESA to solve the growth of particles by dissolution of HNO_3 and HCl. It is recommended to use this option if formation of ammonium nitrate is expected. An example demonstrating the effect of using the MESA/PNG solver is given in section 5.6.

Prescribed concentrations:
Controlled read of concentrations of DMS, NH3, O3, and SOA-1 (gaseous SOA precursor) from the input column in ingeod.dat (every hour) if the the read flag in sensitiv.dat is set to 1. In the case of SOA-1 a second possibility is to allow entrainment from the Free Troposphere (FT) by setting this read flag to 2. The assumed entrainment velocity is 0.6 cm/s and the assumed SOA-1 concentration in the FT is $2x10^7$ molec/cm^3. If read flag is set to 0, time dependent concentrations of these compounds will be calculated by the chemistry solver. In this case, the initial gas-phase concentration, emission strength (if needed) and dry deposition velocity of the chemical species has to be provided in the gas-phase input file inchem.dat.

Dilution with background particles:
Plume dispersion simulation are performed when the flag for dilution with background particles is set >0. Different plume dispersion types, applicable for vehicle exhaust and/or ship exhaust plumes are available. More details are given in section 4.4.

Simulation of fog or cloud cycle:
There are two possibilities to simulate a cloud cycle, using either a prescribed cloud or the formation of a cloud by activation of aerosol particles. For the prescribed cloud (incloud=1 in ingeod.dat), a "droplet mode" forms with user-input values of liquid water content (LWC) and pH (lwcm and pH in ingeod.dat). RH (in ingeod.dat) must be between 0.991 and 1.00. This option is useful to simulate the cloud as chemical reactor for aqueous-phase reactions. For the aerosol activation (incloud=2 in ingeod.dat), the cloud formation follows a prescribed temperature profile,

activation is described by the Köhler equations, and microphysical cloud processes can occur in the formed cloud. More details are given in section 4.3.

2.2 General

The parameters of the trajectory along which the model is run are set in the input file ingeod.dat. Each line of ingeod.dat provides hourly values of a range of meteorological and other parameters. The input is read each hour of the model run. An Excel work sheet (ingeod_prep.xls) is available in the zip file helper_tools.zip. The Excel sheet can be used to prepare the input. Use copy-paste to transfer the content into a text editor (e.g. notepad++, http://notepad-plus-plus.org) and save as ingeod.dat. The input is table-style with 26 columns. The entry in column 11 (incloud) is a (0|1|2) switch. If incloud=1, a droplet distribution will be prescribed in the fourth (CS) mode (see inaero.dat, section 2.3). The droplet number will then be calculated using the liquid water content (column 23) assuming spherical droplets. The pH of the droplets is defined in column 24. The open water fraction (owf) in column 22 was introduced in MAFOR v2.2.
The first column is runtime, which is the total simulation time period in hours (same value in all lines).

Documentation for input file ingeod.dat is given by the following list.

Column	Variable	Description	
01	**runtime**	**simulation time**	**[hours]**
02	**iday**	**day**	**[dd]**
03	**imonth**	**month**	**[mm]**
04	**starttime**	**hour**	**[hh]**
05	**lat_deg**	**latitude**	**[decimal deg]**
06	**lon_deg**	**longitude**	**[decimal deg]**
07	**temp**	**temperature**	**[K]**
08	**press**	**air pressure**	**[Pa]**
09	**RH**	**rel. humidity**	**[-]** **Note: At RH>1.1 the program will stop. RH must be between 0.991 and 1.00 for incloud=1**
10	**zmbl**	**mixing height**	**[m]**
11	**incloud**	**in-cloud flag**	**[-]** **Note: (0|1|2) incloud=1 prescribes droplet distribution in fourth (CS) mode, incloud=2 induces cloud activation**
12	**u10**	**wind speed 10m**	**[m/s]**
13	**rain**	**precipitation**	**[mm/h]**
14	**edms**	**emission DMS**	**[molec/cm2/s]**
15	**eso2**	**emission SO2**	**[molec/cm2/s]**
16	**eh2o2**	**emission H2O2**	**[molec/cm2/s]**
17	**cnh3**	**conc. NH3**	**[molec/cm3]**

18	**camidoh**	**conc. SOA-1**	**[molec/cm3]**
19	**cdms**	**conc. DMS**	**[molec/cm3]**
20	**co3**	**conc. O3**	**[molec/cm3]**
21	**fnuc**	**nucleation scale factor**	**[-]** **Note: used when nucleation option is NUCMEC=5 or 10.** **By default it should be set to 1.0**
22	**owf**	**open water fraction**	**[-]** **Values between 0.0 (land) and 1.0 (open sea)**
23	**lwcm**	**liquid water**	**[m3/m3]** **Note: only used if incloud=1**
24	**pH**	**pH of CS mode**	**[-]** **Note: only used if incloud=1**
25	**dila**	**dispersion parameter**	**[-]** **for plume simulation type 1, 2, 4**
26	**dilcoef**	**dilution coefficient**	**[-]** **for plume simulation type 1, 2, 4**

2.3 Aerosol

2.3.1 Size distribution and aerosol components

The initial aerosol size distribution is provided in the input file inaero.dat. The initial aerosol distribution in the five modes (NU: nucleation mode, NA: nanoparticle mode, AI: Aitken mode, AS: accumulation mode, CS: coarse mode) is based on mass. The geometric mean diameter (GMD) of each mode has to be given based on mass. It is convenient to fill inaero.dat with mass concentrations (in ng/m^3) of aerosol components measured by a Berner Impactor or an Aerosol Mass Spectrometer (AMS). If measurements of the chemical composition of PM1.0, PM2.5, or PM10 are available, the total mass concentration (e.g. PM2.5) should be distributed between different aerosol components using estimated mass fractions of components in each mode. Finally, the total mass concentration MM (in ng/m^3) of each mode is determined by summing up the component mass concentrations in the mode. Table 2.1 lists the aerosol components and their basic properties included in the model.

Table 2.1 Aerosol components and properties in the MAFOR model.

Component	**Name**	**Density (kg m^{-3})**	**Volatility**
Sulfuric acid /sulfate	SULF	1770	Volatile
Organic Carbon (OC)	ORGC	Calculated according to OC fractions (see section 2.7)	Volatile (see section 2.7)
Ammonium	AMMO	1300	Volatile
Nitrate	NITR	1300	Volatile
Methane sulfonate (MSAp)	MSAP	1770	Volatile
Iodic acid/iodate	IODA	4629	Volatile
Sea Salt	SALT	2240	Non-volatile
Primary biological material (PBA)	XXXX	1150	Non-volatile
Soot (EC or BC)	ECBC	1200 [Virtanen et al., 2002]	Non-volatile
Mineral Dust	DUST	1400	Non-volatile

The following example demonstrates how mass concentrations are initialized by estimated the mass fraction of each component and the mass concentration in each mode if only PM10 was measured. It is noted that input mass refers to the dry aerosol, and that water mass concentration per mode is calculated and added by the model.

1. Estimated mass fraction of aerosol components per mode

Mode	H2SO4 (frac.)	OC (frac.)	NH4 (frac.)	NO3 (frac.)	MSAp (frac.)	SALT (frac.)	PBA (frac.)	EC (frac.)	ASH (fraction)	Total
NU	0.00	0.00	0.00	0.00	0.00	0.00	0.00	0.00	0.00	0.00
NA	0.55	0.35	0.05	0.05	0.00	0.00	0.00	0.00	0.00	1.00
AI	0.70	0.10	0.15	0.05	0.00	0.00	0.00	0.00	0.00	1.00
AS	0.50	0.00	0.20	0.05	0.00	0.25	0.00	0.00	0.00	1.00
CS	0.10	0.00	0.00	0.05	0.00	0.85	0.00	0.00	0.00	1.00

2. Measured total mass (=PM10) and estimated total mass concentration per mode

	Total mass	NU	NA	AI	AS	CS
Mass fraction	1.00	0.00	0.01	0.04	0.15	0.80
Mass conc. MM (ng/m^3)	12000	0	120	480	1800	9600

3. Calculated mass concentration of components per mode

Mode	H2SO4 (ng/m^3)	OC (ng/m^3)	NH4 (ng/m^3)	NO3 (ng/m^3)	MSAp (ng/m^3)	SALT (ng/m^3)	PBA (ng/m^3)	EC (ng/m^3)	ASH (ng/m^3)	MM (ng/m^3)
NU	0	0	0	0	0	0	0	0	0	0
NA	66	42	6	6	0	0	0	0	0	120
AI	336	48	72	24	0	0	0	0	0	480
AS	900	0	360	90	0	450	0	0	0	1800
CS	960	0	0	480	0	8160	0	0	0	9600

Next, if the initial number concentration distribution was also monitored, the mass distribution should be adjusted to match the number distribution. This can be done by fitting the mass distribution by variation of the (mass-based) geometric mean diameter (GMD) and/or bandwith (SIGMA) of each mode in inaero.dat such that the calculated number distribution curve matches the measured number distribution curve.

2.3.2 FITAERO

The Fortran program FITAERO performs an automated fitting to create the inaero.dat input file. The program uses the SIMPLEX algorithm for optimization of a non-linear least squares data fitting problem, by finding the minimum of a function (here the initial number size distribution) of more than one independent variable. The downhill simplex method is originally from Nelder and Mead (1965). The method requires only function evaluations, not derivatives. The actual implementation in FITAERO is based on the SIMPLEX code given in an online lesson from Oregon State University (http://oregonstate.edu/instruct/ch490/lessons/lesson10.htm). For multidimensional minimization, the best we can do is to give our algorithm a starting guess for the three parameters (GMD, sigma and mass) as the first point to try. The algorithm then makes its own way downhill through the unimaginable complexity of the 3-dimensional topography, until it encounters a local or global minimum.

Three input files are required to run FITAERO: userfit.inp with the basic configuration, a table-style file of the initial particle concentration dN per size bin, and a table-style file of the mass fractions of the aerosol components in each mode.

Example of userfit.inp:

'./input/initdis1_test.csv'	! Filename of csv-file containing observed Dp dN data (full path)
'./input/massfrac1_test.csv'	! Filename of csv-file containing mass fractions data (full path)
'./output/'	! Output files path name
'./logs/user_log.txt'	! Log file (in output path)
54	! Number of observed size bins
1.00E-06	! DPMAX [in m], in inaero.dat
20	! IMAX, bins per mode in MAFOR, inaero.dat
F	! first column, inaero.dat ('T'/'F')
50.0	! RH [%} in first simulation hour

The first two lines in userfit.inp give the filename (including relative or full path) of the user-provided file of the monitored number size distribution and of the estimated mass fractions. 3rd line is the path of output directory; 4th line is the location and name of the log file that is written by FITAERO; 5th line is the number of size bins of the monitor data; 6th line is DPMAX (diameter of maximum size in m, same value as in inaero.dat); 7th line is IMAX (number of bins per mode in MAFOR, same value as in inaero.dat); 8th line is the T/F flag in inaero.dat; 9th line is the relative humidity (in %) in the first simulation hour.

The DPMAX value is a key parameter for matching the observed (initial) aerosol size distribution with MAFOR. In principle there are three variants:

(1) use 1.E-5 m (10 µm) as DPMAX of the atmospheric aerosol. Then the mode limits internally in the model are approximately 8 nm, 30 nm, 300 nm, and 1500 nm. These are quite sharp borders between the modes (NU–NA, NA–AI, AI–AS, AS–CS).
(2) Use 1.E-6 m m (1 µm) as DPMAX of the atmospheric aerosol. This is typically done for plume simulation for combustion sources. Can also be used for atmospheric simulations if the coarse mode (> 1 µm) is not so important or has not been measured. Then the upper mode limit for the NU mode is still at ~8 nm, but two modes can exist inside the size range 10-100 nm, and a fourth and fifth mode is between 100–1000 nm.
(3) Use a value in the range 2.E-6 to 8.E-6 m to squeeze the modes compared to option (1).

Different DPMAX values can be tested in FITAERO because the three options are implemented in the tool. The recommended DPMAX value for different atmospheric aerosols are listed in the table below.

Classification of aerosol	**Recommended DPMAX (m)**
Marine (clean) background	1.E-5
Marine (coastal) background	4.E-6
Coastal (continental) background	5.E-6
Urban background	8.E-6
Urban background – influenced by road traffic	1.E-6
Ship exhaust plume	1.E-5 or 8.E-6 or 1.E-6
Biomass burning plume	1.E-6
Roadside	1.E-6

Mass fractions of the aerosol components:

As shown in the example file below (massfrac1_test.csv included in the FITAERO input directory), the mass fraction for each MAFOR aerosol component (H2SO4, ORGC, NH4, NO3, MSAp, SALT, BPA, EC, and ASH) is given in lines 2-6 for the modes NU, NA, AI, AS, and CS. The sum in each line is controlled in the last column, and should give 1.00.

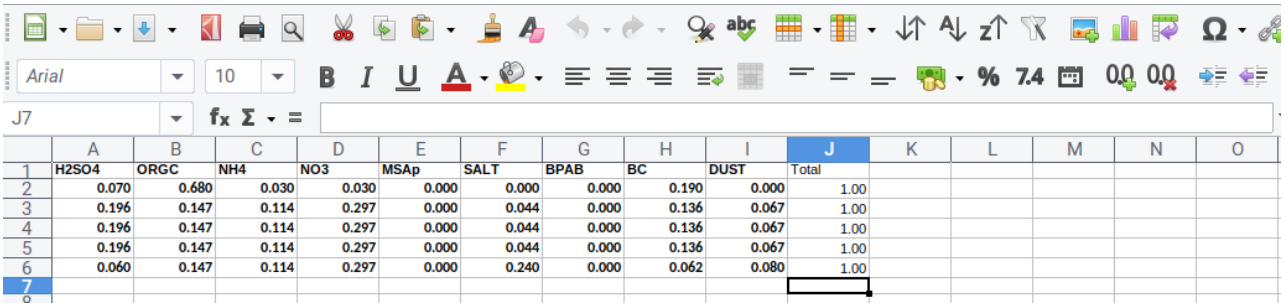

	A	B	C	D	E	F	G	H	I	J
1	H2SO4	ORGC	NH4	NO3	MSAp	SALT	BPAB	BC	DUST	Total
2	0.070	0.680	0.030	0.030	0.000	0.000	0.000	0.190	0.000	1.00
3	0.196	0.147	0.114	0.297	0.000	0.044	0.000	0.136	0.067	1.00
4	0.196	0.147	0.114	0.297	0.000	0.044	0.000	0.136	0.067	1.00
5	0.196	0.147	0.114	0.297	0.000	0.044	0.000	0.136	0.067	1.00
6	0.060	0.147	0.114	0.297	0.000	0.240	0.000	0.062	0.080	1.00
7										

Initial number size distribution:

Comma-separated file (csv format) containing three lines of data. First line: number of size bin in ascending order, diameter (nm) in each bin, number concentration dN (particles per cubic centimeter) in each bin. The file can be created in an Excel sheet and then saved as csv file. Make sure that values are separated by comma (,). An example of the initial number size distribution file can be found in the FITAERO input directory (initdis1_test.csv).

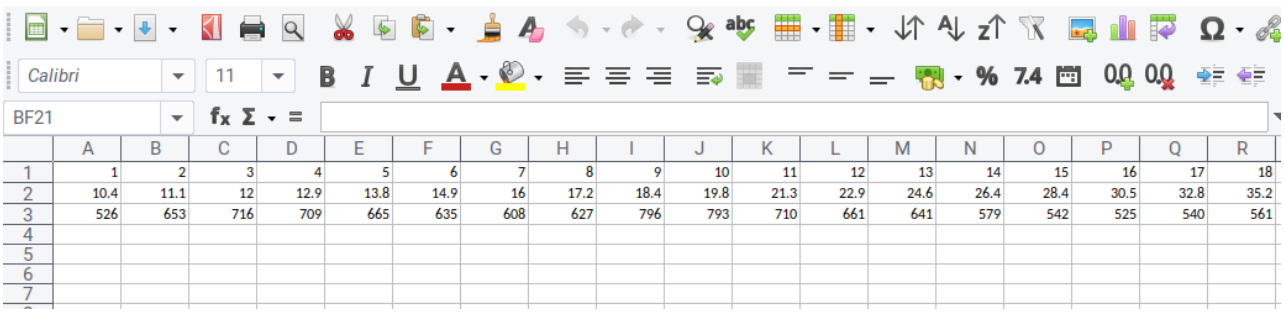

	A	B	C	D	E	F	G	H	I	J	K	L	M	N	O	P	Q	R
1	1	2	3	4	5	6	7	8	9	10	11	12	13	14	15	16	17	18
2	10.4	11.1	12	12.9	13.8	14.9	16	17.2	18.4	19.8	21.3	22.9	24.6	26.4	28.4	30.5	32.8	35.2
3	526	653	716	709	665	635	608	627	796	793	710	661	641	579	542	525	540	561
4																		
5																		
6																		
7																		

How to calculate number concentration dN per bin:
Measurements of the particle number size distribution are usually reported in dN/dlogDp per channel. Make sure that dN/dlogDp is on decadic base (log10). If observations are given on natural base then the dN/dlogDp values have to be multiplied by 2.303. The dlogDp values are calculated for each channel (size bin) straight forward as:

$$dlogDp = log10(Dp_i / Dp_{i-1})$$

starting with the second bin (i=2 and i-1=1) up to the last bin. The dlogDp value of the first bin is the same as the second. Then multiply the series of dN/dlogDp with the corresponding dlogDp value to get the dN value per bin for use in the csv file for the observed initial size distribution.

If particle number concentrations have not been measured for particles > 1 µm diameter then either use DPMAX of 1.E-6 m (in userfit.inp) or add dN values for diameters 1, 2, 3, …, 9 µm with arbitrary small values in the size distribution input file.

The output of FITAERO is inaero.dat, that can be directly used for a MAFOR simulation, and out_sizedis.dat, that contains the comparison between fitted dN and (user-provided) observed dN for the user-provided diameters. It is noted that fitted dN in out_sizedis.dat usually does not align with the observed dN because of the differences in particle density for different aerosol components. Both files are created in the output directory specified in userfit.inp.

FITAERO has been tested for a limited number of cases. It is therefore possible that it does not give a suitable solution for the number concentration and mass fraction data provided by the user. It is hoped that over time, enough experience will be collected for various atmospheric particle distributions in order to adjust the program to better match new cases.

It is possible to modify the inaero.dat file obtained from FITAERO afterwards to better adjust the model to the initial number size distribution. This is described in section 2.3.4.

2.3.3 Aerosol input files for plume simulation

For a plume simulation, the mass distribution of the background aerosol has to be entered in inbgair.dat. The values in inbgair.dat should be taken from a monitored background aerosol mass distribution, e.g. speciated PM2.5 together with estimated mass fractions in the different modes. It is not necessary to provide inbgair.dat for a standard run of the model.

An Excel work sheet (inaero_prep.xls) is available in the zip file helper_tools.zip. The first work sheet of the Excel document can be used to prepare the input of inbgair.dat and inaero.dat. Use copy-paste to transfer the content into a text editor. FITAERO can also be used to create the input files (inbgair.dat requires some modification). After a first version of inbgair.dat and inaero.dat are created, the model should be run for a short time with the input (abrupt the run by control-C or have only one line for the first hour in ingeod.dat). The computed initial distribution should be compared to the monitored number size distribution and the input should be adjusted to better match the monitored distribution (if the aim is to simulate real world observations). This procedure may have to be repeated until agreement is achieved. Note that the number size distribution output of the model, sizedis.res, is based on natural logarithm. For comparison to a monitored size distribution with decadic base, the model output dN/dlogDp has to be multiplied by 2.303.

2.3.4 Modify inaero.dat obtained from FITAERO

The inaero.dat file produced by FITAERO tool can be further modified to improve the match to the observed initial particle number size distribution. To this end, open the Excel document inaero_prep.xls. The second work sheet of the Excel document ("FITAERO") can be used to update the input of inaero.dat. Enter the DPMAX value and the number of bins per mode for the MAFOR run in line 4. Then copy lines 2-6 of inaero.dat and paste to cell A6 either as comma-separated or tab-separated. Also copy the content of the mass fraction csv file (see above) and past to cell A13. In the next step, the geometric mean diameter (GMD), band width (sigma value) and the total mass of one or several of the five modes can be changed in lines 22-26. Changing the GMD allows to shift the simulated mode peak closer to the observed peak. Decreasing sigma centers the mode to the GMD value, increasing sigma flattens the mode. Increasing or decreasing the total mass concentration of a mode to get either higher or lower dN/dlogDp values. A change of GMD or sigma will increase or decrease the simulated number concentration in a size bin, therefore it might be necessary to change the total mass concentration as well. Do not change the compound mass concentrations in lines 22-26.

Modify GMD, sigma and total mass per mode:

Mode	GMD (change)	Sigma (change)	H2SO4	ORG	NH4	NO3	MSAp	SALT	BPAB	BC	DUST	Total Mass (change)
1	9.20E-09	1.35	0.208	0.544	0.024	0.024	0	0	0	0	0	0.80
2	3.43E-08	1.45	23.587	18.643	11.23	23.69	0	5.459	0	19.98	0	103.00
3	1.90E-07	1.85	709.9	561.1	337.9	713.0	0	164.3	0	601.4	0	3100.00
4	3.30E-07	2.10	1603.0	1267.0	763.0	1610.0	0	371.0	0	1358.0	0	7000.00
5	1.60E-06	1.55	1946.5	1538.5	926.5	1955.0	0	450.5	0	1649.0	0	8500.00

After the changes are completed, copy the content of the black frame in lines 32-37 and paste it into a new inaero.dat file in a text editor. Run the model with the updated inaero.dat and abrupt the run by control after about 10 seconds. The computed initial distribution should be compared to the monitored number size distribution and the procedure may have to be repeated until agreement is achieved. Note that the number size distribution output of the model, sizedis.res, is based on natural logarithm. For comparison to a monitored size distribution with decadic base, the model output dN/dlogDp has to be multiplied by 2.303.

2.3.5 Aerosol input files

The initial aerosol size distribution is provided in the input file inaero.dat. This file is always required. The input file inbgair.dat with the background aerosol distribution is required if the switch for dilution is set to 1 in sensitiv.dat. The input file emitpar.dat with constant emission rate for each aerosol component in each mode is required if the switch for particle emission is set to 1 in sensitiv.dat.

Documentation for input file inaero.dat is given by the following list.
Entries of first line:

01	**DPMAX**	**diameter of max. bin [m]** **Note: DPMAX can be 1e-5 (10 µm) or 1e-6 (1 µm)**
02	**IMAX**	**number of bins per mode**

Following lines: one line for each mode NU, NA, AI, AS, CS. in one line, the order is:

01	**Number-Option: F/T**	**If T (true), the initial mass and number concentration will be corrected to maintain the mass of the input (exactly as provided in inaero.dat). The option choice has to be the same in all lines.**
02	**GMD**	**geometric mean diameter [m]**
03	**SIGMA**	**band width [-]**
04	**NUMBER**	**number concentration [#/m3]. Value is not used.**
05	**MSULF**	**sulfate mass concentration [ng/m3]**
06	**MORGC**	**total organic mass (OC) concentration [ng/m3]**
07	**MAMMO**	**ammonium mass concentration [ng/m3]**
08	**MNITR**	**nitrate mass concentration [ng/m3]**
09	**MMSAP**	**methane sulfonate (MSAp) mass concentration [ng/m3]**
10	**MSALT**	**sea-salt concentration [ng/m3]**
11	**MXXXX**	**primary biological aerosol (PBA) mass concentration] [ng/m3]**
12	**MECBC**	**EC or BC mass concentration] [ng/m3]**
13	**MDUST**	**mineral dust mass concentration] [ng/m3]**

Documentation for input file inbgair.dat is given by the following list. Following lines: one line for each mode NU, NA, AI, AS, CS. in one line, the order is:

01	**GMD**	**geometric mean diameter [m]**
02	**SIGMA**	**band width [-]**
03	**MSULF**	**sulfate mass concentration [ng/m3]**
04	**MORGC**	**total organic mass (OC) concentration [ng/m3]**
05	**MAMMO**	**ammonium mass concentration [ng/m3]**
06	**MNITR**	**nitrate mass concentration [ng/m3]**

07	**MMSAP**	**methane sulfonate mass concentration [ng/m3]**
08	**MSALT**	**sea-salt concentration [ng/m3]**
09	**MXXXX**	**primary biological aerosol mass concentration [ng/m3]**
10	**MECBC**	**EC or BC mass concentration [ng/m3]**
11	**MDUST**	**mineral dust mass concentration [ng/m3]**

In the sixth line of inbgair.dat follow the background gas phase concentrations:

01	**BGNO**	**background concentration of NO [molecules/cm^3]**
02	**BGNO2**	**background concentration of NO2 [molecules/cm^3]**
03	**BGSO2**	**background concentration of SO2 [molecules/cm^3]**
04	**BGO3**	**background concentration of O3 [molecules/cm^3]**
05	**BGNH3**	**background concentration of NH3 [molecules/cm^3]**
06	**BGSULF**	**background concentration of H2SO4 [molecules/cm^3]**
07	**BGPIOV**	**background concentration of PIOV [molecules/cm^3]**
08	**BGPSOV**	**background concentration of PSOV [molecules/cm^3]**

Documentation for input file emitpar.dat is given by the following list. Following lines: one line for each mode NU, NA, AI, AS, CS. in one line, the order is:

01	**GMD**	**geometric mean diameter of emission [m]**
02	**SIGMA**	**band width [-]**
03	**ESULF**	**sulfate emission rate [ng/m^2/s]**
04	**EORGC**	**total organic mass (OC) emission [ng/m^2/s]**
05	**EAMMO**	**ammonium emission [ng/m^2/s]**
06	**ENITR**	**nitrate emission [ng/m^2/s]**
07	**EMSAP**	**methane sulfonate emission [ng/m^2/s]**
08	**ESALT**	**sea-salt emission [ng/m^2/s]**
09	**EXXXX**	**primary biological aerosol emssion [ng/m^2/s]**
10	**EECBC**	**EC or BC emission [ng/m^2/s]**
11	**EDUST**	**mineral dust emission [ng/m^2/s]**

2.4 Gas phase

The initial gas phase concentration, the dry deposition velocity and emission rate for a range of compounds are set in the input file inchem.dat. A list of 81 gas-phase compounds is included in inchem.dat. An Excel work sheet (inchem_prep.xls) is available in the zip file helper_tools.zip. The Excel sheet can be used to prepare the input of inchem.dat. Use copy-paste to transfer the content into a text editor and save as inchem.dat.

Documentation for input file inchem.dat is given by the following list.

One line per chemical compound.

The entry in each line is:

01	**compound name**	
02	**compound index**	
03	**gas phase concentration**	**[molecules/cm3]**
04	**emission rate**	**[molecules/cm2/s]**
05	**dry deposition velocity**	**[cm/s]**

Note that compounds between no. 20 and no. 40 are only dummy entries and will be ignored by the program (except those of I2, CH3I and DMSO). Also entries for compound no. 43 (CO2) are ignored. SOA compounds are given in the last nine lines (they can all have emissions).

Emissions of DMS, SO2 and H2O2 given in inchem.dat are not used instead the emissions are taken from ingeod.dat and can vary every hour.

Concentrations of DMS, NH3, O3 and SOA-1 can be prescribed in ingeod.dat and can vary every hour. For this their read flags in sensitiv.dat have to be set to 1. For SOA-1 the read flag can be set to 2, which allows entrainment from free troposphere (entrainment velocity: 0.6 cm/s, FT concentration: 2 ppt). If the read flag is 0, then the time dependent concentrations of the compounds will be calculated by the chemistry solver using the initial concentrations in inchem.dat. NH3 has been added to inchem.dat as compound no. 72.

Marine emissions of I2 (specified by the user) are only activated when open water fraction is < 20 %. The open water fraction is prescribed in ingeod.dat.

Marine emissions of C5H8 and BLOV are automatically activated when open water fraction is >0 % during daytime. The sea-air flux of C5H8 and BLOV is assumed to be 4.4×10^{8} and 2.6×10^{7} molecules/cm^2/s (Bruggemann et al., 2017). This flux is added to any emission rate provided by the user in inchem.dat.

2.5 Aqueous phase

The concentration of 14 compounds in the aqueous solution of the droplet mode (see section 2.2) can be initialized in the input file inaqchem.dat. The input file inaqchem.dat is only required if the switch for aqueous phase chemistry is 1 in sensitiv.dat. Compound no. 14 (in_DOC_a) is the dissolved organic carbon.

An Excel work sheet (inaqchem_prep.xls) is available in the zip file helper_tools.zip. The Excel sheet can be used to prepare the input of inchem.dat. Use copy-paste to transfer the content into a text editor and save as inchem.dat.

Documentation for input file inaqchem.dat is given by the following list.

One line per chemical compound.

The entry in each line is:

01 aq. compound name

02 compound index

03 concentration in CS mode [molecules/cm3(air)]

2.6 Organics

The parameters for the organic vapor and the organic aerosol are given in the input file organic.dat. The parameters for defining the fractal geometry and density of soot particles have to be specified in organic.dat as well. The standard values for soot are DENEC = 1200 kg/m^3 [Lemmetty et al., 2008], rs = 13.5 nm and Dfrac = 1.7 [Jacobson and Seinfeld (2004)].

Documentation for input file organic.dat is given by the following list.

1st Line:

DENOC	**particle density organics [kg/m3]**
surfin	**surface tension from input or function [0|1]**
surf_org	**surface tension organics [kg/s2]**

2nd Line:

DENEC	**particle density of soot [kg/m3]**
rs	**radius of primary spherules in soot [nm]**
Dfrac	**fractal dimension of soot [-]**

Next lines contain the properties of nine organic vapor classes of the 2D VBS (i.e. BSOV, BLOV, BELV, ASOV, ALOV, AELV, PIOV, PSOV, PELV):

3rd Line:

nc_bsov	**number of carbon atoms for BSOV**
no_bsov	**number of oxygen atoms for BSOV**
hvap_bsov	**enthalpy of vaporization for BSOV [kJ/mol]**
csat0_bsov	**saturation concentration C0 for BSOV [ug/m^3]**

4th Line:

nc_blov	**number of carbon atoms for BLOV**
no_blov	**number of oxygen atoms for BLOV**
hvap_blov	**enthalpy of vaporization for BLOV [kJ/mol]**
csat0_blov	**saturation concentration C0 for BLOV [ug/m^3]**

5th Line:

nc_belv	**number of carbon atoms for BELV**
no_belv	**number of oxygen atoms for BELV**
hvap_belv	**enthalpy of vaporization for BELV [kJ/mol]**
csat0_blov	**saturation concentration C0 for BELV [ug/m^3]**

6th Line:

nc_asov	**number of carbon atoms for ASOV**
no_asov	**number of oxygen atoms for ASOV**
hvap_asov	**enthalpy of vaporization for ASOV [kJ/mol]**
csat0_asov	**saturation concentration C0 for ASOV [ug/m^3]**

7th Line:

nc_alov	**number of carbon atoms for ALOV**
no_alov	**number of oxygen atoms for ALOV**
hvap_alov	**enthalpy of vaporization for ALOV [kJ/mol]**
csat0_alov	**saturation concentration C0 for ALOV [ug/m^3]**

8th Line:

nc_aelv	**number of carbon atoms for AELV**
no_aelv	**number of oxygen atoms for AELV**
hvap_aelv	**enthalpy of vaporization for AELV [kJ/mol]**
csat0_aelv	**saturation concentration C0 for AELV [ug/m^3]**

9th Line:

nc_piov	**number of carbon atoms for PIOV**
no_ piov	**number of oxygen atoms for PIOV**
hvap_ piov	**enthalpy of vaporization for PIOV [kJ/mol]**
csat0_ piov	**saturation concentration C0 for PIOV [ug/m^3]**

10th Line:

nc_psov	**number of carbon atoms for PSOV**
no_ psov	**number of oxygen atoms for PSOV**
hvap_ psov	**enthalpy of vaporization for PSOV [kJ/mol]**
csat0_ psov	**saturation concentration C0 for PSOV [ug/m^3]**

11th Line:

nc_pelv	**number of carbon atoms for PELV**
no_ pelv	**number of oxygen atoms for PELV**
hvap_ pelv	**enthalpy of vaporization for PELV [kJ/mol]**
csat0_ pelv	**saturation concentration C0 for PELV [ug/m^3]**

Next lines contain the mole fraction of SOA components in mode NU to CS:

12th to 20th Line:

gamma-oc1(NU)	**mole fraction of SOA-1 in mode NU (0,..,1)**
gamma-oc1(NA)	**mole fraction of SOA-1 in mode NA (0,..,1)**
gamma-oc1(AI)	**mole fraction of SOA-1 in mode AI (0,..,1)**
gamma-oc1(AS)	**mole fraction of SOA-1 in mode AS (0,..,1)**
gamma-oc1(CS)	**mole fraction of SOA-1 in mode CS (0,..,1)**
gamma-oc2(NU)	**mole fraction of SOA-2 in mode NU (0,..,1)**
gamma-oc2(NA)	**mole fraction of SOA-2 in mode NA (0,..,1)**
gamma-oc2(AI)	**mole fraction of SOA-2 in mode AI (0,..,1)**
gamma-oc2(AS)	**mole fraction of SOA-2 in mode AS (0,..,1)**
gamma-oc2(CS)	**mole fraction of SOA-2 in mode CS (0,..,1)**
gamma-oc3(NU)	**mole fraction of SOA-3 in mode NU (0,..,1)**
gamma-oc3(NA)	**mole fraction of SOA-3 in mode NA (0,..,1)**
gamma-oc3(AI)	**mole fraction of SOA-3 in mode AI (0,..,1)**
gamma-oc3(AS)	**mole fraction of SOA-3 in mode AS (0,..,1)**
gamma-oc3(CS)	**mole fraction of SOA-3 in mode CS (0,..,1)**
gamma-oc4(NU)	**mole fraction of SOA-4 in mode NU (0,..,1)**
gamma-oc4(NA)	**mole fraction of SOA-4 in mode NA (0,..,1)**
gamma-oc4(AI)	**mole fraction of SOA-4 in mode AI (0,..,1)**
gamma-oc4(AS)	**mole fraction of SOA-4 in mode AS (0,..,1)**
gamma-oc4(CS)	**mole fraction of SOA-4 in mode CS (0,..,1)**
gamma-oc5(NU)	**mole fraction of SOA-5 in mode NU (0,..,1)**
gamma-oc5(NA)	**mole fraction of SOA-5 in mode NA (0,..,1)**
gamma-oc5(AI)	**mole fraction of SOA-5 in mode AI (0,..,1)**
gamma-oc5(AS)	**mole fraction of SOA-5 in mode AS (0,..,1)**
gamma-oc5(CS)	**mole fraction of SOA-5 in mode CS (0,..,1)**

gamma-oc6(NU)	**mole fraction of SOA-6 in mode NU (0,..,1)**
gamma-oc6(NA)	**mole fraction of SOA-6 in mode NA (0,..,1)**
gamma-oc6(AI)	**mole fraction of SOA-6 in mode AI (0,..,1)**
gamma-oc6(AS)	**mole fraction of SOA-6 in mode AS (0,..,1)**
gamma-oc6(CS)	**mole fraction of SOA-6 in mode CS (0,..,1)**
gamma-oc7(NU)	**mole fraction of SOA-7 in mode NU (0,..,1)**
gamma-oc7(NA)	**mole fraction of SOA-7 in mode NA (0,..,1)**
gamma-oc7(AI)	**mole fraction of SOA-7 in mode AI (0,..,1)**
gamma-oc7(AS)	**mole fraction of SOA-7 in mode AS (0,..,1)**
gamma-oc7(CS)	**mole fraction of SOA-7 in mode CS (0,..,1)**
gamma-oc8(NU)	**mole fraction of SOA-8 in mode NU (0,..,1)**
gamma-oc8(NA)	**mole fraction of SOA-8 in mode NA (0,..,1)**
gamma-oc8(AI)	**mole fraction of SOA-8 in mode AI (0,..,1)**
gamma-oc8(AS)	**mole fraction of SOA-8 in mode AS (0,..,1)**
gamma-oc8(CS)	**mole fraction of SOA-8 in mode CS (0,..,1)**
gamma-oc9(NU)	**mole fraction of SOA-9 in mode NU (0,..,1)**
gamma-oc9(NA)	**mole fraction of SOA-9 in mode NA (0,..,1)**
gamma-oc9(AI)	**mole fraction of SOA-9 in mode AI (0,..,1)**
gamma-oc9(AS)	**mole fraction of SOA-9 in mode AS (0,..,1)**
gamma-oc9(CS)	**mole fraction of SOA-9 in mode CS (0,..,1)**

Next lines contain reaction rate factors:

21th Line:

fech3so2_dec	**scal. Factor activation energy of CH3SO2 decomposition**

See section 2.7 for more details on the properties of the organic vapors and regarding the formation of SOA. In the nine lines for the organic mole fraction, one is for each SOA-type. By this, it is possible to prescribe the organic composition in each mode of the existing particles. For each mode (5 columns, NU, NA, AI, AS, CS) the values distributed over the 9 SOA-types have to add up to 1 (in each column). If there is organic mass in the existing aerosol, the values in organic.dat must be non-zero. For example, if the nucleation mode should consist 25 % of each SOA-1 to SOA-4 and the other modes of SOA-2, then the lines in organic.dat would be:

0.25 0.00 0.00 0.00 0.00
0.25 1.00 1.00 1.00 1.00
0.25 0.00 0.00 0.00 0.00
0.25 0.00 0.00 0.00 0.00
0.00 0.00 0.00 0.00 0.00
0.00 0.00 0.00 0.00 0.00
0.00 0.00 0.00 0.00 0.00
0.00 0.00 0.00 0.00 0.00
0.00 0.00 0.00 0.00 0.00

Parameters for controlling the gas phase chemistry of DMS are in line 20. Currently, the only parameter to vary is a scaling factor for the activation energy of the thermal decomposition of the CH_3SO_2 radical. A standard value of fech3so2_dec is 0.90.

2.7 Dispersion and deposition data

The parameters for plume dispersion (dilution) and dry deposition of particles are given in the input file dispers.dat.

Documentation for input file dispers.dat is given by the following list.

1st Line:

hmix_st	**mixing height @ station**	**[m]**
dst_st	**distance @ station**	**[m]**
hsta_st	**stack height above ground**	**[m]**
ta_st	**temperature @ station**	**[K]**

2nd Line:

dil2_b	**Type 2 dilution parameter for concentration**	**[-]**
dil2_c	**Type 2 dilution parameter for concentration**	**[s]**
dil2_d	**Type 2 dilution parameter for temperature**	**[-]**
dil2_e	**Type 2 dilution parameter for temperature**	**[s]**
dil2_f	**Type 2 dilution parameter for temperature**	**[-]**

3rd Line:

DR_fin	**Type 3 dilution: final dilution ratio after PD**	**[-]**
tau_c	**Type 3 dilution: dilution lifetime concentration**	**[s]**
T_fin	**Type 3 dilution: final temperature after PD**	**[-]**
tau_d	**Type 3 dilution: dilution lifetime temperature**	**[s]**
BGH2O	**Type 3 dilution: background H2O concentration**	**[molecules cm^{-3}]**

4th Line:

u0	**Type 4 dilution: initial exhaust gas velocity**	**[m/s]**
sigw	**Type 4 dilution: entrainment velocity**	**[m/s]**
tend1	**Type 4 dilution: width of line source 1**	**[m]**
tbeg2	**Type 4 dilution: downwind distance of line source 2**	**[m]**
tend2	**Type 4 dilution: width of street**	**[m]**

5th Line:

ustar	**friction velocity**	**[m/s]**
znot	**surface roughness**	**[m]**
ADEP	**dry deposition parameter A**	
BDEP	**dry deposition parameter B**	

6th Line:

zcap	**height of canopy**	**[m]**
dcol	**collector size**	**[m]**
Fplus	**roughness parameter (Hussein et al (2012)**	**[-]**

7th Line:

vupdra	**updraft velocity (value range 0 … 0.5)**	**[m/s]**
sst	**sea surface temperature**	**[K]**
sal	**salinity of seawater**	**[g/kg]**

For all types of plume simulations (see section 4.4) hmix_st, dst_st, hsta_st, and ta_st have to be provided in line 1. These are also the parameters required for plume simulation of Type 1.

For the plume simulation Type 2 (see section 4.4), in addition values for parameters dil2_b, dil2_c, dil2_d, dil2_e, and dil2_f have to be provided.

The plume simulation of Type 3 (diesel exhaust after treatment and ageing chamber) is described in more detail in section 4.4. For Type 3, the parameters DR_fin, tau_c, T_fin, tau_d and BGH2O have to be provided in line 3.

The plume simulation of Type 4 considers particle emissions from two road traffic line sources (two-stage dilution from road to ambient). The setup of Type 4 is described in more detail in section 4.4. For Type 4, the parameters u0, sigw, tend1, tbeg2, tend2 have to be provided in line 4.

Dry deposition of particles is parameterized by ustar (friction velocity) and znot (surface roughness length). For dry deposition to water surface (ocean) it is recommended to use the parameterization by Schack et al. (1985). For this the dry deposition flag in sensitiv.dat has to be set to 1. The default set of parameters for water surfaces is: ustar=1.17, znot=0.001, ADEP=1.7, and BDEP=51.8. Table 2.2 shows the parameter values for other surfaces. For dry deposition to a canopy with rough surface (e.g. forest) it is recommended to use the option 2 (Kouznetsov and Sovief (2012). The control parameters zcap (canopy height z) and dcol (collector size d_c) can be changed in dispers.dat. Typical values for dcol are 0.002 m for bare soil, 0.002 m for conifer forest and 0.02 m for broad-leaf forest. A logarithmic wind profile is assumed in the canopy. For dry deposition to rough surfaces it is recommended to use option 3 (Hussein et al. (2012). The control parameter for the roughness of a surface, Fplus, can be changed in dispers.dat.

Table 2.2 Dry depositon of particles: parameter sets for option 1. Adopted from Schack et al. (1985). Values for F+ adapted from Hussein et al. (2012).

Surface	**ustar** Friction velocity (m/s)	**znot** Surface Roughness (m)	**ADEP**	**BDEP**	**Fplus** F^+
Rye grass		0.008	8.99	186	
Crushed Gravel (road)	1.33	0.0013	4.0	121	0.55
Sticky Artificial Grass	0.50	0.01	2.39	885	0.4
Artificial Grass	0.19	0.0012	27.3	400	1.6
Grass	0.36	0.01			0.5
Water	1.17	0.001	1.7	51.8	0.2
Water	0.44	0.0002	0.19	18.8	0.5
Moss		0.0037	9.41	422	

Option 4 (Zhang et al., 2001) is suitable for any rough surface and be used with the parameters of option 2 (zcap and dcol).

Figure 2.1 shows a comparison of dry deposition velocity option 1 (black line), option 2 (red line), and option 3 (blue line) for water with ustar=1.17, znot=0.001 and average particle density of 1400 kg/m^3.

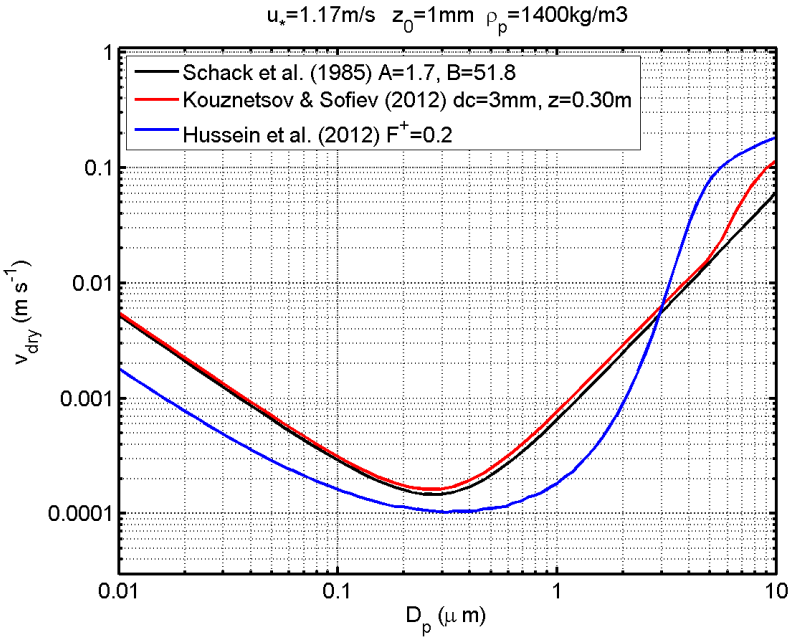

Figure 2.1 Dry deposition of particles with option 1 (black line), option 2 (red line), and option 3 (blue line).

2.8 Chamber Data

Two input files are required for the simulation of chamber experiments: incham.dat and monitor.dat. The two input files are only required if the chamber experiment switch in sensitiv.dat is set to 1. The input file incham.dat is used to control the chamber experiment simulation. The input file monitor.dat provides input of parameters monitored during a chamber experiment for every minute. Currently only chamber experiments on the photo-oxidation of amines have been simulated with the model and therefore the input file incham.dat is very specific for amines, but it is possible to simulate chamber experiments for various VOC. The wall loss of organic vapors is treated as in Zhang et al. (2014) by using a first-order wall loss rate and the organic aerosol equivalent wall to account for evaporation of organics from the chamber walls. The wall loss of VOC and major gaseous oxidation products is approximated by the wall loss rate of O_3, given by the model user. The wall loss of particles (diffusion to surfaces and sedimentation) is controlled in sensitiv.dat, by setting the deposition flag to 0 (no wall loss) or 1 (wall loss activated).

Documentation for input file incham.dat is given by the following list.

Entries in first line:

IAM	**selected amine (1-6; 1: MEA, 2: methylamine, 3: dimethylamine, 4: trimethylamine, 5: methylmethanimine, 6: AMP) [ignore if not an amine experiment]**	
IOZ	**read O3 conc from monitor.dat**	
KP_NIT	**dissociation constant Amine-NO3 (molec/cm3)2**	
F_HONO	**scaling factor HONO source**	
ya_soan1	**SOA-1 yield (0-1)**	
ya_soan2	**SOA-2 yield (0-1)**	
fco	**scaling factor Amine-NO3 condensation rate**	

Entries in second line:

fkoh_mea	**scaling factor k(MEA+OH)**	**(Note: only for IAM=1)**
cami	**nucleation constant (m3/molec/s)**	
K_DIL	**dilution rate constant for gases (s-1)**	
L_MEA	**MEA wall loss rate constant (s-1)**	**(Note: only for IAM=1)**
L_NO2	**NO2 wall loss rate constant (s-1)**	
L_HNO3	**HNO3 wall loss rate constant (s-1)**	
L_O3	**O3 wall loss rate constant (s-1)**	

Entries in third line:

DILPAR	**dilution rate constant for particles (s-1)**
V_CHAM	**Volume of the chamber (m3)**
S_CHAM	**Total surface area of the chamber (m2)**

S_SED	**Sedimentation surface area of the chamber (m2)**
S_DIF	**Diffusion surface area of the chamber (m2)**
CWIN	**Equivalent wall organic aerosol (mg/m3)**

For the EUPHORE chamber, the following values apply: DILPAR = $7x10^{-6}$ s^{-1}, V_CHAM = 177 m^3, S_CHAM = 177 m^2 (giving a surface on volume ratio S/V = 1), S_SED = 65 m^2, S_DIF = 130 m^2, and CWIN = 10 mg/m^3. The typical range of the equivalent wall organic aerosol is 2-20 mg/m^3.

Documentation for input file monitor.dat is given by the following list.
One line for every minute of the simulation. In one line, the order is:

c(O3)	**concentration of O3 in ppbv**
c(NO)	**concentration of NO in ppbv**
c(NO2)	**concentration of NO2 in ppbv**
jno2m	**measured j(NO2) in s-1**
temp	**measured temperature in K**
c(IPN)	**concentration of isopropylnitrite (IPN) in ppbv (0.0 if not present)**

3 Output Files

All output files generated by the MAFOR model are in table-style ASCII format. Every 60 second of the simulation a new line is added to the output files (note exception for plume dispersion simulations, section 4.4). The first column of the output file is the time of day in seconds.

For every simulation the following output files are generated:

Concentrations (gas phase and aq. phase)	concout.res
Mass concentration (aerosol components)	aerconc.res
Number size distribution	size_dis.res
Mass size distribution	size_dism.res
Total number concentration	total_n.res
Wet aerosol diameter	wetdp.res
Dispersion parameters	plume.res
SOA distribution	soadis.res
Debugging information	debug.res

3.1 Concentration output

The output file concout.res contains the concentrations of all compounds of the chemical mechanism in the gas phase and aqueous phase (unit: molecules/cm^3(air)).

The last four columns of concout.res are: liquid water content (units m3/m3) of NU, AI, AS, and CS mode.

Appendix A provides a list of indices of the compounds in concout.res for use with MATLAB plotting scripts.

3.2 Aerosol output

The format of the number size distribution output file size_dis.res is (table R x C, R rows and C columns):

Line (1:R,1)	time of day	[s]	
Line (1,2:C)	dry diameter per bin	[m]	
Line (2,2:C)	dlogDp per bin	[-]	Note: natural log
Line (3:R,2:C)	dN/dlogDp per bin	[#/m3]	Note: natural log

The format of the output file of the mass size distribution of dry particles, size_dism.res is (table M x N, M rows and N columns):

Line (1:R,1)	time of day	[s]	
Line (1:R,2:C)	dM/dlogDp per bin	[kg/m3]	Note: natural log

For plume dilution type 3 and type 4 the output format of size_dism.res is

Line (1:R,1)	time of day	[s]
Line (1,2:C)	dM/dlogDp per bin	[kg/m3]
Line (2,2:C)	dSulfate/dlogDp per bin	[ng/m3]
Line (3,2:C)	dMSAp/dlogDp per bin	[ng/m3]

Line (4,2:C)	dNitrate/dlogDp per bin	[ng/m3]
Line (5,2:C)	dAmine/dlogDp per bin	[ng/m3]
Line (6,2:C)	dAmmonium/dlogDp per bin	[ng/m3]
Line (7,2:C)	dSOA-1/dlogDp per bin	[ng/m3]
Line (8,2:C)	dSOA-2/dlogDp per bin	[ng/m3]
Line (9,2:C)	dSOA-3/dlogDp per bin	[ng/m3]
Line (10,2:C)	dSOA-4/dlogDp per bin	[ng/m3]
Line (11,2:C)	dSOA-5/dlogDp per bin	[ng/m3]
Line (12,2:C)	dSOA-6/dlogDp per bin	[ng/m3]
Line (13,2:C)	dSOA-7/dlogDp per bin	[ng/m3]
Line (14,2:C)	dSOA-8/dlogDp per bin	[ng/m3]
Line (15,2:C)	dSOA-9/dlogDp per bin	[ng/m3]
Line (16,2:C)	dSalt/dlogDp per bin	[ng/m3]
Line (17,2:C)	dSoot/dlogDp per bin	[ng/m3]
Line (18,2:C)	dDust/dlogDp per bin	[ng/m3]
Line (19,2:C)	dPBA/dlogDp per bin	[ng/m3]
Line (20,2:C)	dWater/dlogDp per bin	[ng/m3]

On line 21 again dM/dlogDp and so on.

The format of the wet diameter output file wetdp.res is (table R x C, R rows and C columns):

Line (1:R,1)	time of day	[s]
Line (1:R,2:C)	wet diameter per bin	[m]

The wet diameter will only be calculated if the switch for condensation of water is 1 in sensitiv.dat. Otherwise the output will be constant dry diameter. Calculation of the wet diameter depends on relative humidity and the aerosol composition.

Documentation for aerosol mass concentration output file aerconc.res is given by the following list (table R x C, R rows and C columns):

Line (1:R,1)	time of day	[s]
Line (1:R,2)	sulfate mass concentration NU mode	[ng/m3]
Line (1:R,3)	sulfate mass concentration NA mode	[ng/m3]
Line (1:R,4)	sulfate mass concentration AI mode	[ng/m3]
Line (1:R,5)	sulfate mass concentration AS mode	[ng/m3]
Line (1:R,6)	sulfate mass concentration CS mode	[ng/m3]
Line (1:R,7)	MSAp mass concentration NU mode	[ng/m3]
Line (1:R,8)	MSAp mass concentration NA mode	[ng/m3]
Line (1:R,9)	MSAp mass concentration AI mode	[ng/m3]
Line (1:R,10)	MSAp mass concentration AS mode	[ng/m3]
Line (1:R,11)	MSAp mass concentration CS mode	[ng/m3]
Line (1:R,12)	iodate mass concentration NU mode	[ng/m3]
Line (1:R,13)	iodate mass concentration NA mode	[ng/m3]
Line (1:R,14)	iodate mass concentration AI mode	[ng/m3]
Line (1:R,15)	iodate mass concentration AS mode	[ng/m3]
Line (1:R,16)	iodate mass concentration CS mode	[ng/m3]
Line (1:R,17)	PBA mass concentration NU mode	[ng/m3]
Line (1:R,18)	PBA mass concentration NA mode	[ng/m3]
Line (1:R,19)	PBA mass concentration AI mode	[ng/m3]
Line (1:R,20)	PBA mass concentration AS mode	[ng/m3]

Line (1:R,21)	PBA mass concentration CS mode	[ng/m3]
Line (1:R,22)	OC mass concentration NU mode	[ng/m3]
Line (1:R,23)	OC mass concentration NA mode	[ng/m3]
Line (1:R,24)	OC mass concentration AI mode	[ng/m3]
Line (1:R,25)	OC mass concentration AS mode	[ng/m3]
Line (1:R,26)	OC mass concentration CS mode	[ng/m3]
Line (1:R,27)	ammonium mass concentration NU mode	[ng/m3]
Line (1:R,28)	ammonium mass concentration NA mode	[ng/m3]
Line (1:R,29)	ammonium mass concentration AI mode	[ng/m3]
Line (1:R,30)	ammonium mass concentration AS mode	[ng/m3]
Line (1:R,31)	ammonium mass concentration CS mode	[ng/m3]
Line (1:R,32)	nitrate mass concentration NU mode	[ng/m3]
Line (1:R,33)	nitrate mass concentration NA mode	[ng/m3]
Line (1:R,34)	nitrate mass concentration AI mode	[ng/m3]
Line (1:R,35)	nitrate mass concentration AS mode	[ng/m3]
Line (1:R,36)	nitrate mass concentration CS mode	[ng/m3]
Line (1:R,37)	EC mass concentration NU mode	[ng/m3]
Line (1:R,38)	EC mass concentration NA mode	[ng/m3]
Line (1:R,39)	EC mass concentration AI mode	[ng/m3]
Line (1:R,40)	EC mass concentration AS mode	[ng/m3]
Line (1:R,41)	EC mass concentration CS mode	[ng/m3]
Line (1:R,42)	dust mass concentration NU mode	[ng/m3]
Line (1:R,43)	dust mass concentration NA mode	[ng/m3]
Line (1:R,44)	dust mass concentration AI mode	[ng/m3]
Line (1:R,45)	dust mass concentration AS mode	[ng/m3]
Line (1:R,46)	dust mass concentration CS mode	[ng/m3]
Line (1:R,47)	seasalt mass concentration NU mode	[ng/m3]
Line (1:R,48)	seasalt mass concentration NA mode	[ng/m3]
Line (1:R,49)	seasalt mass concentration AI mode	[ng/m3]
Line (1:R,50)	seasalt mass concentration AS mode	[ng/m3]
Line (1:R,51)	seasalt mass concentration CS mode	[ng/m3]
Line (1:R,52)	water mass concentration NU mode	[ng/m3]
Line (1:R,53)	water mass concentration NA mode	[ng/m3]
Line (1:R,54)	water mass concentration AI mode	[ng/m3]
Line (1:R,55)	water mass concentration AS mode	[ng/m3]
Line (1:R,56)	water mass concentration CS mode	[ng/m3]

The last aerosol output file is total_n.res. It contains total number concentration and a series of other aerosol parameters. Documentation for output file total_n.res is given by the following list (table R x C, R rows and C columns):

Line (1:R,1)	time of day	[s]
Line (1:R,2)	number concentration of nucleation mode particles with diameter>3nm	[#/m3]
Line (1:R,3)	number concentration of nucleation mode NU	[#/m3]
Line (1:R,4)	number concentration of nucleation mode NA	[#/m3]
Line (1:R,5)	number concentration of Aitken mode AI	[#/m3]
Line (1:R,6)	number concentration of accumulation mode AS	[#/m3]
Line (1:R,7)	number concentration of coarse mode CS	[#/m3]
Line (1:R,8)	number concentration of particles with 10-25 nm diameter	[#/m3]

Line (1:R,9)	number concentration of particles with 25-100 nm diameter	[#/m3]
Line (1:R,10)	loss rate of amine to particles	[1/s]
Line (1:R,11)	coagulation sink	[1/s]
Line (1:R,12)	condensation sink organic vapour	[1/s]
Line (1:R,13)	total growth rate	[m/s]
Line (1:R,14)	nucleation rate	[1/(m3s)]
Line (1:R,15)	number concentration of particles with 25-50 nm diameter	[#/m3]
Line (1:R,16)	number concentration of particles with 50-75 nm diameter	[#/m3]
Line (1:R,17)	number concentration of particles with 75-1000 nm diameter	[#/m3]
Line (1:R,18)	number concentration of particles with 1-2 µm diameter	[#/m3]
Line (1:R,19)	number concentration of particles with >2 µm diameter	[#/m3]
Line (1:R,20)	PNC1, particles with <25 nm diameter	[#/m3]
Line (1:R,21)	PNC2, particles with 25-50 nm diameter	[#/m3]
Line (1:R,22)	PNC3, particles with 50-75 nm diameter	[#/m3]
Line (1:R,23)	PNC4, particles with 75-1000 nm diameter	[#/m3]
Line (1:R,24)	PNC5, particles with 1-2 µm diameter	[#/m3]
Line (1:R,25)	PNC6, particles with >2 µm diameter	[#/m3]
Line (1:R,26)	Ambient supersaturation ratio	[-]
Line (1:R,27)	Fraction of activated particle number	[-]
Line (1:R,28)	Fraction of activated mass	[-]
Line (1:R,29)	Critical particle diameter for activation	[m]
Line (1:R,30)	Air temperature	[K]

3.3 Plume dispersion output

The output file plume.res contains plume height, temperature, dilution rate and other parameters for plume dispersion.

Line (1:R,1)	time of day	[s]
Line (1:R,2)	time of plume travel	[s]
Line (1:R,3)	plume temperature	[K]
Line (1:R,4)	plume height	[m]
Line (1:R,5)	plume width	[m]
Line (1:R,6)	plume area	[m2]
Line (1:R,7)	dilution rate	[1/s]
Line (1:R,8)	gas-phase concentration of H2SO4	[µg/m3]
Line (1:R,9)	gas-phase concentration of PIOV	[µg/m3]
Line (1:R,10)	gas-phase concentration of PSOV	[µg/m3]
Line (1:R,11)	gas-phase concentration of PELV	[µg/m3]
Line (1:R,12)	total particle number emission rate	[1/(m2s)]

3.4 SOA distribution output

The output file soadis.res is given by the following list (table R x C, R rows and C columns):

Line (1:R,1)	time of day	[s]
Line (1:R,2:10)	effective saturation concentration C*	[µg/m3]
Line (1:R,11:19)	SOA gas-phase concentration	[µg/m3]
Line(1:R,20:28)	SOA particle phase concentration	[µg/m3]

4 Running MAFOR

4.1 Trajectory simulation in boundary layer

The most common application of an atmospheric aerosol/chemistry box model is probably the multi-day run of a clear sky situation along a trajectory or at a fixed observation location, assuming a well-mixed (homogeneous) boundary layer. The set of input files for a boundary layer simulation is:

Gas phase:	inchem.dat
Aerosol:	inaero.dat
Organic:	organic.dat
General:	ingeod.dat
Dry deposition	dispers.dat
Configuration:	sensitiv.dat

In sensitiv.dat the switches for aerosol processes should probably be 1 (“switched on”), the chemistry integration switch and the water condensation switch should also be 1. To prescribe the concentrations of DMS, NH3, O3 or SOA-1 the corresponding switches should be 1. All other switches can be 0. In ingeod.dat, lat_deg, lon_deg, temp, press, RH, u10 and zmbl can be taken from an observed or calculated (pseudo-)trajectory. The switch incloud should be 0. A rainfall (drizzle) rate can be entered in the column rain. This rate will be used for wet scavenging of particles (wet deposition switch of 1 in sensitiv.dat). If all lines have the same values for lat_deg and lon_deg, the simulation is at a fixed location. The columns edms, eso2 and eh2o2 can be used to prescribe emissions of DMS, SO2 and H2O2 if the corresponding switches in sensitiv.dat are set to 1. The corresponding entries in the emission column of inchem.dat will not be used. Gas phase concentrations of NH3 can either be prescribed (every simulation hour) by using column cnh3 in ingeod.dat (set NH3 flag in sensitiv.dat to 1) or computed freely as time-dependent concentrations (set NH3 flag in sensitiv.dat to 0) using the supplied initial concentration and emission rate in inchem.dat.

A test example for a boundary layer simulation of a nucleation event is given in section 5.1.

4.2 Chamber experiment

The simulation of a chamber photo-oxidation experiments is the most adequate application of an aerosol/chemistry box model because the chamber volume is well-mixed.

The set of input files for a chamber experiment simulation is:

Gas phase:	inchem.dat
Aerosol:	inaero.dat
Organic:	organic.dat
General:	ingeod.dat
Configuration:	sensitiv.dat
Chamber control	incham.dat
Chamber monitors	monitor.dat

The chamber experiment switch in sensitiv.dat has to be 1, to read the information from incham.dat and moinitor.dat. Simulation of SOA formation in a chamber experiment is currently possible for amine experiments with different amines (incham.dat: switch IAM; 1: MEA, 2: methylamine, 3: dimethylamine, 4: trimethylamine, 5: methylmethanimine), for experiments with alpha-pinene

(APIN) and other terpenes, for isoprene and for aromatic VOC (toluene, xylene, trimethylbenzene). The molar yields of gaseous SOA precursors in the oxidation of these VOC is given in Table 4.2; see Section 4.6.

Simulation of experiments on gas phase oxidation of all the compounds that can be initialized in inchem.dat are possible. Monitored mixing ratios of NO and NO2 in ppb, temperature in K and monitored photolysis rate of NO2 in s^{-1} are read every minute from monitor.dat. In addition, mixing ratio of O3 in ppb will be read from monitor.dat if the switch IOZ is set 1 in incham.dat.

Deposition of particles to the chamber walls is calculated by the model according to wall loss in the EUPHORE photoreactor; the wall loss rate of particles cannot be influenced by the user. The wall loss rate of organic vapors (SOA_gas) is determined by their saturation concentration and the equivalent wall organic aerosol. A test example for a chamber experiment simulation is given in section 5.2.

4.3 Multiphase chemistry of fog or cloud

Multiphase chemistry can also be simulated with the MAFOR model. This simulation considers chemistry in the gas phase and in the aqueous phase of droplets with diameter >1 μm. Fog or cloud events can be prescribed during the simulation in order to simulate a cycle of subsequent dry air and fog or cloud periods. The aerosol processes can also be considered in a multiphase chemistry simulation but this has not been tested thoroughly until now. The set of input files for a multiphase chemistry simulation is:

Gas phase:	inchem.dat
Aerosol:	inaero.dat
Organic:	organic.dat
General:	ingeod.dat
Dry deposition	dispers.dat
Configuration:	sensitiv.dat
Aqueous phase	inaqchem.dat

Option 1: Prescribed fog or cloud

The following entries in ingeod.dat are relevant for the multiphase chemistry simulation: incloud, RH, lwcm and pH. For the hours of the simulation with fog or cloud (line with incloud=1) a droplet distribution in the CS mode will be calculated based on the liquid water content provided in the column lwcm (and the geometric mean diameter of the CS mode) and the pH of the droplets in the CS mode will be set to the value provided in the column pH. The RH value has to be between 0.991 and 1.000. The number of CS mode droplets is calculated based on lwcm. Aqueous phase chemistry will be calculated in the CS mode if aqueous phase partitioning and chemistry is on. Time dependent concentrations of the aqueous phase compounds in the CS droplet mode will be calculated and written to the output in concout.res. The liquid water content of the CS mode is written to the last column of concout.res.

The input file inaqchem.dat is read by the program if the aqueous chemistry switch is set to 1. The entries in inaqchem.dat will be used to initialize the aqueous phase composition in the droplets of the coarse (CS) mode if the simulation starts with fog or cloud (incloud=1 in ingeod.dat).

If incloud=0 follows the lines with incloud=1 in ingeod.dat then the fog evaporates and all droplets disappear, all dissolved gases will evaporate and the ionic compounds will remain stored in a “virtual” aqueous phase. The in-cloud produced mass of sulfate, MSAp, ammonium, and organic acids is added to the reconstructed coarse particle mode after cloud evaporation.

a) Simulation without aerosol processes during cloud:
In sensitiv.dat all switches in the first and third line should be set to 0. In the second line only the chemistry integration should be 1. In the fourth line all the switches for partitioning to aqueous phase and for aqueous phase chemistry should be 1.

b) Simulation with aerosol processes during cloud:
In sensitiv.dat all switches for aerosol processes can be activated to enable cloud microphysical processes. If the coagulation option 1 is used then interstitial aerosol scavenging of small particles by collision with the droplets in CS mode occurs. In the fourth line all the switches for partitioning to aqueous phase and for aqueous phase chemistry should be 1.

A test example for multiphase chemistry of a fog cycle is given in section 5.4.

Option 2: Cloud formation model

The cloud processing is enabled during one hour if the cloud switch is on (switch incloud=2 in ingeod.dat). RH is set to 98% at the beginning of the cloud formation in the program. A cloud or fog cycle for the current hour and the aerosol particles are activated along a temperature profile similar to that in Pandis et al. (1990a, Fig. 1 therein). Air entrainment into the cloud is not considered. The cloud formation model is used to simulate the cloud droplet spectrum for the air of the entire box volume cooling adiabatically for a specified updraft speed. The particles of a certain size bin are described as droplets when either the supersaturation of the environment exceeds their critical supersaturation or their diameter exceeds the critical diameter. When both of these criteria are not met, the particles will be referred to as interstitial aerosol.

The life cycle of the fog or cloud is divided into three periods: 1) the conditioning period, when relative humidity rises from the initial value to saturation, 2) the rapid growth period once RH exceeds the critical RH, and 3) the dissipation period when RH decreases below saturation. In the conditioning period, gas-phase chemistry and aerosol dynamics processes continue as in the situation without cloud. At the end of the conditioning period, partitioning of gases to droplets and aqueous phase chemistry begins. In the rapid growth period, droplets grow unstably resulting in the creation of a fog or cloud with considerable liquid water content. Aerosol operators are switched off during that period and the cloud droplet microphysics operator takes over. In the dissipation period, droplets evaporate and shrink to the size of wet particles.

Figure 4.1 shows the temperature profile and typical liquid water content in Aitken mode (blue), Accumulation mode (black) and coarse mode (red) during a cloud or fog cycle. The amplitude of the temperature profile can be controlled by the updraft velocity.

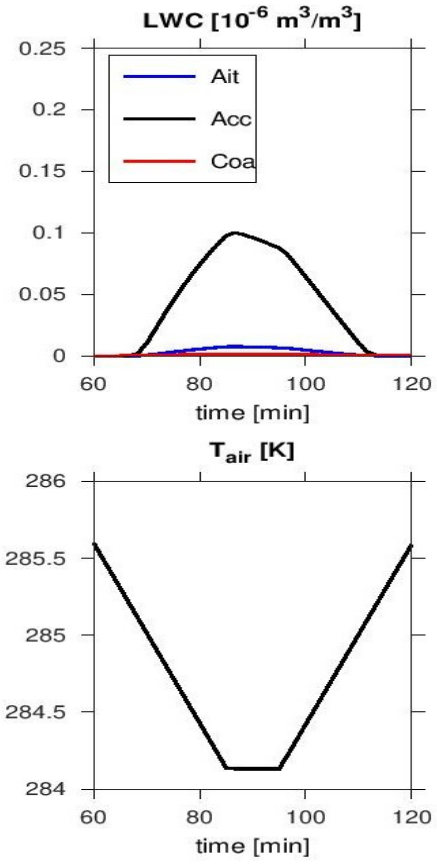

Figure 4.1 Temperature profile and liquid water content during a cloud/fog cycle.

The condensation and evaporation of water follows the description of Pruppacher and Klett (1997), with the kinetic factor, the modified diffusion coefficient for water vapor and the modified diffusion coefficient of air calculated according to Abdul-Razzak et al. (1998) and Seinfeld and Pandis (2006). The radiation heating or cooling of droplets is considered. The Köhler theory is used to relate the aerosol size distribution and composition to the number of activated particles as a function of maximum supersaturation. The fraction of activated particles in terms of total number and mass concentration is written to the output file total_n.res. Equilibrium supersaturation is modeled using Köhler theory, with the Kelvin effect and the Raoult effect calculated according to Abdul-Razzak and Ghan (2000). However, instead of the hygroscopicity parameter, the dynamically calculated species concentrations in the liquid droplet are used. The effect of partly dissociated soluble gases and slightly soluble matter due to the explicit computation of aqueous phase concentrations in the droplet modes is also considered. The Kelvin effect considers the surface tension reduction by organic surfactants, i.e. dissolved organic acids in the droplet modes.

In the fourth line of sensitiv.dat, all the switches for partitioning to aqueous phase and for aqueous phase chemistry should be 1. The partitioning of gases to the droplets of AI, AS and CS modes and aqueous phase chemistry in the three bulk modes is considered, given that LWC is higher than $1x10^{-10}$ m^3/m^3, and aqueous phase reactions will cause the transformation of the dissolved gases and ions. In dispers.dat, the value of the updraft velocity (7th line, first entry) determines the cooling rate and controls the supersaturation of the environment. The liquid water content and the pH in the respective droplet modes are calculated dynamically and cannot be prescribed to the simulation.

Processes of droplet microphysics operator during the cloud cycle are activated by setting the flag of the corresponding aerosol process in sensitiv.dat to 1. The following cloud processes are implemented:

1) Collision / coalescence of particles and droplets) by Brownian diffusion. The collection kernel describes the interaction of two colliding particles and/or droplets. The collision partners are assumed to fall with their terminal velocities. The smaller collision partner will be collected by the larger collision partner as soon as it is inside the swept volume of the collector. The collection kernel for collision / coalescence of droplets and/or particles in cloud or fog is active when the coagulation option is 1 in sensitiv.dat.

2) Interstitial scavenging of aerosol particles: removal of interstitial (non-activated) particles by larger droplets through Brownian diffusion. Enabled with coagulation option 1.

3) In-cloud condensation. The mass increase of activated aerosols by the uptake of water-soluble chemical species and by chemical reactions within the droplets is calculated dynamically. This may result in the change of mass concentrations of sulfate, MSA, nitrate, ammonium, amines, chloride, iodate, and organics. The mass transfer rate of a species from the gas phase to the aqueous droplet is translated to condensation fluxes that move particles between the size sections of the particle distribution. Enabled with condensation option 1.

4) Gravitational settling of droplets. Enabled with deposition option 1.

4.4 Plume dispersion

The processes during the dilution of a plume from a industrial or traffic source are of great interest and therefore the possibility to perform a simulation of plume dispersion (along a x-axis) was implemented in MAFOR. The set of input files for a boundary layer simulation is:

Gas phase:	inchem.dat
Aerosol:	inaero.dat
Background aerosol	inbgair.dat
Organic:	organic.dat
General:	ingeod.dat
Dilution	dispers.dat
Configuration:	sensitiv.dat

The presumed situation is the dilution of an aerosol or gas mixture present close to an emission source (emission and the early stage of the plume is not implemented in MAFOR) with increasing time (distance along the x-axis), by entrainment of background air.

MAFOR offers four types of dilution parameterizations which assume a circular cross-section of the plume, in the following termed “Plume dispersion Type 1”, “Plume dispersion Type 2”, “Plume dispersion Type 3”, and “Plume dispersion Type 4”. When choosing the dilution options 1 or 2, a model time step of t = 0.1 s will be automatically applied. When choosing the dilution options 3 or 4, a model time step of t = 0.01 s will be automatically applied. The latter will increase the run time of the simulation. Calculations with option 3 and 4 are limited to 60 s and 120 s simulation time, respectively. Option 1 and 2 gives output every second while option 3 and 4 gives output every 0.1 s.

Further, MAFOR offers three types of dilution parameterizations which assume a semi-elliptic cross-section of the plume, in the following termed “Plume dispersion Type 5”, “Plume dispersion Type 6”, and “Plume dispersion Type 7”. For options 5-7, a model time step of t = 0.1 s will be applied and output is given every second. These three types are intended specifically for the dispersion of ship exhaust plumes. In the ship plume study by Karl et al. (2020), the “Plume dispersion Type 1” has been used.

Plume dispersion Type 1

The dilution of the traffic-influenced aerosol by background air was approximated by fitting a power-law function $y = a \cdot x^{-b}$ (where $x = u \cdot t$ with “u” the wind speed and “t” the time); where *a* is “dila” and *b* is “dilcoef” in the input file ingeod.dat. Temperature of the plume decreases correspondingly. The change of plume height with time is calculated according to the plume dispersion equations presented by Pohjola et al. (2003). The dilution switch in sensitiv.dat has to be set to 1 for dispersion Type 1.

Plume dispersion Type 2

The dilution of the traffic-influenced aerosol concentrations by background air was approximated by fitting a power-law function of the form: $y = (t+b)^c$ (with “t” being the time), where *b* is “dil2_b” and *c* is “dil2_c” in the input file organic.dat. Parameter “dil2_c” can take values between 0 and -2. The temperature in the plume is approximated with a separate function of the form: $T_{pl} = d \cdot (t+e)^f + T_{air}$, where *d* is “dil2_d”, *e* is “dil2_e”, and *f* is “dil2_f” in the input file dispers.dat. Values of the Type 2 parameters have to be provided in line 2 of the input file dispers.dat. The change of plume height with time is calculated according to the plume dispersion equations presented by Pohjola et al. (2003). The dilution switch in sensitiv.dat has to be set to 2 for dispersion Type 2.

Plume dispersion Type 3

The dilution of diesel exhaust in a laboratory dilution system with zero air is modelled by the exponential equation $DR(t) = DR\_fin^{1/tau\_c}$, (with "t" being the time) where "DR_fin" is the final dilution rate after the primary diluter (PD) and "tau_c" is the dilution time constant for concentrations, i.e. the time in which the system has achieved the final dilution ratio. The temperature during dilution is assumed to follow Newtonian cooling, with $T_{pl}(t) = T\_fin+(T1-T\_fin) \cdot exp(-t/tau\_d)$, where "T_fin" is the final exhaust temperature after PD and "tau_d" is the dilution time constant for temperature, i.e. the time when the remaining excess temperature is ~37% (=1/e %) of the raw exhaust temperature T1. The value of the raw exhaust temperature is "ta_st" in dispers.dat. Further, "BGH2O" is the background H2O concentration in the diluting air. Values of the Type 3 parameters have to be provided in line 3 of the input file dispers.dat. The dilution switch in sensitiv.dat has to be set to 3 for dispersion Type 3. Type 3 produces output every 0.1 s. Wall loss of H_2SO_4 in the aeging chamber (when time is > tau_d) can be taken into account by setting ICHAM to 2 in sensitiv.dat. The wall of sulphuric acid is treated according to Vouitsis et al. (2005).

Plume dispersion Type 4

Two-component dilution scheme for the dilution of vehicular traffic exhaust between the road edge and ambient air for a street with two line emission sources (air parcel moving over the street and picking up emissions). In the first dilution stage (along the width of the street until kerbside) the dilution function is derived from the jet plume model of Vignati et al. (1999), which considers the entrainment of fresh air due to the jet effect of the exhaust gas. For this model, the initial exhaust gas velocity "u0" and entrainment velocity "sigw" have to be provided in line 4 of the input file dispers.dat. In the second dilution stage, from kerbside to ambient the power-law function (as in Type 1) is used, for which parameter values of "dila" and "dilcoef" have to be provided in ingeod.dat. The remaining parameters describe the geometry of the traffic line sources in the street. One line source represents the vehicular traffic into one direction and can in principle consist of several lanes. The configuration of Type 4 considers two line sources. The geometry parameters are given in line 4 of dispers.dat: the width of line source no. 1 "tend1", the downwind distance of line source no. 2 "tbeg2", and the total width of the street "tend2". The dilution switch in sensitiv.dat has to be set to 4 for dispersion Type 4.

Plume dispersion Type 5

Type 5 represents Gaussian dispersion with a semi-elliptic plume cross section. The dilution rate is given by $\lambda_{dil}(t) = 1/A_{pl} * dA_{pl}/dt$, where A_{pl} is the cross-section area of the plume. The time-dependent plume width and height are described by two power-laws. Type 5 can be used for dispersion scenarios of ship exhaust plumes. The plume dispersion parameters for Type 5 cannot be changed by the user. The dilution switch in sensitiv.dat has to be set to 5 for dispersion Type 5.

Plume dispersion Type 6

Modification of the Gaussian dispersion based on the formulation of Konopka (1995) that consider a horizontal and linear shear flow. Type 5 is recommended for dispersion scenarios of ship exhaust plumes in ports or close to shoreline. The plume dispersion parameters for Type 6 cannot be changed by the user. The dilution switch in sensitiv.dat has to be set to 6 for dispersion Type 6.

Plume dispersion Type 7

Valid for dispersion of ship plumes under convective conditions in the marine boundary layer (open sea) based on the parameterization of dispersion rates by Chosson et al. (2008). The plume dispersion parameters for Type 7 cannot be changed by the user. The dilution switch in sensitiv.dat has to be set to 7 for dispersion Type 7.

General notes:
Currently only dispersion of an (emitted) aerosol, NO, NO_2, SO_2, SO_3, H_2SO_4, NH_3 and the organic vapor compounds in a plume can be simulated. The dilution of other gases is not yet implemented. In the input file sensitiv.dat, the switch for dilution with background particles needs to be set to 1 in order to read the input file inbgair.dat which contains the background aerosol distribution and composition. The gas-phase concentrations in inchem.dat will be used as the initial concentrations inside the plume when the dispersion run is performed.

The gas-phase concentrations of the background air (NO, NO_2, SO_2, O_3, NH_3, H_2SO_4, PIOV, PSOV) have to be given in inbgair.dat. Therefore O_3 concentration in inchem.dat should be zero or a very small value. The background O_3 is now given in inbgair.dat; O_3 will entrain into the plume with increasing time with a plume entrainment rate having the same value as the dilution rate.

In the input file ingeod.dat, the values of the dispersion parameters should be entered in the columns dila and dilcoef. Realistic parameter values of “dila” and “dilcoef” in ingeod.dat have to be provided for Type 1, Type 2 and Type 4.

In the input file dispers.dat, in line 1 the values for hmix_st (initial plume height), dst_st (distance of starting point from source), hsta_st (height of stack above the ground), and ta_st (plume temperature at starting point) need to be entered for all plume dispersion simulations. These values characterize the initial state of the plume and depends on the distance of the starting point location (=station) from the emission source point.

In plume dispersion simulations the box height corresponds to the plume height instead of the boundary layer height (given in ingeod.dat). The height of the box is therefore increased with time and is recalculated every time step. Meteorological data is updated every hour using the values in ingeod.dat.

During plume dispersion runs the output file plume.res contains plume height, temperature, dilution rate and other parameters for plume dispersion. The output of aerosol mass concentrations is written to aerconc.res and the changing SOA distribution is written to soadis.res.

A test example for plume dispersion Type 1 from a traffic-related aerosol is given in section 5.5 . A test example for plume dispersion Type 3 for the evolution of diesel exhaust particles in a laboratory dilution system is given in section 5.3.

4.5 Nucleation

MAFOR can be used with 14 different nucleation mechanisms to simulate new particle formation. Nucleation will be used if the nucleation switch is set to 1. Then one of the nucleation options 1-14 can be selected. The parameterized nucleation schemes have been described in detail by Karl et al. (2012a).

Table 4.1 shows a brief summary of the nucleation options.
Note that the referenced literature must be cited in all publications that use MAFOR with the corresponding nucleation option.

Table 4.1 Nucleation options in the MAFOR model.

Option no.	Nucleation mechanism	Reference (must be cited)
1	kinetic H_2SO_4	Kulmala et al., 2006
2	homogeneous H_2SO_4-H_2O	Vehkamäki et al., 2002 Vehkamäki et al., 2003
3	homogeneous H_2SO_4-H_2O-NH_3	Merikanto et al., 2007 Merikanto et al., 2009
4	homogeneous & ion-mediated H_2SO_4-H_2O-NH_3	Yu et al., 2018 Yu et al., 2020
5	activation H_2SO_4	Kulmala et al., 2006
6	kinetic HNO_3-AMINE	Karl et al., 2012b
7	combination H_2SO_4 (activation & ion-mediated)	Karl et al., 2011 Karl et al., 2012a
8	"OS1" activ H_2SO_4-ORG	Karl et al., 2012a
9	"OS2" kinet H_2SO_4-ORG	Karl et al., 2012a
10	"OS3" total H_2SO_4-ORG	Karl et al., 2012a
11	neutral & ion-induced H_2SO_4-H_2O	Määttänen et al., 2018a,b
12	diesel H_2SO_4-ORG	Pirjola et al., 2015
13	ACDC, H_2SO_4-H_2O-NH_3	Henschel et al. (2016) Baranizadeh et al. (2016)
14	activation HIO_3	Kulmala et al. (2006) Vuollekoski et al. (2009)
15	Neutral & ion-induced HIO_3 nucleation	Zhao et al. (2024)

The nucleation rate calculated by the following nucleation mechanisms can be scaled by a value provided in column fnuc in ingeod.dat: activation H2SO4 (option 5), combination (option 7) and “OS3” (option 10). If it is not desired to scale the nucleation rate, the values in column fnuc should be set to 1.

The organic compound that is involved in the nucleation options 8-10 (“OS1”, “OS2, and “OS3”) and 12 is SOA-2 (see section 2.7; in the above list denoted as “ORG”). The gas phase concentration of SOA-2 is initialized in inchem.dat. Currently it is not possible to fix SOA-2 gas phase concentration at a constant value. SOA-2 is formed by chemical reactions. Examples are: reaction of amines with OH radical, reaction of isoprene peroxy radicals with HO2 and NO, TMB + OH, APIN + O3, reaction of monoterpene peroxy radical with HO2 and NO.

The ion-mediated binary nucleation (option 4) based on the look-up table parameterization of Yu (2010) has been replaced in v2.0 by the more recent look-up table version for ion-mediated ternary nucleation, short TIMN (Yu et al., 2018; Yu et al., 2020). TIMN includes ternary nucleation of H2SO4-NH3-H2O and binary homogeneous nucleation. This option provides the calculation of the nucleation rate due to ion-mediated nucleation based on the look-up table program by Yu et al. (2020) as function of temperature, relative humidity, sulfuric acid concentration, and ammonia concentration, while the ionization rate is set to 2.4 ion pairs cm^{-3} s^{-1} and surface area of aerosol is set to 10 µm m^{-2}. For sulfuric acid concentration $<5x10^5$ molecules cm^{-3}, the steady state assumption given by Karl et al. (2011) is used.

Nucleation of sulfuric acid/iodic acid clusters (option 14) assumes sulfuric acid induced activation, according to a parametrization for OIO nucleation in Vuollekoski et al. (2009). Nucleated clusters are inserted at 1.5 nm diameter in size.

4.6 Secondary organic aerosol

Nine SOA compounds are available in the MAFOR model to represent the different categories, volatility and formation routes of secondary organic aerosol. Biogenic secondary oxidized vapors are represented by BSOV (semi-volatile), BLOV (low-volatile) and BELV (extremely low-volatile). Aromatic secondary oxidized vapors are represented by ASOV (semi-volatile), ALOV (low-volatile) and AELV (extremely low-volatile). Primary emitted organic vapors, such as long-chained n-alkanes are represented by PIOV (intermediate volatility), PSOV (semi-volatile) and PELV (extremely low-volatile). All SOA compounds are represented by a gas phase component and a particle phase component.

The initial gas phase concentrations of the SOA gas phase components are entered in inchem.dat. Vapor concentrations of BSOV ("COV", SOA-1) can be prescribed to the simulation in ingeod.dat when the switch read SOA-1 in sensitiv.dat is set to 1.

By default, the molecular stoichiometric yield of BSOV (SOA-1) is set to 0.40 for its formation in chemical reaction while it is zero for all other SOA compounds. The default molar yield of BLOV (SOA-2) and BELV (SOA-3) are set to 0. The yields of BSOV and BLOV in the photo-oxidation of terpenes can be changed by the user in chamber simulations (in incham.dat), but not in other types of model simulations.

Table 4.2 gives an overview of the molar yields used in SOA forming reactions of biogenic VOC and aromatic VOC in the MAFOR model.

Table 4.2 SOA formation reactions: molar yields of SOA precursors in the MAFOR model. ELV - extremely low volatile vapor (BELV or ALV), LV – low volatile vapor (BLOV or ALOV), SV – semi-volatile vapor (BSOV or ASOV). Molar yields adopted from: Tsimpidi et al. (2010), Ceulemans et al. (2012) and Couvidat et al. (2012).

Reaction type →	**VOC + Ox**			**RO2 + NO**		**RO2 + HO2**	
SOA forming system	**ELV**	**LV**	**SV**	**LV**	**SV**	**LV**	**SV**
Isoprene + OH	0	0	0	0.003	0.101	0.024	0.119
Terpene + OH	0	0	0	0.052	0.184	0*	0.40*
Terpene + O3	0.07 **	0.13 **	0	0.052	0.184	0*	0.40*
Toluene + OH	0.04	0	0	0.097	0.748	0.780	0
Xylene + OH	0	0.063	0.424	0	0	0	0
TMB + OH	0	0.04	0	0	0	0	0

* Molar yield can be defined by the model user in chamber simulations (incham.dat).
** Only in reactions alpha-pinene + O3 and beta-pinene + O3.
Terpene: alpha-pinene (APINENE), beta-pinene (BPINENE), camphene (CAMPHENE), carene (CARENE), sabinene (SABINENE).
Aromatics: toluene (TOLUENE), xylene (LXYL), trimethylbenzene (LTMB).

The yields of SOA-1 and SOA-2 can be changed by the user in the input file incham.dat (for chamber simulations) in the following reactions (see section 4.2):

- Reactions of amines with the OH radical: MMA + OH, MEA + OH, DMA + OH, CH2NH3 + OH, TMA + OH
- For alpha-pinene (APIN), beta-pinene (BPIN), camphene (CAMPHENE), carene (CARENE), and sabinene (SABINENE) in the reaction of monoterpene peroxy radicals with HO2.

The primary emitted organic vapors (PIOV, PSOV, PELV) are not formed in any chemical reaction. However, they are inter-converted by oxidative aging, oligomerization and fragmentation.

The chemical properties of the condensable organic vapors are defined in the input file organic.dat. They can be changed according to the vapor properties that shall be used in the simulation. The default values of the nine SOA components are listed in Table 4.3.

The particle density of the organic aerosol can be changed in organic.dat. The default value is 1570 kg m^{-3}.

Table 4.3 Properties of organic components in the MAFOR model. ΔHvap is the enthalpy of vaporization, C^0 is the saturation concentration over the pure liquid and p_s^0 is the vapor pressure of the pure liquid.

SOA component	**Name in inchem.dat**	**Number carbon atoms (nC) ***	**Number oxygen atoms (nO) ***	**ΔHvap * [kJ mol^{-1}]**	**C^0 (298 K) * [μg m^{-3}]**	**p_L^0 (298 K) ** [Pa]**	**Reference ΔHvap**
SOA-1	KPP_BSOV	10	2.5	50	2.1	$3.06 \cdot 10^{-5}$	Couvidat et al. (2012)
SOA-2	KPP_BLOV	10	2.5	50	0.03	$4.37 \cdot 10^{-7}$	Couvidat et al. (2012)
SOA-3	KPP_BELV	20	7	50	0.0001	$9.0 \cdot 10^{-10}$	Couvidat et al. (2012)
SOA-4	KPP_ASOV	7	2	50	1.0	$1.8 \cdot 10^{-5}$	Couvidat et al. (2012)
SOA-5	KPP_ALOV	7	2	50	0.01	$2.0 \cdot 10^{-7}$	Couvidat et al. (2012)
SOA-6	KPP_AELV	14	8	50	0.0001	$9.0 \cdot 10^{-10}$	Couvidat et al. (2012)
SOA-7	KPP_PIOV	21	0	108	100	$8.05 \cdot 10^{-4}$	Chickos and Wilson (1997)
SOA-8	KPP_PSOV	26	0	135	0.6	$3.80 \cdot 10^{-6}$	Chickos and Wilson (1997)
SOA-9	KPP_PELV	34	0	177	0.0002	$9.97 \cdot 10^{-10}$	Chickos and Wilson (1997)

* Values can be changed by the model user.

** Vapor pressure of the pure liquid calculated based on the given value of C^0.

Enthalpy of vaporization:

The temperature dependence of the saturation concentration C^0 is calculated in MAFOR based on the Clausius-Clapeyron equation, using the value of the enthalpy of vaporization provided by the model user in organic.dat. Default values of $\Delta Hvap = 50$ kJ mol^{-1} for the biogenic and aromatic organic vapors can be used (or replaced by a more appropriate value). For the primary emitted (carbon-chain like) vapors, it is recommended to calculate ithe enthalpy of vaporization by the formula given by Chickos and Wilson (1997): $\Delta Hvap$ (kJ mol^{-1}) = 5.43·nC – 3.3.

Initial mole fractions in the organic aerosol:

The initial organic aerosol (mass component OC in input file inaero.dat) has to be speciated in the input file organic.dat. The mole fraction of the SOA compounds (gamma-oc) in each mode has to be entered in organic.dat. The respective mole fractions should add up to 1 for each mode.

Nucleation involving organic vapors:

BLOV (SOA-2) can be used as nucleating component when setting nucleation options 8, 9, 10, or 12 (see section 2.7).

Plume simulations:

In plume simulations, the SOA gas phase components are diluted with the same rate as the aerosol components.

SOA partitioning:

Three different theoretical approaches are offered to simulate SOA concentrations: **1)** by explicitly calculating the condensation/evaporation driving force, which is the difference between the species concentration in the bulk gas and the concentration just above the particle surface (Jacobson, 1997), **2)** by a hybrid approach of condensation / evaporation and the absorptive partitioning into an organic liquid according to Kerminen et al. (2000), and **3)** by extension of the hybrid approach to also consider the physical adsorption of organics to the surfaces of primary particles (dust and soot) according to Pankow (1994). The first approach is the default, for the second the SOA-partition option in sensitiv.dat has to be set to 1 and for the third the SOA-partition option in sensitiv.dat has to be set to 2. It is noted that the third approach is still under development and should only be used for testing.

4.7 Condensation of sulfuric acid, methane sulfonic acid and iodic acid

Relevant property data of sulfuric acid (H_2SO_4), methane sulfonic acid (MSA, CH_3SO_3H), and iodic acid (HIO_3) for condensation is compiled in Table 4.4.

Table 4.4 Relevant physicochemical properties of H2SO4, MSA and iodic acid in the MAFOR model.

Comp.	Name in inchem. dat	MW (g mol^{-1})	Density of pure liquid (kg m^{-3})	Surface tension (kg s^{-2})	Acc. coeff.	Sat. Vapour pressure p_s^0 (Pa) at 280 K	Ref. p_s
H2SO4	KPP_ H2SO4	98.08	1851	0.052	0.5	6.5x10^{-4} (at X_a=0.9)	Bolsaitis and Elliott (1990)
MSA	KPP_ CH3SO3H	96.11	1507	0.053	0.13	1.5x10^{-2} *	Kreidenweis and Seinfeld (1988)
HIO3	---	175.91	4629	0.052	0.5	2.2x10^{-9}	EPISuite predicted

* If temperature > T_{trans}, then MSA is treated as ELVOC with saturation vapor pressure of 1x10^{-11} Pa. T_{trans} = 252 – 0.691*RH + 0.0349*RH^2 – 5.6x10^4*RH^3 + 3.32x10^6*RH^4 (Hodshire et al., 2019).

The saturation vapor pressure of sulfuric acid over particles, p_s^0, is calculated as function of temperature and of the mole fraction of H_2SO_4 (X_a). The data by Bolsaitis and Elliott was fit with a multiple regression plot to derive an expression for the dependency, see Figure 4.2.

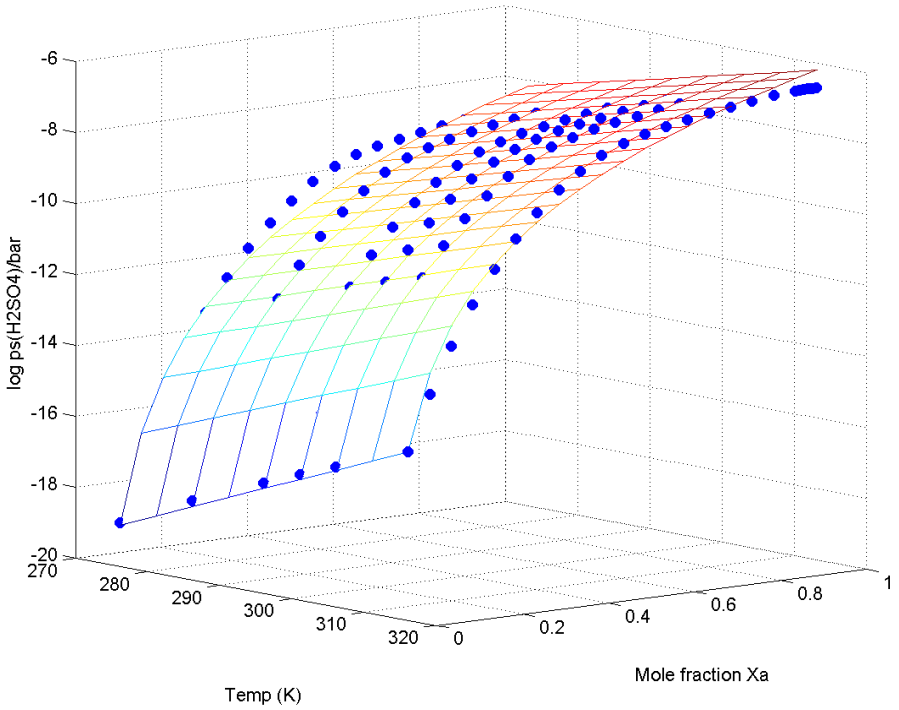

Figure 4.2 Multiple regression plot for sulfuric acid saturation vapor pressure (as log(H_2SO_4/bar)).

To correct the condensation flux of H2SO4, MSA, and HIO3 by the Kelvin effect, set option "Kelvin effect considered" to 1 in file "sensitiv.dat".

4.8 Coagulation

Particle coagulation is a process in which smaller particles collide with each other and coalesce completely to form larger particles. A semi-implicit solution is applied to coagulation (Jacobson, 2005a). The semi-implicit solution yields an immediate volume-conserving solution for coagulation with any time step. Brownian coagulation coefficients Ki,j between particles in size bin i and j are calculated according to Fuchs (1964) assuming spherical particles. If colliding particles result in a particle that has exactly the same size as particles in size bin i, the particle is attributed to bin i, and the number concentration of bin i increases. In all other cases, particles are redistributed among the nearest size bins according to the resulting particle's volume. When coagulation option 2 is chosen, the effect of the fractal geometry of soot particles on coagulation is taken into account by considering the effect on radius, diffusion coefficient and the Knudsen number in the Brownian collision kernel. It is assumed that the collision radius is equal to the fractal (outer) radius of the aggregate of primary spherules (with radius rs). The fractal parameters, rs = 13.5 nm and the fractal dimension Df = 1.7, were adopted from Jacobson and Seinfeld (2004). These parameters can be changed by the model user in organic.dat.

Van der Waals forces and viscous interactions can affect the coagulation rate of small particles. It has been shown that Van-der-Waals forces can enhance the coagulation rate of particles with diameter < 50 nm by up to a factor of five (Jacobson and Seinfeld, 2004). When coagulation option 3 is used, an empirical enhancement factor, V_E is applied that depends on the value of the particle pair Knudsen number (Karl et al., 2016). When coagulation option 4 is used, an exact solution of the enhancement by van der Waals forces and viscous forces using the interpolation formula for the van der Waals collision kernel between the free-molecular and continuum regimes (Jacobson, 2005a, page 513) is applied. The Hamaker constant of water, $A_H/kT = 20$ is used for all particle types.

When coagulation option 5 is used, both the effect of fractal geometry and the effect of van der Waals/viscous forces (exact solution) are considered. Figure 4.3 illustrates the effect of using the different options on the coagulation rate for the collision with 10-nm particles.

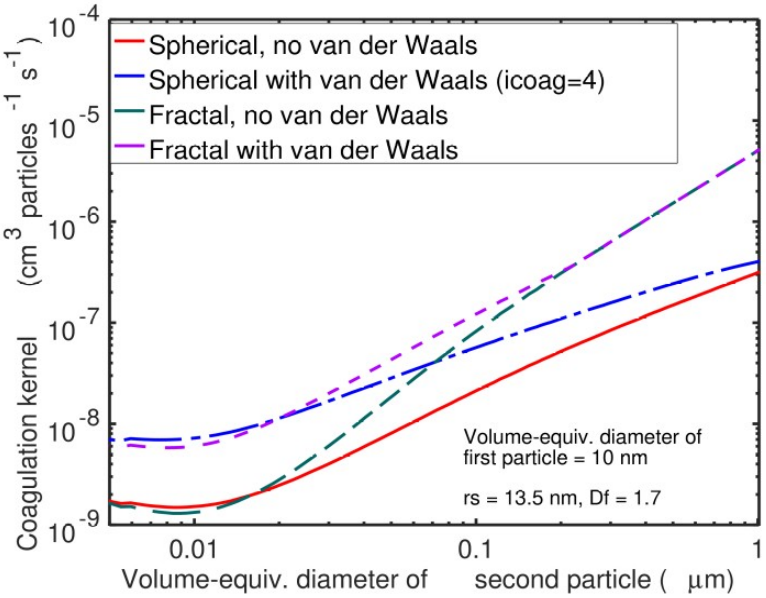

Figure 4.3 Effect of fractal geometry and van der Waals forces when the volume-equivalent diameter is 10 nm and the volume-equivalent diameter of the second particle varies from 5 to 1000 nm. Red line: option 1, blue line: option 4, green line: option 2, purple line: option 5.

4.9 Emission of particles

Continuous emission of a particle size spectrum

Emission of primary particles controlled by input file emitpar.dat. This causes a continuous emission of particles during the simulation. The emitted size spectrum of particles and their chemical composition can be provided per mode (NU, AI, AS, CS) in the input file emitpar.dat. Particle emissions are activated in sensitiv.dat by setting the "emission of particles" option to 1. The source strength of the particles cannot be varied during the simulation. The particle emission rates have to be given in units ng m^{-2} s^{-1}.

Sea-air flux of sea-salt particles

Emission of sea-salt particles (short: sea-salt emission) is implemented using the empirical parameterization of Salter et al. (2015) for the size range of 10 nm to 10 µm. Through the use of air entrainment as a function of wind speed, Salter et al. could scale their laboratory measurements of particle production to wind speed, avoiding the difficulties associated with defining the "white area" of the whitecap in a laboratory setup. The wind speed dependence is described by the dependence of the air entrainment flux into the oceanic water column on the 10 m wind speed. The wind speed dependence of $(u10)^{3.41}$ follows the suggestion in Salter et al. (2015).

Sea-salt emissions depend on wind speed (u10 in m/s, ingeod.dat), sea surface temperature (SST in K) and salinity (SAL in g/kg). The latter two can be set to constant values in dispers.dat. The dependence on salinity is added to the parameterization of Salter et al. by correcting the size of emitted particles by $(SAL/35)^{1/3}$, based on the plots published by Martensson et al. (2003). Figure 4.4 shows the size-dependent sea-salt particle flux dF/dlogDp for different wind speed and SST (for SAL = 35 g/kg).

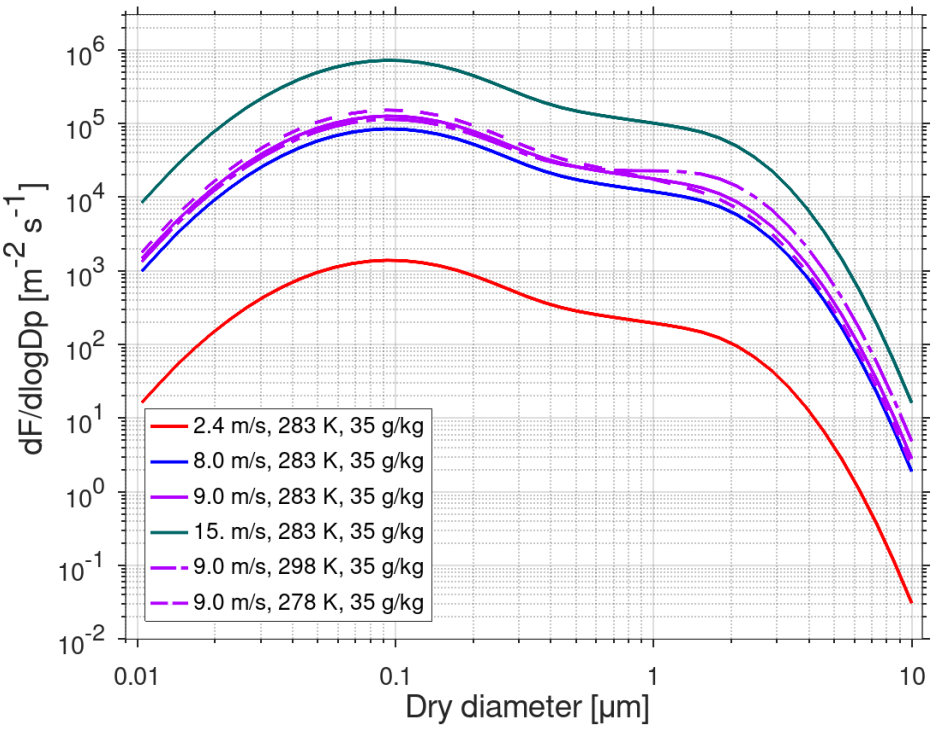

Figure 4.4 Dependence of the sea-salt flux (dF/dlogDp) on wind speed and sea surface temperature with the implemented parameterization by Salter et al. (2015).

Sea-salt emissions are activated in a run by choosing the option 2 for ”emission of particles” in sensitiv.dat. Sea-salt particle emissions are scaled with the open water fraction (owf) that is provided in the input file ingeod.dat.

Continuous emission after cloud

A third option is the continuous particle emission after cloud dissipation. Emission of primary particles controlled by input file emitpar.dat. The emission begins after the end of a cloud phase indicated by the cloud flag in input file ingeod.dat. The emission of sea-salt particles happens simultaneously during the simulation. Thjs type of combined emission is designed for simulation of arctic marine cases. The combined particle emission is activated by choosing the option 3 for ”emission of particles” in sensitiv.dat.

5 Test examples

Four set of test examples including all necessary input files, reference output files and reference plot graphics are available for download and briefly described in this chapter. The reference plots have been generated with GNU Octave v9.2.0. Matlab scripts for plotting graphics are provided in subdirectory “matlab”. The scripts work in Matlab and Octave. When using MATLAB, figure plots have to be saved as *.bmp files instead of *.jpg files. The corresponding line in the plot script has to be changed from:

```
print -djpg '{plot directory}/figureplot.jpg'
```

to:

```
print -dbmp '{plot directory}/figureplot.bmp'
```

MAFOR model output needs to be moved to subdirectory “output” to apply the plot scripts.

5.1 Nucleation event

5.1.1 Description

Simulation of 10 hours at a fixed location in the Arctic Ocean follows an observed new particle formation event with nucleation of new particles and growth by condensation of sulphuric acid, MSA (from oxidation of DMS) and one organic vapor ("COV", BSOV). Model results for the number size distribution are compared to measured data. Number size distribution of particles is plotted 1) as a series of snapshots and 2) as sequential time series (contour plot). Observation data and model simulation (using MAFOR v1.2) for this nucleation event on DOY 209 (Arctic Ocean Expedition in 1996) have been published by Karl et al. (2012a). The model simulation was modified for the test example.

5.1.2 Input

The input file sensitiv.dat for this example is shown below:

sensitiv.dat

```
1  1  1  1  1  1  7  0
2  1  1  0  0  0  1  0
3  1  0  1  1  0  0  0
4  1  0  0
```

In this example, all aerosol processes are switched on; the nucleation option 7 (combination H2SO4) is selected. Condensation of organics and sulphuric compounds is allowed. Chemistry integration switch is on; DMS and SOA-1 concentrations are read from ingeod.dat. Water condensation to particles is on. The debug switch is set to 1 to obtain debugging information in debug.res.

The input file ingeod.dat for this example is shown below:

ingeod.dat

```
1  10 29 7 11 83.46 66.03 272.46 101300. 0.873 60.00 0 2.96 0.00 0.0 1.D09 0.0 1.13D09 40.E+07 7.39D08 0.00 1.50 0.00 7.0 90.0 0.5
2  10 29 7 12 83.46 66.03 272.47 101300. 0.879 60.00 0 2.48 0.00 0.0 1.D09 0.0 1.13D09 40.E+07 1.28D09 0.00 1.50 0.00 7.0 90.0 0.5
3  10 29 7 13 83.46 66.03 272.33 101300. 0.884 60.00 0 2.54 0.00 0.0 1.D09 0.0 1.13D09 40.E+07 4.89D08 0.00 1.50 0.00 7.0 90.0 0.5
4  10 29 7 14 83.46 66.03 272.48 101300. 0.897 60.00 0 2.60 1.00 0.0 1.D09 0.0 1.13D09 40.E+07 3.26D09 0.00 1.50 0.00 7.0 90.0 0.5
5  10 29 7 15 83.46 66.03 272.03 101300. 0.895 60.00 0 2.30 1.00 0.0 1.D09 0.0 1.13D09 40.E+07 3.89D09 0.00 1.50 0.00 7.0 90.0 0.5
6  10 29 7 16 83.46 66.03 271.91 101300. 0.885 60.00 0 2.50 1.00 0.0 1.D09 0.0 1.13D09 40.E+07 3.65D09 0.00 1.50 0.00 7.0 90.0 0.5
7  10 29 7 17 83.46 66.03 271.83 101300. 0.878 60.00 0 2.49 0.70 0.0 1.D09 0.0 1.13D09 40.E+07 1.29D09 0.00 1.50 0.00 7.0 90.0 0.5
8  10 29 7 18 83.46 66.03 271.79 101300. 0.886 60.00 0 2.58 0.60 0.0 1.D09 0.0 1.13D09 40.E+07 0.70D09 0.00 1.50 0.00 7.0 90.0 0.5
9  10 29 7 19 83.46 66.03 271.89 101300. 0.898 60.00 0 2.69 0.50 0.0 1.D09 0.0 1.13D09 40.E+07 0.50D09 0.00 1.50 0.00 7.0 90.0 0.5
10 10 29 7 20 83.46 66.03 275.82 101300. 0.894 60.00 0 2.67 0.40 0.0 1.D09 0.0 1.13D09 40.E+07 2.34D09 0.00 1.50 0.00 7.0 90.0 0.5
```

In column 13 (rain) of ingeod.dat a rain rate between 0.40 and 1.00 mm/h is entered which will cause wet scavenging of particles. The incloud switch is set to zero during the simulation. NH3, DMS, and SOA-1 (vapour) concentrations are prescribed to the run. A constant concentration of 4E+08 (molecules cm^{-3}) of SOA-1 is used during the simulation. The nucleation rate is scaled by a factor (fnuc) of 1.50. Entries in the last four columns are not relevant to the simulation.

The input file dispers.dat is shown below:

dispers.dat

```
1  1.10     12.0     0.25     300.0
2  0.00     -0.4     5.00     0.00    -0.8
3  12.0     300.0    0.03     0.12    1.0E16
4  0.230    0.290    7.00     13.0    22.5
5  1.17     0.001    1.70     51.8
6  0.30     0.003    0.20
7  0.10     275.0    31.0
8
```

Entries in the first four lines are not used in the simulation (input for plume dispersion). The fifth line shows entries for dry deposition of particles over a water surface (section 2.7) which are used when the dry deposition flag in sensitiv.dat is set 1.

5.1.3 Result plots

The plots created with the MATLAB scripts sizedis_arctic.m and profile_arctic.m are shown below.

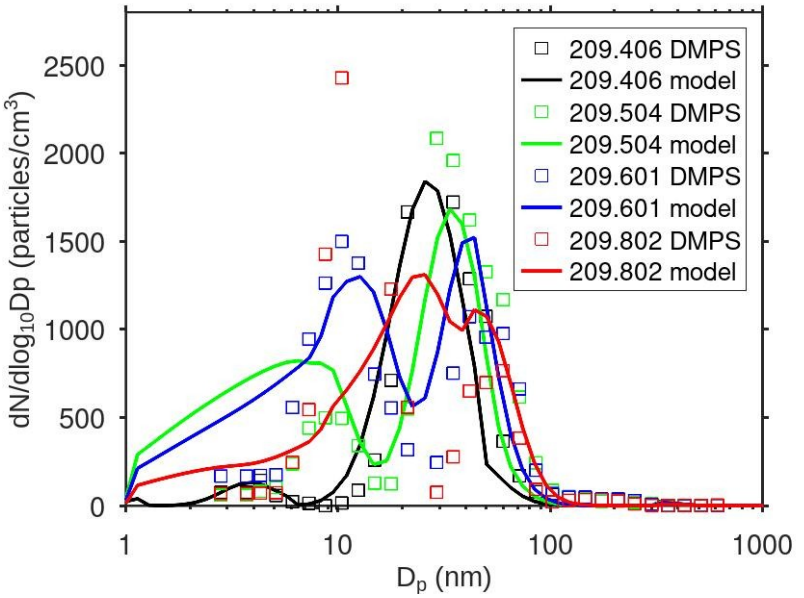

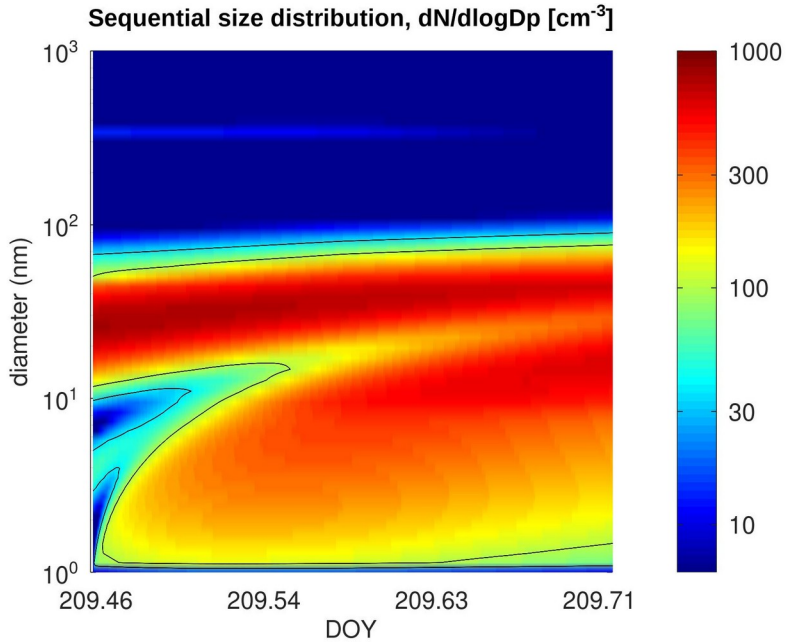

5.2 Chamber experiment

5.2.1 Description

Simulation of 5 hours of a photo-oxidation experiment of a gaseous mixture of monoethanolamine (MEA, 2-aminoethanol) and NO_x in the photoreactor EUPHORE (http://euphore.es) that took place on May 11th, 2009. In the experiment MEA was added into the dark chamber between 07:07 UT and 07:45 UT. At 08:57 UT, NO was injected and at 12:48 the chamber roof was opened. Immediately at 10:52 UT a particle burst was observed. The chamber was closed at 16:39. In the simulation of the experiment nucleation is based on a new HNO_3-amine parameterization (nucleation option 6 in sensitiv.dat), and particle growth by condensation of SOA-1 and SOA-2 and condensation of ethanolaminium nitrate (salt) is enabled. The experiment data and model simulation (using MAFOR v1.0) has been published in the report by Nielsen et al. (2010).

5.2.2 Input

The input file sensitiv.dat for this example is shown below:

sensitiv.dat

```
1   1     0     1     1     1     6     1
2   0     1     1     0     0     1     0
3   0     0     0     1     0     1     0
4   0     0     0
```

Condensation, coagulation and nucleation (nucleation option 6: kinetic HNO3-AMINE) are switched on in sensitiv.dat. Dry deposition is switched on to enable particle loss to the chamber walls. The chamber experiment switch is set to 1 to enable reading of incham.dat (control parameters) and monitor.dat (chamber monitor data). Condensation of organics and amine nitrate is enabled. SOA-1 and SOA-2 form in the reaction of MEA + OH with the molar yields that are specified in incham.dat. Chemistry integration and SOA-partitioning (option 1) switch is on. A dry aerosol is simulated (no condensation of water).

The input file ingeod.dat for this example is shown below:

ingeod.dat

```
1   5  11  5   12.0   39.33  0.27   296.5  101300. 0.03   1.00   0   0.0 0.0 0.0 0.0 0.0 0.0 0.0 0.0 0.0 0.0 1.00   1.00E-11   7.00   86.49   0.92332
2   5  11  5   13.0   39.33  0.27   299.2  101300. 0.06   1.00   0   0.0 0.0 0.0 0.0 0.0 0.0 0.0 0.0 0.0 0.0 1.00   1.00E-11   7.00   86.49   0.92332
3   5  11  5   14.0   39.33  0.27   301.0  101300. 0.03   1.00   0   0.0 0.0 0.0 0.0 0.0 0.0 0.0 0.0 0.0 0.0 1.00   1.00E-11   7.00   86.49   0.92332
4   5  11  5   15.0   39.33  0.27   300.8  101300. 0.03   1.00   0   0.0 0.0 0.0 0.0 0.0 0.0 0.0 0.0 0.0 0.0 1.00   1.00E-11   7.00   86.49   0.92332
5   5  11  5   16.0   39.33  0.27   299.7  101300. 0.03   1.00   0   0.0 0.0 0.0 0.0 0.0 0.0 0.0 0.0 0.0 0.0 1.00   1.00E-11   7.00   86.49   0.92332
```

Most entries of the input file ingeod.dat are set to zero or ignored by the model, except time, geographic position (of the chamber), temperature, pressure and relative humidity.

The input file incham.dat for this example is shown below:

incham.dat

```
1   1        1          8.0E16    10.5       0.33      0.06      1.00
2   3.00    2.0E-26    2.00E-5    7.00E-6    1.15E-5   8.20E-5   3.00E-6
3   7.E-6    177.0     177.0      65.0       130.0     10.0
4
```

First line: from the available amines, MEA is chosen and ozone concentration is read from monitor.dat. HONO chamber source is scaled by factor of 10. Molar stoichiometric yield of SOA-1 is 0.33 and of SOA-2 is 0.06. The rate constant of the reaction MEA + OH is scaled by factor of 3. The dilution rate of gases and particles in the chamber is set to $7x10^6$ s^{-1}. It is referred to section 2.8 for the other entries in incham.dat.

5.2.3 Result plots

The plots created with the MATLAB script monitor_chamber.m are shown below.

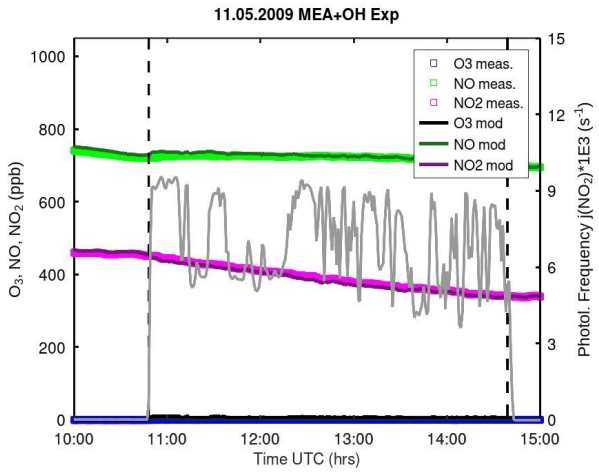

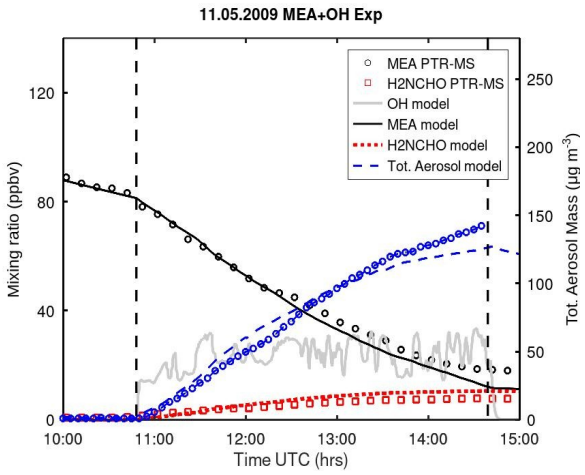

The organic aerosol is plotted with the MATLAB script soadis_chamber.m below on the left side, including concentrations of the SOA components (SOA-1, SOA-2, SOA-3) in the gas phase (color dashed lines) and in the particle phase (color solid lines). The modeled total OC (black dashed line) consists fully of modeled SOA (gray line). After the first hour of the experiment, measured OC mass from the Aerosol Mass Spectrometer (AMS) shows a steeper increase than modeled OC. The sequential particle number distribution created with the MATLAB script profile_chamber.m on the right.

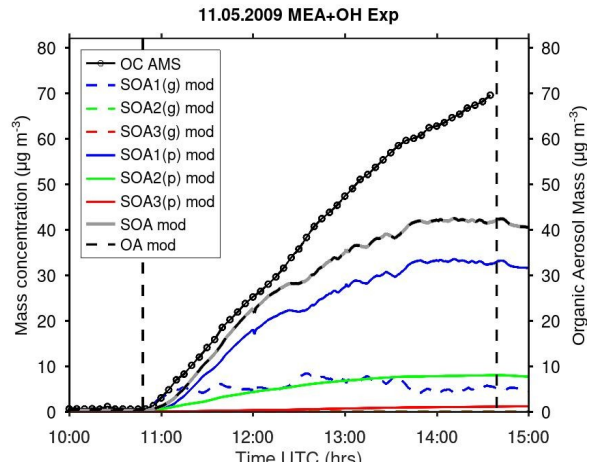

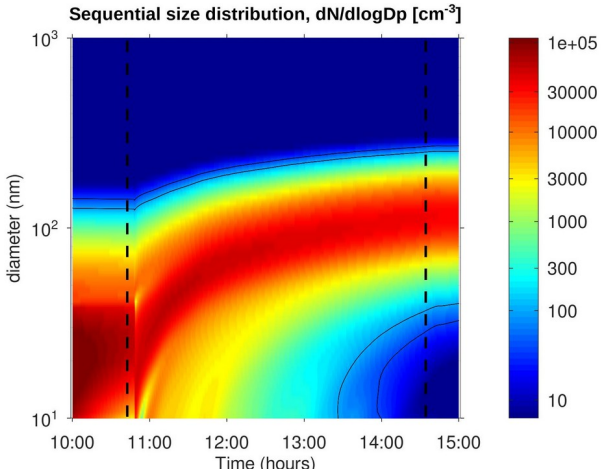

5.3 Diesel exhaust dilution and aging

5.3.1 Description

Simulation of an experimental laboratory system of diesel exhaust dilution and aging for a total duration of 60 seconds. The system consists of a primary diluter with relative humidity close to zero and a dilution ratio of 12; followed by an aging chamber to ensure adequate residence time for the condensational growth of the nucleation mode particles in the cooled and diluted aerosol sample. The initial raw exhaust particle distribution at t = 0.0 s was assumed to be entirely non-hygroscopic. It is divided into the core mode between 5-15 nm consisting of non-volatile organic matter (OM_{nv}) and the soot mode consisting of elemental carbon. The simulations of the diesel exhaust treatment system (using MAFOR v1.8) are published in Pirjola et al. (2015).

5.3.2 Input

The input file sensitiv.dat for this example is shown below:

sensitiv.dat

```
0       0       1       1       1       12      0
2       1       0       0       0       0       1
0       0       0       1       3       0       0
1       0       0
```

Aerosol processes condensation of H_2SO_4 with unity accommodation, organic vapors (SOA-2 [COV_s] and SOA-9 [COV_l]; Kelvin effect taken into account), coagulation, nucleation (option 12, diesel H2SO4-ORG), dilution with particle-free background air and condensation of water are switched on. The wall loss of H_2SO_4 in the aging chamber (chamber option 2) is not activated in this example. Dilution is according to plume type 3. The parameters for this dilution type are in 3rd line of dispers.dat:

dispers.dat

```
0.025   0.00    0.00    697.0
0.00    -0.4    5.00    0.00    -0.8
6.5     300.0   0.03    0.12    1.0E16
0.230   0.290   7.00    13.0    22.5
1.33    0.0013  4.00    121.0
0.01    0.002   0.20
0.1     280.0   33.0
```

The start temperature (ta_st) of the raw exhaust is 697.0 K. The final temperature of the diluted exhaust is 300.0 K. The dilution ends at 0.12 s. (tau_d in line 3). Initial concentrations of H_2SO_4, SOA-2 and SOA-9 are given in inchem.dat. For H_2SO_4 a continuous source from the walls of $1x10^{12}$ molecules cm^{-3} s^{-1} is prescribed.

5.3.3 Result plots

The plots created with the MATLAB scripts sizedis_diesel_wetdp.m and massdis_diesel.m are shown below. Four time steps are plotted in the figures (0.0 s, 0.1 s, 0.9 s, 2.7 s) showing the evolution of the aerosol distribution in terms of particle numbers, particle mass (top panel) and particle mass composition (bottom panel). The particle number distribution is compared to results from a simulation with AEROFOR (e.g. Pirjola, 1999; Pirjola and Kulmala, 2001) and with measured records from SMPS after 2.7 s.

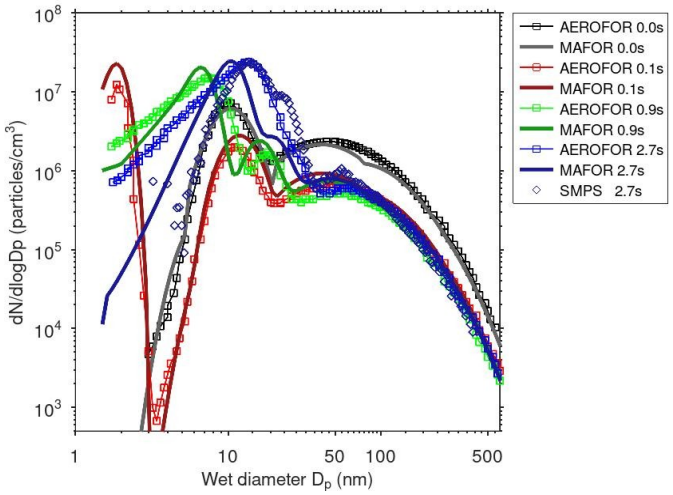
dN/dlogDp (particles/cm3)
Wet diameter Dp (nm)
AEROFOR 0.0s
MAFOR 0.0s
AEROFOR 0.1s
MAFOR 0.1s
AEROFOR 0.9s
MAFOR 0.9s
AEROFOR 2.7s
MAFOR 2.7s
SMPS 2.7s

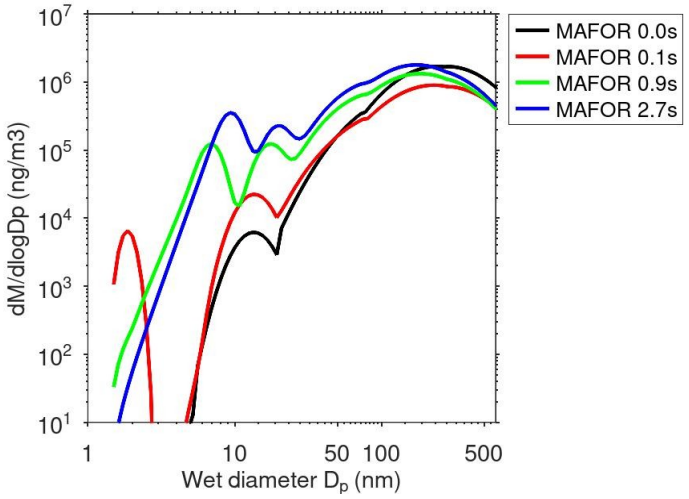
dM/dlogDp (ng/m3)
Wet diameter Dp (nm)
MAFOR 0.0s
MAFOR 0.1s
MAFOR 0.9s
MAFOR 2.7s

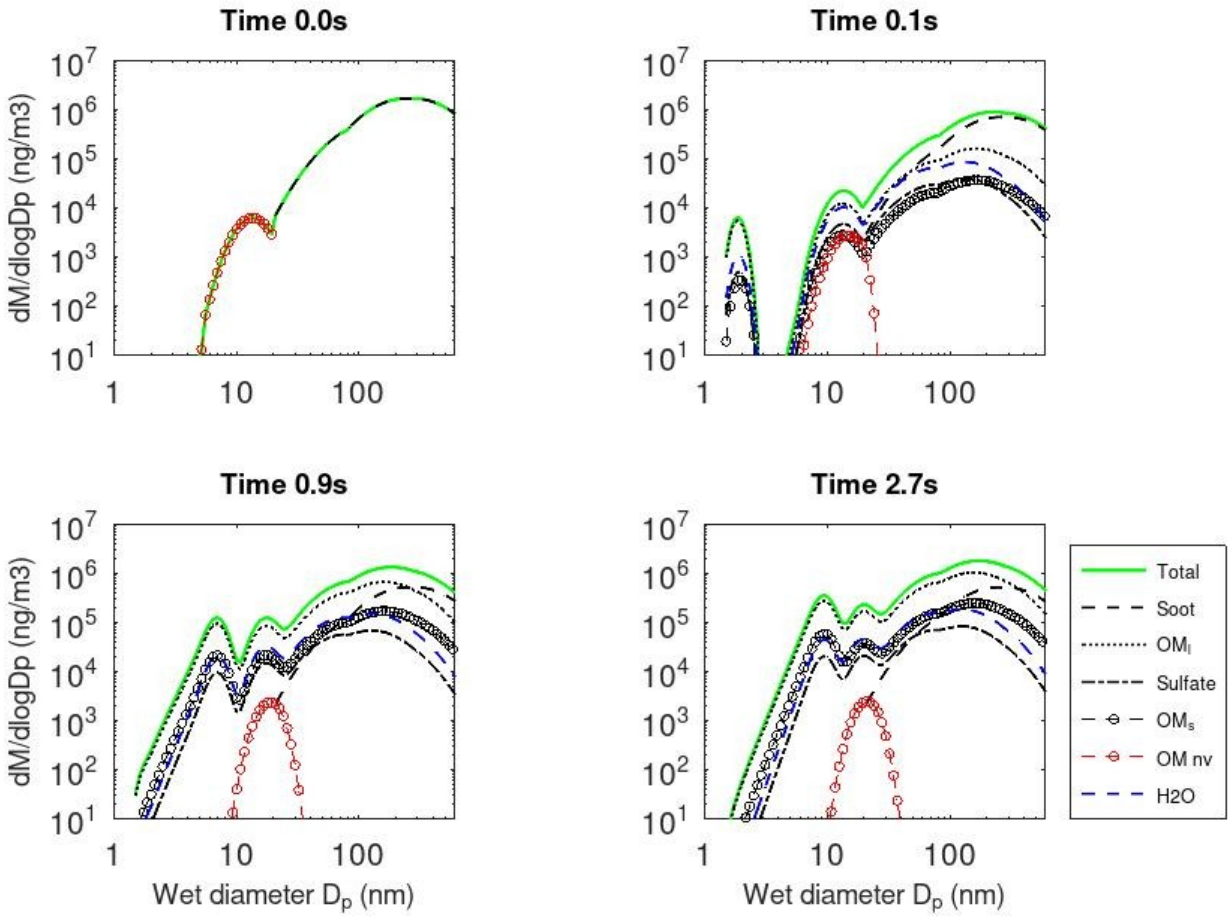
Time 0.0s
Time 0.1s
Time 0.9s
Time 2.7s
dM/dlogDp (ng/m3)
Wet diameter Dp (nm)
Total
Soot
OMl
Sulfate
OMs
OM nv
H2O

5.4 Fog cycle chemistry

5.4.1 Description

Scenario represents typical summertime photochemical and meteorological conditions for a refinery area at the west coast of Norway which is best described as moderately polluted marine boundary layer. The scenario is based on monthly average concentrations of pollutants and other atmospheric constituents. Continuous emission of nitrous acid (HONO) is added and the emission rate is adjusted to produce maximum concentrations of 300 pptv HONO. The simulation time is 72 hours (3 days) with a fog cycle. Each fog event starts at 2 a.m. and ends at 10 a.m. (8 hours). Fog forms at approximately 2 a.m. and fog dissipates at approximately 10 a.m. so that three full fog events are simulated. The simulation starts at 5 a.m. of the first day in a fog period. By doing so, the chemical composition of fog droplets is initialized with the aqueous phase concentrations (in inaqchem.dat). The amplitude of the liquid water content during fog ranges from 9 to 200 mg m^{-3}. The pH value of fog droplets is prescribed to be fixed at 5.1. Continuous emissions of dimethyl sulphide (DMS), dimethylamine (DMA), and a series of VOC (C_2H_6, C_3H_8, C_2H_4, and toluene) are added (in inchem.dat).

5.4.2 Input

The input file sensitiv.dat for this example is shown below:

sensitiv.dat

1	0	0	0	0	0	0	0
2	0	0	0	0	0	1	0
3	0	0	0	1	0	0	0
4	1	1	1				

All aerosol processes are switched off. The switch for chemistry integration, aqueous phase partitioning and aqueous phase chemistry is set to 1. The condensation of water to particles is allowed but this does not affect the water content of coarse mode droplets during fog; instead their water content is calculated based on the prescribed droplet distribution by using the switch incloud=1 in the input file ingeod.dat.

The first lines of the input file ingeod.dat for this example are shown below:

ingeod.dat

1	74	15	6	5	60.48	5.02	285.26	101300	0.991	1000.00	1	5.00	0.00	6.00E+09	0.00	4.00E+09	0.00	0.00	0.00	0.00	1.00	0.00	2.00E-07	5.10	86.49	0.92
2	74	15	6	6	60.48	5.02	285.96	101300	0.991	1000.00	1	5.00	0.00	6.00E+09	0.00	4.00E+09	0.00	0.00	0.00	0.00	1.00	0.00	1.96E-07	5.10	86.49	0.92
3	74	15	6	7	60.48	5.02	285.81	101300	0.991	1000.00	1	5.00	0.00	6.00E+09	0.00	4.00E+09	0.00	0.00	0.00	0.00	1.00	0.00	1.65E-07	5.10	86.49	0.92
4	74	15	6	8	60.48	5.02	286.35	101300	0.991	1000.00	1	5.00	0.00	6.00E+09	0.00	4.00E+09	0.00	0.00	0.00	0.00	1.00	0.00	1.03E-07	5.10	86.49	0.92
5	74	15	6	9	60.48	5.02	286.63	101300	0.991	1000.00	1	5.00	0.00	6.00E+09	0.00	4.00E+09	0.00	0.00	0.00	0.00	1.00	0.00	9.00E-09	5.10	86.49	0.92
6	74	15	6	10	60.48	5.02	286.62	101300	0.755	1000.00	0	5.00	0.00	6.00E+09	0.00	4.00E+09	0.00	0.00	0.00	0.00	1.00	0.00	1.00E-11	5.10	86.49	0.92
7	74	15	6	11	60.48	5.02	286.77	101300	0.748	1000.00	0	5.00	0.00	6.00E+09	0.00	4.00E+09	0.00	0.00	0.00	0.00	1.00	0.00	1.00E-11	5.10	86.49	0.92
8	74	15	6	12	60.48	5.02	286.82	101300	0.741	1000.00	0	5.00	0.00	6.00E+09	0.00	4.00E+09	0.00	0.00	0.00	0.00	1.00	0.00	1.00E-11	5.10	86.49	0.92
9	74	15	6	13	60.48	5.02	287.03	101300	0.735	1000.00	0	5.00	0.00	6.00E+09	0.00	4.00E+09	0.00	0.00	0.00	0.00	1.00	0.00	1.00E-11	5.10	86.49	0.92
10	74	15	6	14	60.48	5.02	287.13	101300	0.726	1000.00	0	5.00	0.00	6.00E+09	0.00	4.00E+09	0.00	0.00	0.00	0.00	1.00	0.00	1.00E-11	5.10	86.49	0.92
11	74	15	6	15	60.48	5.02	287.25	101300	0.724	1000.00	0	5.00	0.00	6.00E+09	0.00	4.00E+09	0.00	0.00	0.00	0.00	1.00	0.00	1.00E-11	5.10	86.49	0.92
12	74	15	6	16	60.48	5.02	287.19	101300	0.715	1000.00	0	5.00	0.00	6.00E+09	0.00	4.00E+09	0.00	0.00	0.00	0.00	1.00	0.00	1.00E-11	5.10	86.49	0.92
13	74	15	6	17	60.48	5.02	287.29	101300	0.723	1000.00	0	5.00	0.00	6.00E+09	0.00	4.00E+09	0.00	0.00	0.00	0.00	1.00	0.00	1.00E-11	5.10	86.49	0.92
14	74	15	6	18	60.48	5.02	287.02	101300	0.741	1000.00	0	5.00	0.00	6.00E+09	0.00	4.00E+09	0.00	0.00	0.00	0.00	1.00	0.00	1.00E-11	5.10	86.49	0.92
15	74	15	6	19	60.48	5.02	286.65	101300	0.760	1000.00	0	5.00	0.00	6.00E+09	0.00	4.00E+09	0.00	0.00	0.00	0.00	1.00	0.00	1.00E-11	5.10	86.49	0.92
16	74	15	6	20	60.48	5.02	286.37	101300	0.771	1000.00	0	5.00	0.00	6.00E+09	0.00	4.00E+09	0.00	0.00	0.00	0.00	1.00	0.00	1.00E-11	5.10	86.49	0.92
17	74	15	6	21	60.48	5.02	285.97	101300	0.797	1000.00	0	5.00	0.00	6.00E+09	0.00	4.00E+09	0.00	0.00	0.00	0.00	1.00	0.00	1.00E-11	5.10	86.49	0.92
18	74	15	6	22	60.48	5.02	285.90	101300	0.811	1000.00	0	5.00	0.00	6.00E+09	0.00	4.00E+09	0.00	0.00	0.00	0.00	1.00	0.00	1.00E-11	5.10	86.49	0.92
19	74	15	6	23	60.48	5.02	285.58	101300	0.807	1000.00	0	5.00	0.00	6.00E+09	0.00	4.00E+09	0.00	0.00	0.00	0.00	1.00	0.00	1.00E-11	5.10	86.49	0.92
20	74	16	6	00	60.48	5.02	285.47	101300	0.821	1000.00	0	5.00	0.00	6.00E+09	0.00	4.00E+09	0.00	0.00	0.00	0.00	1.00	0.00	1.00E-11	5.10	86.49	0.92
21	74	16	6	01	60.48	5.02	285.26	101300	0.832	1000.00	0	5.00	0.00	6.00E+09	0.00	4.00E+09	0.00	0.00	0.00	0.00	1.00	0.00	1.00E-11	5.10	86.49	0.92
22	74	16	6	02	60.48	5.02	285.16	101300	0.991	1000.00	1	5.00	0.00	6.00E+09	0.00	4.00E+09	0.00	0.00	0.00	0.00	1.00	0.00	9.00E-09	5.10	86.49	0.92
23	74	16	6	03	60.48	5.02	285.14	101300	0.991	1000.00	1	5.00	0.00	6.00E+09	0.00	4.00E+09	0.00	0.00	0.00	0.00	1.00	0.00	1.03E-07	5.10	86.49	0.92
24	74	16	6	04	60.48	5.02	285.34	101300	0.991	1000.00	1	5.00	0.00	6.00E+09	0.00	4.00E+09	0.00	0.00	0.00	0.00	1.00	0.00	1.65E-07	5.10	86.49	0.92
25	74	16	6	05	60.48	5.02	285.26	101300	0.991	1000.00	1	5.00	0.00	6.00E+09	0.00	4.00E+09	0.00	0.00	0.00	0.00	1.00	0.00	2.00E-07	5.10	86.49	0.92
26	74	16	6	06	60.48	5.02	285.96	101300	0.991	1000.00	1	5.00	0.00	6.00E+09	0.00	4.00E+09	0.00	0.00	0.00	0.00	1.00	0.00	1.96E-07	5.10	86.49	0.92
27	74	16	6	07	60.48	5.02	285.81	101300	0.991	1000.00	1	5.00	0.00	6.00E+09	0.00	4.00E+09	0.00	0.00	0.00	0.00	1.00	0.00	1.65E-07	5.10	86.49	0.92
28	74	16	6	08	60.48	5.02	286.35	101300	0.991	1000.00	1	5.00	0.00	6.00E+09	0.00	4.00E+09	0.00	0.00	0.00	0.00	1.00	0.00	1.03E-07	5.10	86.49	0.92
29	74	16	6	09	60.48	5.02	286.63	101300	0.991	1000.00	1	5.00	0.00	6.00E+09	0.00	4.00E+09	0.00	0.00	0.00	0.00	1.00	0.00	9.00E-09	5.10	86.49	0.92
30	74	16	6	10	60.48	5.02	286.62	101300	0.755	1000.00	0	5.00	0.00	6.00E+09	0.00	4.00E+09	0.00	0.00	0.00	0.00	1.00	0.00	1.00E-11	5.10	86.49	0.92

The fog periods during the simulation are triggered by the setting the switch incloud (column 11) to 1 in the input file ingeod.dat. For the input lines with incloud=1, the lwcm in column 23 and the pH in column 24 will be read by the model and used to calculate the coarse mode droplet distribution. Emissions of DMS (edms, column 14) and emissions of H2O2 (eh2o2, column 16) are read by the model. A line with incloud=0 following a line with incloud=1 has the effect to trigger the

immediate evaporation of fog water (no droplets remain) and gases that are dissolved in fog droplets.

5.4.3 Result plots

The plots created with the MATLAB scripts conc_aqchem.m and profile_aqchem.m are shown below. The upper graphic shows aqueous phase concentrations in the droplet mode in the upper panel and gas phase concentrations in air in the lower panel. In the lower graphic, fog periods are visualized as droplet mode peaks (light blue spots) in the sequential size distribution.

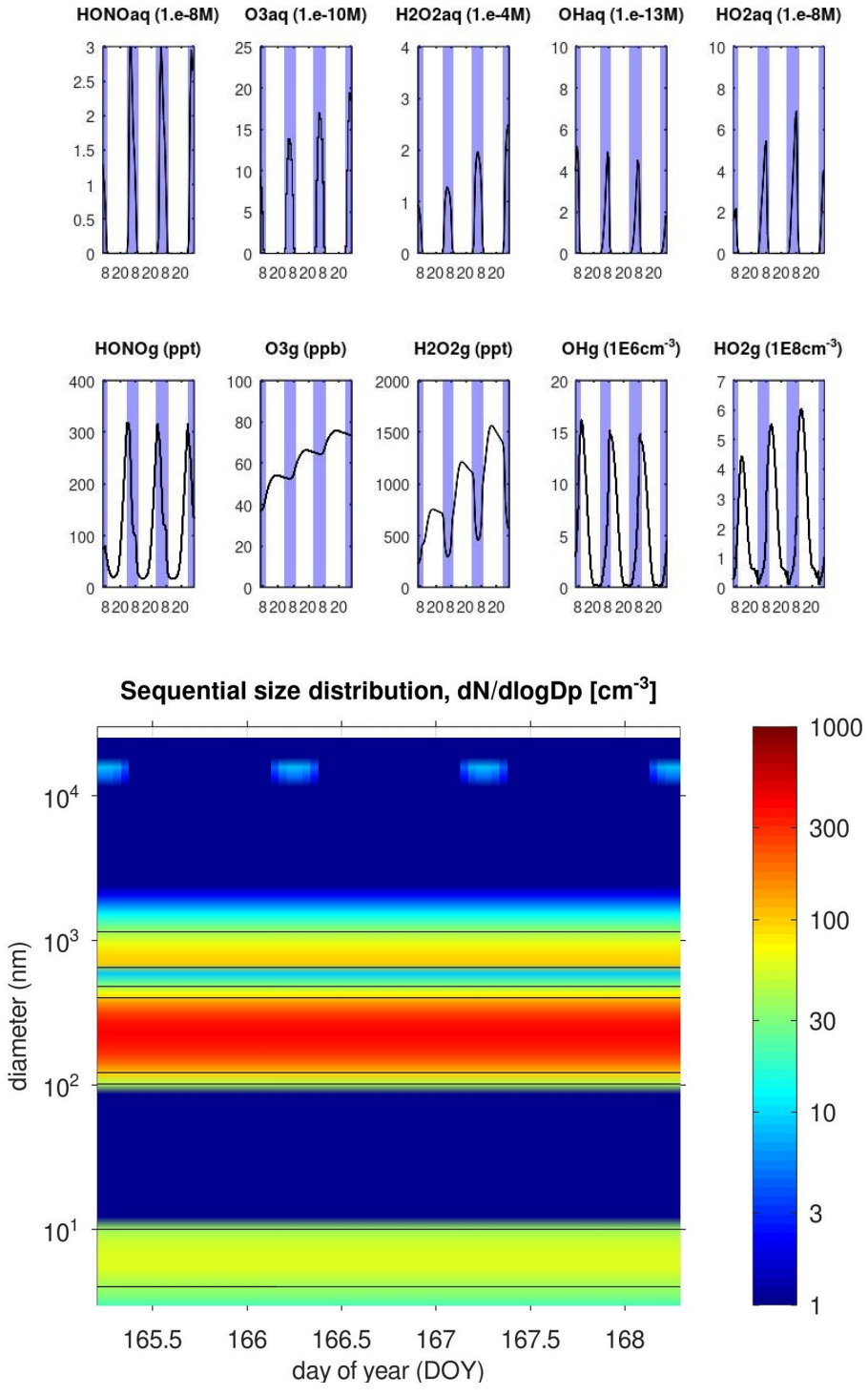

5.5 Traffic plume

5.5.1 Description

In this plume simulation the dispersion of particle downwind of a motorway in the Netherlands are compared to measurements. Aerosol processes considered in the model are condensation/evaporation of n-alkanes, coagulation and dry deposition of particles. Two different n-alkanes, C22H46 (C22) and C28H58 (C28), were used to represent vehicular exhaust gases with different volatility which can condense onto the particles during their transport away from the road. The dilution of the traffic-influenced aerosol by background air was approximated by fitting a power-law function $y = a \cdot x^{-b}$ (where $x = u \cdot t$ with "u" the wind speed and "t" the time) to the measured EC concentrations with distance to road. The mass concentration as function of distance from the road (increasing simulation time) and the particle number size distributions at different distances from the road are plotted in this example. Monitored data and model simulation (using MAFOR v1.2) have been published by Keuken et al. (2012). The model simulation was modified for the test example.

5.5.2 Input

The input file sensitiv.dat for this example is shown below:

sensitiv.dat

```
2   0   1   1   0   6   0
0   1   0   0   0   0   1
0   0   0   1   1   0   0
1   0   0
```

In this example the aerosol processes coagulation, dry deposition and condensation are switched on. The chemistry integration is switched off. Condensation of organics (here: n-alkanes) is switched on, the Kelvin effect during condensation of n-alkanes is considered (last switch in 2nd line). The debug switch is set to 1 to obtain debugging information in debug.res. The dilution switch is set to 1 in order to enable the plume simulation type 1 and reading of the input file inbgair.dat which contains the background aerosol mass composition and distribution. The condensation of water to particles is allowed during the run. Dry deposition option 2 is used.

The simulation is for 1 hour and therefore ingeod.dat has only one line. In column 24 and 25, the dilution parameters are provided. Entries in columns 14-23 are ignored.

The input file inaero.dat is shown below:

inaero.dat

```
1.00E-06    24
F   1.00E-08    1.45    0.00E+00    0.0000  0.0000  0.000   0.000   0   0   0   0   0
F   2.50E-08    1.40    6.50E+03    11.55   57.05   5.05    12.20   0   2.55    0   21.60   0
F   4.90E-08    1.50    4.10E+04    417.60  327.64  181.80  435.60  0   91.80   0   345.66  0
F   1.70E-07    1.80    8.70E+03    1600.80 4255.80 696.90  1669.80 0   351.90  0   3324.80 0
F   3.00E-07    1.70    1.70E+02    928.000 3128.000    404.000 968.000 0   204.000 0   1968    400
```

The input file inbgair.dat for the background aerosol looks like this:

inbgair.dat

```
1.0E-08 1.45    0.0000  0.0000  0.000   0.000   0.0 0.0 0.0 0.0 0.0
2.5E-08 1.40    11.55   9.05    5.05    12.20   0.0 2.55    0.0 9.60    0.0
1.3E-07 2.10    417.6   327.6   181.8   435.6   0.0 91.8    0.0 345.6   0.0
1.7E-07 1.80    1600.8  1255.8  696.9   1669.8  0.0 351.9   0.0 1324.8  0.0
3.0E-07 1.70    928.000 728.000 404.000 968.000 0.0 204.000 0.0 768.000 0.0
1.20E+10    4.78E+10    0.00E+00    9.31E+11    1.00E+06    1.00E+05    0.00E+00    0.00E+00
```

In the input file organic.dat the carbon number of the n-alkanes is entered and the initial molar fraction (gamma-oc) of SOA-7 and SOA-8 in the organic aerosol (OC) for the modes NU, AI, AS, CS has to be entered. The start concentration of n-alkane 1 and n-alkane 2 vapour (in molecules cm^{-3}) is entered in inchem.dat (KPP_PIOV, KPP_PSOV). For both species a concentration of $0.75x10^{10}$ molecules cm^{-3} was used in this example.

The input file organic.dat is shown below:

organic.dat

```
1570.   1      0.050
1200.   13.5   1.7
10      2.5     50      2.1
10      2.5     50      0.03
20      7       50      0.0001
7       2       50      1.0
7       2       50      0.01
14      8       50      0.0001
22      0      113      34.1
28      0      145      0.074
34      0      177      0.0002
0.00        0.00        0.00        0.00        0.00
0.00        0.00        0.00        0.00        0.00
0.00        0.00        0.00        0.00        0.00
0.00        0.00        0.00        0.00        0.00
0.00        0.00        0.00        0.00        0.00
0.00        0.00        0.00        0.00        0.00
0.00        0.00        0.00        0.00        0.00
1.00        1.00        1.00        1.00        1.00
0.00        0.00        0.00        0.00        0.00
0.90
```

The input file dispers.dat is shown below:

dispers.dat

```
1.10        12.0        0.25        300.0
0.00        -0.4        5.00        0.00    -0.8
12.0        300.0       0.03        0.12    1.0E16
0.230       0.290       7.00        13.0    22.5
1.33        0.0013      4.00        121.0
0.01        0.002       0.20
0.1         280         33.0
```

Entries in the first line characterize the initial conditions of the plume, i.e. the initial mixing height, the distance of the start location from the emission source (motorway), the height of the exhaust pipe above ground, and the initial plume air temperature. The second, third and fourth line contain parameters for Type 2, Type 3 and Type 4 dilution which are ignored in this run. The Fourth and fifth line show entries for dry deposition of particles onto the road surface (section 2.7).

5.5.3 Result plots

The plots created with the MATLAB scripts aermass_plume.m are shown on the next page. The upper left plot displays the particle mass concentrations as function of time and the upper right plot shows the modelled and measured number concentrations in different distances to road relative to the roadside concentration.

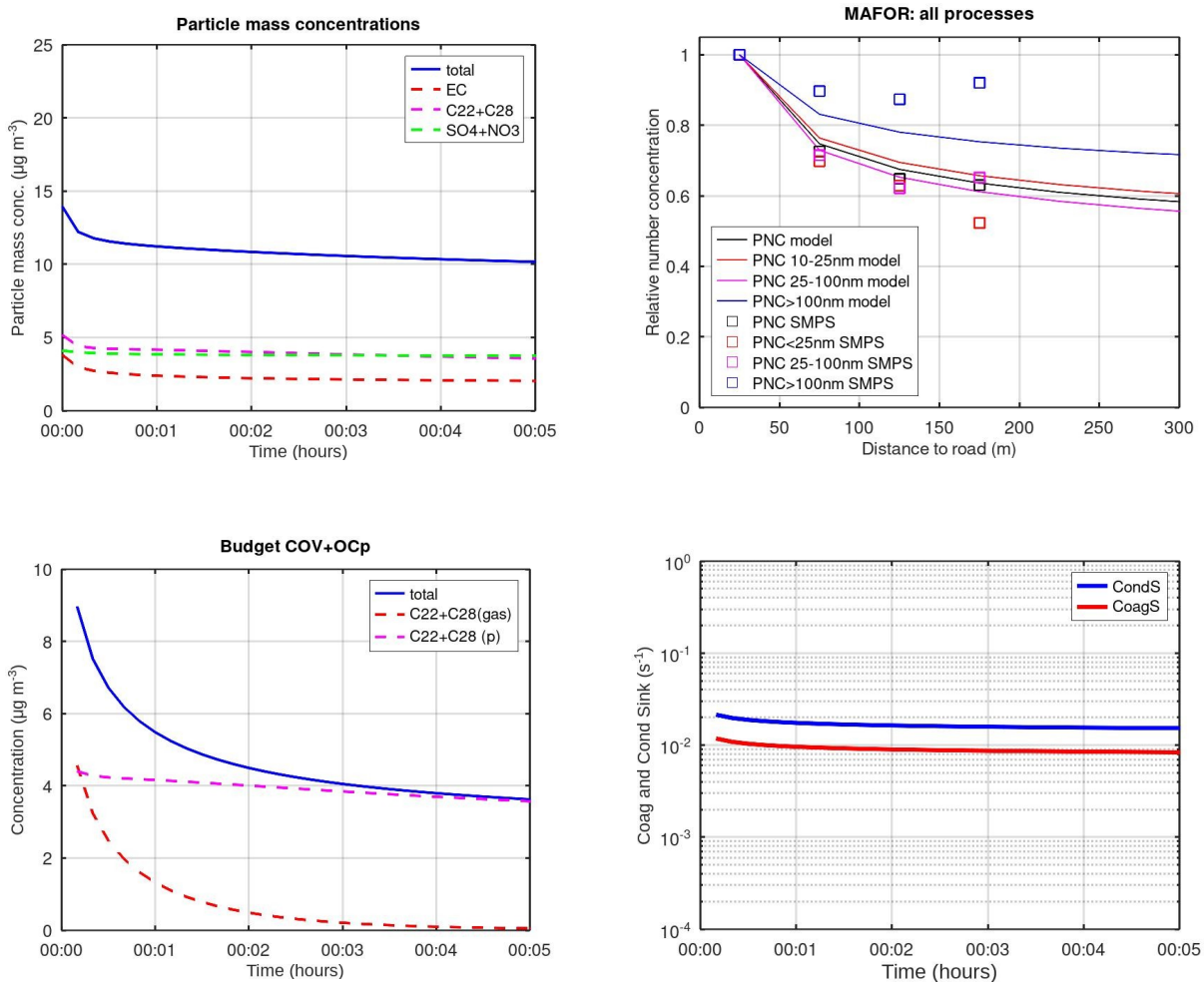

The lower left plot displays the budget of OC in gas phase and particle phase and the lower right plot displays the coagulation sink (red line) and condensation sink (blue line) with increasing time (corresponds to distance from road). The number size distribution plot (left) and the mass size distribution plot (right) created with the MATLAB scripts sizedis_plume.m is shown below.

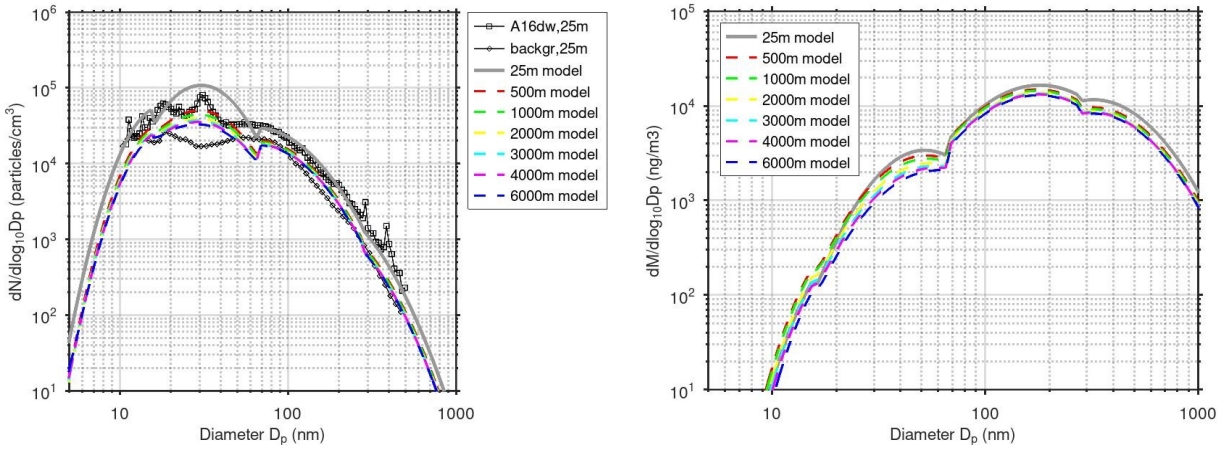

5.6 Ammonium nitrate aerosol

5.6.1 Description

In this scenario, the formation of ammonium nitrate particles is simulated for the conditions at the regional background station Cabauw in the Netherlands with emissions of ammonia from agriculture and NO_X from local traffic and long-range transport. Chemical composition of $PM_{2.5}$ in Cabauw, as in the BOP report ["Composition and origin of Particulate Matter in the Netherlands" [Schaap, M., Weijers, E.P., Mooibroek, D., Nguyen, L., Hoogerbrugge, R. (2010)] was used to derive mass fraction of aerosol components. The average size distribution data for 2011, provided by M.P. Keuken, was fitted using the derived mass fractions. The simulation time is 10 hours on a summer day. Typical values are used as initial concentrations of relevant gases. Initial NH_3 and HNO_3 are 1.0×10^{11} cm^{-3} (2.82 µg/m^3) and 2.0×10^{10} cm^{-3} (2.09 µg/m^3), respectively. Emissions of NH_3 and NO_2 are 5.0×10^{10} cm^2 s^{-1} and 5.0×10^{10} cm^2 s^{-1}, respectively. Two simulations are done: one using dynamic condensation/evaporation (ICONW1) and one using in addition dissolutional growth of nitric acid employing the thermodynamic equilibrium solver MESA (ICONW2).

5.6.2 Input

The input file sensitiv.dat for the ICONW1 run is shown below:

sensitiv.dat

```
1  1  1  1  1  0  7  0
2  1  1  0  1  0  1  0
3  0  0  0  1  0  0  0
4  1  0  0
5
```

For ICONW2 run, sensitiv.dat has to be changed as follows:

sensitiv.dat

```
1  1  1  1  1  0  7  0
2  1  1  0  1  0  1  0
3  0  0  0  1  0  0  0
4  2  0  0
5
```

Nucleation is turned off in both simulations. Condensation of sulphate, organics and ammonium is on in both runs. The switch for chemistry integration is set to 1. In ICONW1, the water condensation switch is set to 1 and in ICONW2, this switch is 2 to activate the coupling to MESA. The results from the two runs have to be saved to different sub-folders (named iconw1 and iconw2) of the output folder. Temperature is constant at 290 K and RH is constant at 87% in the input file ingeod.dat,

The first lines of the input file ingeod.dat for this example are shown below:

ingeod.dat

```
1   10 24 8  10 51.9703 4.9262 290.00 101300. 0.870  200.00 0  2.96 0.00 0.0 0.D09  0.0 9.92D09 00.E+07 7.39D08 0.00  3.50 0.00 7.0 90.0  0.5
2   10 24 8  11 51.9703 4.9262 290.00 101300. 0.870  200.00 0  2.48 0.00 0.0 0.D09  0.0 9.92D09 00.E+07 1.28D09 0.00  3.50 0.00 7.0 90.0  0.5
3   10 24 8  12 51.9703 4.9262 290.00 101300. 0.870  200.00 0  2.54 0.00 0.0 0.D09  0.0 9.92D09 00.E+07 4.89D08 0.00  3.50 0.00 7.0 90.0  0.5
4   10 24 8  13 51.9703 4.9262 290.00 101300. 0.870  200.00 0  2.60 0.00 0.0 0.D09  0.0 9.92D09 00.E+07 3.26D09 0.00  3.50 0.00 7.0 90.0  0.5
5   10 24 8  14 51.9703 4.9262 290.00 101300. 0.870  200.00 0  2.30 0.00 0.0 0.D09  0.0 9.92D09 00.E+07 3.89D09 0.00  3.50 0.00 7.0 90.0  0.5
6   10 24 8  15 51.9703 4.9262 290.00 101300. 0.870  200.00 0  2.50 0.00 0.0 0.D09  0.0 9.92D09 00.E+07 3.65D09 0.00  3.50 0.00 7.0 90.0  0.5
7   10 24 8  16 51.9703 4.9262 290.00 101300. 0.870  200.00 0  2.49 0.00 0.0 0.D09  0.0 9.92D09 00.E+07 1.29D09 0.00  3.50 0.00 7.0 90.0  0.5
8   10 24 8  17 51.9703 4.9262 290.00 101300. 0.870  200.00 0  2.58 0.00 0.0 0.D09  0.0 9.92D09 00.E+07 0.70D09 0.00  3.50 0.00 7.0 90.0  0.5
9   10 24 8  18 51.9703 4.9262 290.00 101300. 0.870  200.00 0  2.69 0.00 0.0 0.D09  0.0 9.92D09 00.E+07 0.50D09 0.00  3.50 0.00 7.0 90.0  0.5
10  10 24 8  19 51.9703 4.9262 290.00 101300. 0.870  200.00 0  2.67 0.00 0.0 0.D09  0.0 9.92D09 00.E+07 2.34D09 0.00  3.50 0.00 7.0 90.0  0.5
```

The initial concentration and emission rate of NH3 is provided in the input file inchem.dat. Time-dependent concentrations of ammonia are calculated, which are influenced by condensation and evaporation to/from the particulate phase. The particle size distribution changes dynamically through the simulation

5.6.3 Result plots

The plots created with the MATLAB scripts mesatest_aermass.m, mesatest_sizediswet.m and mesatest_nprofile.m. The concentration time series of the total particle mass and of the various aerosol components are displayed in the upper panel. The decline of NaCl in ICONW2 is due to depletion of chloride in the sea-salt particles (degassing of HCl through displacement by HNO_3). MESA solver recalculates Kp(NH_4NO_3) and the other solution terms of the mixed inorganic aerosol every 90 s, after changes of the number concentration and the composition in each size bin, leading to stepwise increase of nitrate. In ICONW2, the quicker equilibration of ammonia leads to higher final NH_4 concentrations. Less nitrate is formed in the case of growth by dissolution. In the middle panel, the number size distributions are shown at certain times up to 300 minutes after starting with the size distribution fitted to measurements with SMPS. The lower panel, the particle growth during the simulation is visualized as sequential size distribution.

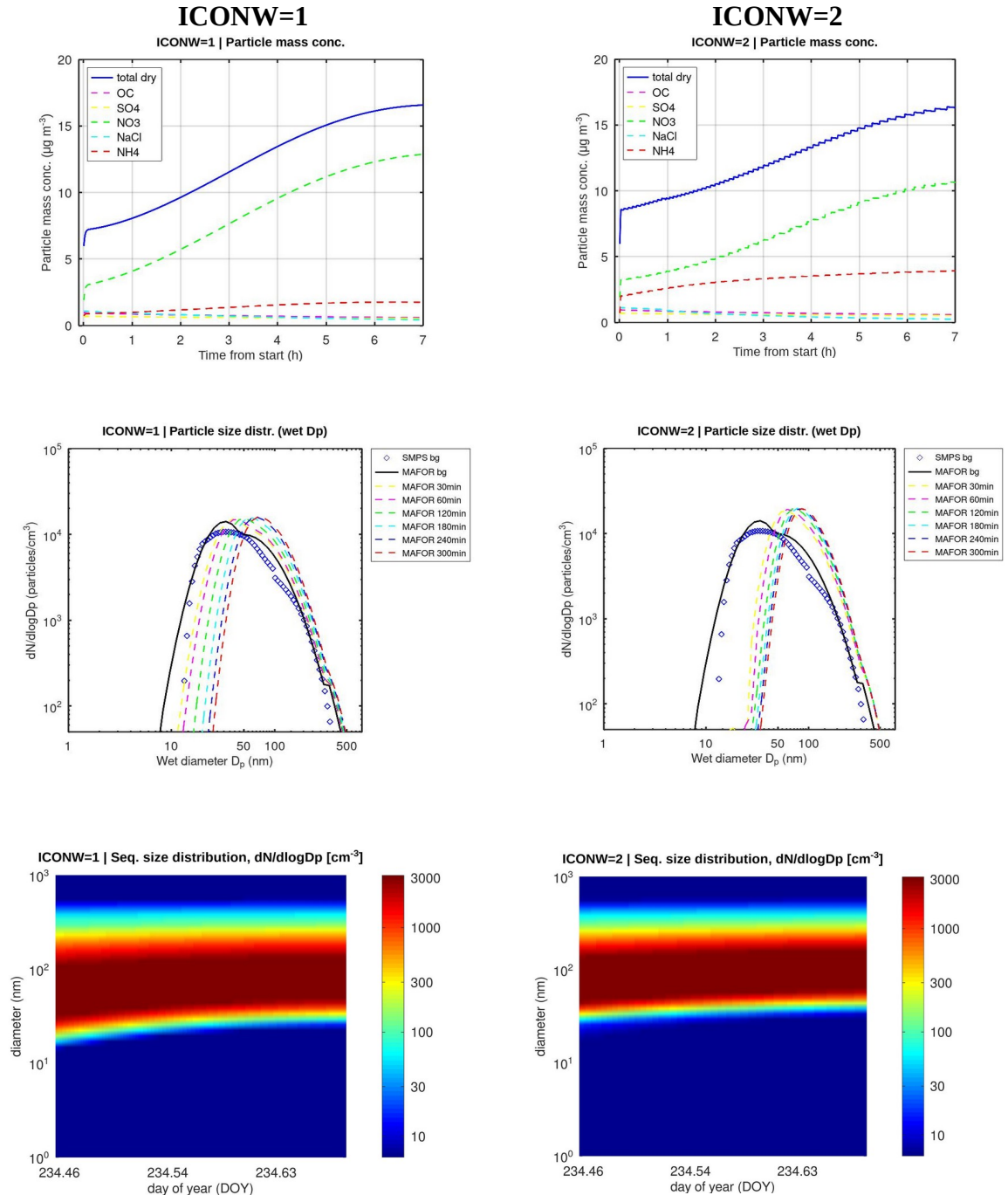

6 References

Abdul-Razzak, H., Ghan, S. J., and C. Rivera-Carpio, A parameterization of aerosol activation, Single aerosol type, J. Geophys. Res., 103, D6, 6123-6131, 1998.

Abdul-Razzak, H. and S. J. Ghan, A parameterization of aerosol activation, 2. Multiple aerosol types, J. Geophys. Res., 105, D5, 6837-6844, 2000.

Baranizadeh, E., Murphy, B. N., Julin, J., Falahat, S., Reddington, C. L., Arola, A., Ahlm, L., Mikkonen, S., Fountoukis, C., Patoulias, D., Minikin, A., Hamburger, T., Laaksonen, A., Pandis, S. N., Vehkamäki, H., Lehtinen, K. E. J., Riipinen, I., Implementation of state-of-the-art ternary new particle formation scheme to the regional chemical transport model PMCAMx-UF in Europe, Geosci. Model Dev., 9, 2741–2754, doi:10.5194/gmd-9-2741-2016, 2016.

Bolsaitis, P. and J. F. Elliott, Thermodynamic Activities and equilibrium partial pressures for aqueous sulfuric acid solutions, J. Phys. Chem. Eng. Data., 35, 69-85, 1990.

Bruggemann, M., Hayeck, N., Bonnineau, C., Pesce, S., Alpert P. A., Perrier, S., Zuth, C., Hoffmann, T., Chen, J., and George, C., Interfacial photochemistry of biogenic surfactants: a major source of abiotic volatile organic compounds, Faraday Discuss., 200, 59-74, doi:10.1039/c7fd00022g, 2017.

Ceulemans, K., Compernolle, S. and J.-F. Müller, Parameterising secondary organic aerosol from α-pinene using a detailed oxidation and aerosol formation model, Atmos. Chem. Phys., 12, 5343-5366, doi:10.5194/acp-12-5343-2012, 2012.

Chickos, J. S. and J. A. Wilson, Vaporization enthalpies at 298.15 K of the n-alkanes from C_{21} to C_{28} and C_{30}, J. Chem. Eng. Data, 42, 190-197, 1997.

Chosson, F., Paoli, R., and Cuenot, B., Ship plume dispersion rates in convective boundary layers for chemistry models, Atmos. Chem. Phys., 8, 4841-4853, www.atmos-chem-phys.net/8/4841/2008/, 2008.

Couvidat, F., Debry, E., Sartelet, K., and C. Seigneur, A hydrophylic/hydophobic organic (H_2O) aerosol model: Development, evaluation and sensitivity analysis, J. Geophys. Res., 117, D10304, 1-19, doi:10.1029/2011JD017214, 2012

Donahue, N. M., Epstein, S. A., Pandis, S. N., and A. L. Robinson, A two-dimensional volatility basis set: 1. organic-aerosol mixing thermodynamics, Atmos. Chem. Phys., 11, 3303-3318, doi:10.5194/acp-11-3303-2011, 2011.

Fuchs, N. A., The Mechanics of Aerosols, Pergamon, New York, 1964.

Henschel, H., Kurtén, T., and Vehkamäki, H., Computational study on the effect of hydration on new particle formation in the sulfuric acid/ammonia and sulfuric acid/dimethylamine Systems, J. Phys. Chem. A, 120, 1886–1896, doi:10.1021/acs.jpca.5b11366, 2016.

Hodshire, A. L., Campuzano-Jost, P., Kodros, J. K., Croft, B., Nault, B. A., Schroder, J. C., Jimenez, J. L., and Pierce, J. R., The potential role of methanesulfonic acid (MSA) in aerosol formation and growth and the associated radiative forcings, Atmos. Chem. Phys. 19, 3137-3160, doi:10.5194/acp-19-3137-2019, 2019.

Hussein, T., Smolik, J., Kerminen, V. M., and M. Kulmala, Modeling dry deposition of aerosol particles onto rough surfaces, Aerosol Sci. Technol. 46:1, 44-59, 2012.

Jacobson, M. Z., Numerical techniques to solve condensational and dissolutional growth equations when growth is coupled to reversible aqueous reactions. Aerosol Sci. Technol., 27, 491-498, 1997.

Jacobson, M. Z., Analysis of aerosol interactions with numerical techniques for solving coagulation, nucleation, condensation, dissolution, and reversible chemistry among multiple size distributions, J. Geophys. Res., 107(D19), 4366, doi: 10.1029/2011JD002044, 2002.

Jacobson, M. Z., Fundamentals of Atmospheric Modeling, Second Edition, Cambridge University Press, 2005a.

Jacobson, M. Z., A solution to the problem of nonequilibrium acid/base gas-particle transfer at long time step, Aerosol Sci. Technol., 39(2), 92-103, doi:10.1080/027868290904546, 2005b.

Jacobson, M. Z. and Seinfeld, J. H., Evolution of nanoparticle size and mixing state near the point of emissions, Atmos. Environ., 38, 1839-1850, 2004.

Karl, M., Gross, A., Pirjola, L., and C. Leck, A new flexible multicomponent model for the study of aerosol dynamics in the marine boundary layer, Tellus B, 63(5), 1001-1025, doi: 10.1111/j.1600-0889.2011.00562.x, 2011.

Karl, M., Leck, C., Gross, A. and L. Pirjola, A study of new particle formation in the marine boundary layer over the central Arctic Ocean using a flexible multicomponent aerosol dynamic model, Tellus B, 64, 17158, doi: 10.3402/ tellusb.v64i0.17158, 2012a.

Karl, M., Dye, C., Schmidbauer, N., Wisthaler, A., Mikoviny, T., D'Anna, B., Müller, M., Clemente, E., Muñoz, A., Porras, R., Ródenas, M., Vázquez, M. and T. Brauers, Study of OH-initiated degradation of 2-aminoethanol, Atmos. Chem. Phys., 12, 1881-1901, 2012b.

Karl, M., Kukkonen, J., Keuken, M. P., Lutzenkirchen, S., Pirjola, L., and Hussein, T., Modeling and measurements of urban aerosol processes on the neighborhood scale in Rotterdam, Oslo and Helsinki, Atmos. Chem. Phys., 16, 4817-4835, 2016.

Karl, M., Pirjola, L., Karppinen, A., Jalkanen, J.-P., and Ramacher, M. O. P., Kukkonen, J., Modeling of the concentrations of ultrafine particles in the plumes of ships in the vicinity of major harbors, J. Environ. Res. Public Health, 17, 777, 1-24, doi:10.3390/ijerph17030777, 2020.

Kerminen, V.-M., Virkkula, A., Hillamo, R., Wexler, A. S., and M. Kulmala, Secondary organics and atmospheric cloud condensation nuclei production, J. Geophys. Res., 105(D7), 9255-9264, 2000.

Keuken, M., Henzing, J. S., Zandveld, P., van den Elshout, S., and M. Karl, Dispersion of particle numbers and elemental carbon from road traffic, a harbor and an airstrip in the Netherlands, Atmos. Environ., 54, 320-327, 2012c.

Konopka, P., Analytical Gaussian Solutions for Anisotropic Diffusion in a Linear Shear Flow, J. Non-Equilib. Thermodyn., 20, 78-91, 1995.

Kouznetsov, R. and M. Sovief, A methodology for evaluation of vertical dispersion and dry deposition of atmospheric aerosol, J. Geophys. Res., 117, D01202, 1-17, doi:10.1029/2011JD016366, 2012.

Kreidenweis, S. M. and J. H. Seinfeld, Nucleation of sulfuric acid-water and methanesulfonic acid-water solution particles: Implications for the atmospheric chemistry of organosulfur species, Atmos. Environ. 22(2), 283-296, 1998.

Kulmala, M., Lehtinen, K. E. J., and A. Laaksonen, Cluster activation theory as an explanation of the linear dependence between formation rate of 3 nm particles and sulphuric acid concentration, Atmos. Chem. Phys., 6, 787-793, 2006.

Kulmala, M., Kerminen, V.-M., Anttila, T., Laaksonen, A., and C. D. O'Dowd, Organic aerosol formation via sulphate cluster activation, J. Geophys. Res., 109, D04205, doi:10.1029/2003JD003961, 2004.

Leaitch, W. R., Strapp, J. W., and G. A. Isaac, Cloud droplet nucleation and cloud scavenging of aerosol sulphate in polluted atmospheres, Tellus, 38B, 328-344, 1986.

Lehtinen, K. E. J. and M. Kulmala, A model for particle formation and growth in the atmosphere with molecular resolution in size, Atmos. Chem. Phys., 3, 251-257, 2003.

Lemmetty, M., Rönkkö, T., Virtanen, A., Keskinen, J., and L. Pirjola, The effect of sulphur in diesel exhaust aerosol: Models compared with measurements, Aerosol Sci. Technol., 42(11), 916-929, doi:10.1080/02786820802360682, 2008.

Martensson, E. M., Nilsson, E. D., de Leeuw, G., Cohen, L. H., and H.-C. Hansson, Laboratory simulations and parameterization of the primary marine aerosol production, J. Geophys. Res., 108(D9), 4297, doi:10.1029/2002JD002263, 2003.

Merikanto, J., Napari, I., Vehkamäki, H., Anttila, T., and M. Kulmala, New parameterization of sulfuric acid-ammonia-water ternary nucleation rates at tropospheric conditions, J. Geophys. Res., 112, D15207, doi:10.1029/2006JD007977, 2007.

Merikanto, J., Napari, I., Vehkamäki, H., Anttila, T., and M. Kulmala, Correction to "New parameterization of sulfuric acid-ammonia-water ternary nucleation rates at tropospheric conditions", J. Geophys. Res., 114, D09206, doi:10.1029/2009JD012136, 2009.

Määttänen, A., Merikanto, J., Henschel, H., Duplissy, J., Makkonen, R., Ortega, I. K., and H. Vehkamäki, New parameterizations for neutral and ion-induced sulfuric acid-water particle formation in nucleation and kinetic regimes, J. Geophys. Res.: Atmospheres, 123, 1269-1296, doi:10.1002/2017JD027429, 2018a.

Määttänen, A., Merikanto, J., Henschel, H., Duplissy, J., Makkonen, R., Ortega, I. K., and H. Vehkamäki, (2018, April 13). Revised release of a Fortran code including the particle formation parameterizations published in Määttänen et al., JGR D, 2018 (Version v1.0). Journal of Geophysical Research Atmospheres., Zenodo, http://doi.org/10.5281/zenodo.1217782, 2018b.

Nelder, J. A. and Mead, R., The Computer Journal, vol. 7, pp. 308-313.

Nielsen, C. J., D'Anna, B., Dye, C., George, C., Graus, M., Hansel, A., Karl, M., King, S., Musabila, M., Müller, M., Schmidbauer, N., Stenstrøm, Y., and A. Wisthaler, Atmospheric Degradation of Amines. Summary Report: Gas phase oxidation of 2-aminoethanol (MEA). CLIMIT project no. 193438, NILU OR 8/2010, Norwegian Institute for Air Research, Kjeller, Norway, 2010. Available at http://www.nilu.no.

Pandis, S. N., Seinfeld, J. H., and C. Pilinis, Chemical composition differences in fog and cloud droplets of different sizes, Atmos. Environ., 24A(7), 1957-1969, 1990a.

Pankow, J. F., An absorption model of gas/particle partitioning of organic compounds in the atmosphere, Atmos. Environ., 28(2), 185-188, 1994.

Pirjola, L., Effects of the increased UV radiation and biogenic VOC emissions on ultrafine aerosol formation, J. Aerosol. Sci., 30, 355–367, 1999.

Pirjola, L. and Kulmala, M., Development of particle size and composition distribution with a novel aerosol dynamics model, Tellus, 53B, 491-509, 2001.

Pirjola, L., Karl, M., Rönkkö, T., and F. Arnold, Model studies of volatile diesel exhaust particle formation: Organic vapours involved in nucleation and growth?, Atmos. Chem. Phys. Discuss., 2015, 15, 4219-4263, doi:10.5194/acpd-15-4219-2015, 2015.

Pohjola, M., Pirjola, L., Kukkonen, J., and M. Kulmala, Modelling of the influence of aerosol processes for the dispersion of vehicular exhaust plumes in street environment, Atmos. Environ., 37, 339-351, 2003.

Pruppacher, H. R. and J. D. Klett Microphysics of Clouds and Precipitation, Kluwer Academic Publishers, Dordrecht, The Netherlands, 1997.

Sander, R., Kerkweg, A., Jöckel, P., and J. Lelieveld, Technical note: The new comprehensive atmospheric chemistry module MECCA, Atmos. Chem. Phys., 5, 445 – 450, 2005.

Sander, A., Baumgaertner, A., Cabrera-Perez, D., Frank, F., Gromov, S., Grooß, J.-U., Harder, H., Huijnen, V., Jöckel, P., Karydis, V. A., Niemeyer, K. E., Pozzer, A., Riede, H., Schultz, M. G., Taraborrelli, D., and Tauer, S., The community atmospheric chemistry box model CAABA/MECCA-4.0. Geosci. Model Dev., 12, 1365-1385, https://doi.org/10.5194/gmd-12-1365-2019, 2019.

Sandu, A. and R. Sander, Technical note: Simulating chemical systems in Fortran90 and Matlab with the Kinetic PreProcessor KPP-2.1. Atmos. Chem. Phys., 6, 187 – 195, 2006.

Sandu, A., Verwer, J. G., Van Loon, M., Carmichael, G. R., Potra, F. A., Dabdub, D. and J. H. Seinfeld, Benchmarking stiff ODE solvers for atmospheric chemistry problems .1. Implicit vs explicit. Atmospheric Environment, 31, 3151 – 3166, 1997.

Salter, M. D., Zieger, P., Acosta Navarro, J. C., Grythe, H., Kirkevag, A., Riipinen, I., and E. D. Nilsson, An empirically derived inorganic sea spray source function incorporating sea surface temperature. Atmos. Chem. Phys., 15, 11047 – 11066, https://doi.org/10.5194/acp-15-11047-2015, 2015.

Schack, C. J., Jr., S. E. Pratsinis, and S. K. Friedlander, A general correlation for deposition of suspended particles from turbulent gases to completely rough surfaces, Atmospheric Environment, 19(6), 953-960, doi:10.1016/0004-6981(85)90240-9, 1985.

Seinfeld, J. H. and S. N. Pandis, Atmospheric Chemistry and Physics, From Air Pollution to Climate Change, 2nd Edition, John Wiley & Sons, Inc., Hoboken New Jersey, 2006.

Slinn, W. G. N., Precipitation scavenging, In: Atmospheric Sciences and Power Production - 1979, Chap. 11 Divsion of Biomedical Environmental Research, U.S. Department of Energy, Washington, DC, 1983.

Tsimpidi, A. P., Karydis, V. A., Zavala, M., Lei, W., Molina, L., Ulbrich, L. M., Jimenez, J. L., and S. N. Pandis, Evaluation of the volatility basis-set approach for the simulation of organic aerosol formation in the Mexico City metropolitan area, Atmos. Chem. Phys., 10, 525-546, www.atmos-chem-phys.net/10/525/2010/, 2010.

Vehkamäki, H., Kulmala, M., Napari, I., Lehtinen, K. E. J., Timmreck, C., Noppel, M., and A. Laaksonen, An improved parameterization for sulphuric acid-water nucleation rates for tropospheric and stratospheric conditions, J. Geophys. Res., 107, D22, 4622, doi:10.1029/2002JD002184, 2002.

Vehkamäki, H., Kulmala, M., Napari, I., Lehtinen, K. E. J., and M. Noppel, Modelling binary homogeneous nucleation of water – sulfuric acid vapours: Parameterisation for high temperature emissions, Environ. Sci. Technol., 37, 3392-3398, doi:10.1021/es0263442, 2003.

Vignati, E., Berkowicz, R., Palmgren, F., Lyck, E., and Hummelshøj, P., Transformation of size distributions of emitted particles in streets, Sci. Tot. Environ., 235, 37-49, 1999.

Virtanen, A., Ristimäki, J., Marjamäki, M., Vaaraslahti, K., Keskinen, J., and Lappi, M., Effective Density of Diesel Exhaust Particles as a Function of Size, SAE Tech. Pap. Ser. 2002-01-0056, 2002.

Vouitsis, E., Ntziachristos, L., and Samaras, Z.: Modelling of diesel exhaust aerosol during laboratory sampling, Atmos. Environ., 39, 1335-1345, 2005.

Vuollekoski, H., Kerminen, V.-M., Anttila, T., Sihto, S.-L., Vana, M., Ehn, M., Korhonen, H., McFiggans, G., O'Dowd, C. D., and Kulmala, M., Iodine dioxide nucleation simulations in coastal and remote marine environments, J. Geophys. Res., 114, D02206, doi:10.1029/2008JD010713, 2009.

Yu, F., Ion-mediated nucleation in the atmosphere: Key controlling parameters, implications, and look-up table. J. Geophys. Res.,115, D03206, doi:10.1029/2009JD012630, 2010.

Yu, F., Nadykto, A. B., Herb, J., Nazarenko, K. M., and Uvarova, L. A., H2SO4-H2O-NH3 ternary ion-mediated nucleation (TIMN): Kinetic-based model and comparison with CLOUD measurements, Atmos. Chem. Phys., 18, 17451-17474, doi:10.5194/acp-18-17451-2018, 2018.

Yu, F., Nadykto, A. B., Luo, G., and Herb, J., H2SO4-H2O binary and H2SO4-H2O-NH3 ternary homogeneous and ion-mediated nucleation: look-up table version 1.0 for 3-D modeling application, Geosci. Model Dev., 13, 2663-2670, doi:10.5194/gmd-13-2663-2020, 2020.

Zaveri, R. A., Easter, R. C.,and Wexler, A. S., A new method for multicomponent activity coefficients of electrolytes in aqueous atmospheric aerosols, J. Geophys. Res., 110, D02201, doi:10.1029/2004JD004681, 2005a.

Zaveri, R. A., Easter, R. C., and Peter, L. K., A computationally efficient Multicomponent Equilibrium Solver for Aerosols (MESA), J. Geophys. Res., 110, D24203, doi:10.1029/2004JD005618, 2005b.

Zaveri, R. A., Easter, R. C., Fast, J. D., and Peters, L. K.:,Model for Simulating Aerosol Interactions and Chemistry (MOSAIC), J. Geophys. Res., 113, D13204, doi:10.1029/2007JD008782, 2008.

Zhang, L., Gong, S., Padro, J., and Barrie, L.: A size-segregated particle dry deposition scheme for an atmospheric aerosol module, Atmos. Environ., 35, 549–560, doi:10.1016/S1352-2310(00)00326-5, 2001

Zhang, X., Cappa, C. D., Jathar, S. H., McVay, R. C., Ensberg, J. J., Kleeman, M. J., and Seinfeld, J. H.: Influence of vapor wall loss in laboratory chambers on yields of secondary organic aerosol, P. Natl. Acad. Sci. USA, 111, 5802–5807, 2014.

Zhao, B., Donahue, N. D., Zhang, K., Mao, L., Shrivastava, M., Ma, P.-L., Shen, J., Wang, S., Sun, J., Gordon, H., Tang, S., Fast, J., Wang, M., Gao, Y., Yan, C., Singh, B., Li, Z., Huang, L., Lou, S., Lin, G., Wang, H., Jiang, J., Ding, A., Nie, W., Qi, X., Chi, X., and Wang, L.: Global variability in atmospheric new particle formation mechanisms, Nature, 631, 98–125, doi:10.1038/s41586-024-07547-1, 2024.

7 Appendix A: List of species indices

MAFOR v2.2.0 Species	aq. Mode	matlab no
ind_CH2ClI		2
ind_CH2I2		3
ind_I2O2		4
ind_IPN		5
ind_CH3CHOCH3		6
ind_I2O3		7
ind_I2O4		8
ind_INO		9
ind_Nap_a01	a01	10
ind_Nap_a02	a02	11
ind_Nap_a03	a03	12
ind_N2O		13
ind_LNITROGEN		14
ind_LCARBON		15
ind_IPART		16
ind_OCS		17
ind_LSULFUR		18
ind_BELV		19
ind_AELV		20
ind_CH3NO		21
ind_MEANHA		22
ind_HOCH2CH2NO		23
ind_H2NCOCH3		24
ind_TMADF		25
ind_HOCH2CONHCHO		26
ind_CH2CNH2CH3		27
ind_DMCNH		28
ind_H2NCCHOHCH3		29
ind_HNCCH3MOH		30
ind_H2NCCH2MOH		31
ind_HOETNHCH2CHO		32
ind_HOCH2CONETOH		33
ind_AMPOX		34
ind_AMPNA		35
ind_DEANCHO		36
ind_CHEXOL		37
ind_CHEXOOH		38
ind_DEANCOCH2OH		39
ind_CH3SOO2H		40
ind_CH3SO4H		41
ind_DMSO2OOH		42
ind_CH3CHO_a01	a01	43
ind_HO2m_a01	a01	44
ind_IO3m_a01	a01	45
ind_CH3SO3m_a01	a01	46
ind_D1O_a01	a01	47
ind_CH3CO3_a01	a01	48
ind_CH3NHNHCH3_a01	a01	49
ind_NH2C2H4NH2_a01	a01	50
ind_DOCO_a01	a01	51
ind_CH3CHO_a02	a02	52
ind_HO2m_a02	a02	53
ind_IO3m_a02	a02	54
ind_CH3SO3m_a02	a02	55
ind_D1O_a02	a02	56
ind_CH3CO3_a02	a02	57
ind_CH3NHNHCH3_a02	a02	58
ind_NH2C2H4NH2_a02	a02	59
ind_DOCO_a02	a02	60
ind_CH3CHO_a03	a03	61
ind_HO2m_a03	a03	62
ind_IO3m_a03	a03	63
ind_CH3SO3m_a03	a03	64
ind_D1O_a03	a03	65
ind_CH3CO3_a03	a03	66
ind_CH3NHNHCH3_a03	a03	67
ind_NH2C2H4NH2_a03	a03	68
ind_DOCO_a03	a03	69
ind_ROO6R5O2		70
ind_ROO6R3O		71
ind_Cl2O2		72
ind_PIOV		73
ind_PELV		74
ind_PSOV		75
ind_DMOCNH2MOH		76
ind_CHEX		77
ind_CH3SOCH2		78
ind_CH3CO2H_a01	a01	79
ind_DOC_a01	a01	80
ind_CH3CO2H_a02	a02	81
ind_DOC_a02	a02	82
ind_CH3CO2H_a03	a03	83
ind_DOC_a03	a03	84
ind_BIACET		85
ind_NC4H10		86
ind_CPDKETENE		87
ind_NCPDKETENE		88
ind_MNCPDKETENE		89
ind_CH3CCl3		90
ind_CH3SCH2		91
ind_CH3COOm_a01	a01	92
ind_HOOCH2SCO_a01	a01	93
ind_CH3COOm_a02	a02	94
ind_HOOCH2SCO_a02	a02	95
ind_CH3COOm_a03	a03	96
ind_HOOCH2SCO_a03	a03	97
ind_C3H8		98
ind_METACETHO		99
ind_CH3COOHCHCHO		100

a01, a02, a03: Aqueous phase species in Aitken(AI), Accumulation(AS) and Coarse(CS) modes. respectively.

Continued.

ind_HCOCCH3CHOOH		101
ind_IC4H10		102
ind_CO23C4CO3H		103
ind_NMBOBCO		104
ind_PBZQCO		105
ind_PTLQCO		106
ind_NOPINDCO		107
ind_NOPINDOOH		108
ind_OH2MENTHEN6ONE		109
ind_OClO		110
ind_C3H7I		111
ind_NAMP		112
ind_AMPAN		113
ind_CHEXO		114
ind_HSO3		115
ind_DMSO2		116
ind_DMSO2O		117
ind_HOOCH2SOO		118
ind_MSOON		119
ind_MSPN		120
ind_IO_a01	a01	121
ind_ICl2m_a01	a01	122
ind_CH3NCO_a01	a01	123
ind_NCOm_a01	a01	124
ind_C2H4C2O4mm_a01	a01	125
ind_C2H5C2O4m_a01	a01	126
ind_IO_a02	a02	127
ind_ICl2m_a02	a02	128
ind_CH3NCO_a02	a02	129
ind_NCOm_a02	a02	130
ind_C2H4C2O4mm_a02	a02	131
ind_C2H5C2O4m_a02	a02	132
ind_IO_a03	a03	133
ind_ICl2m_a03	a03	134
ind_CH3NCO_a03	a03	135
ind_NCOm_a03	a03	136
ind_C2H4C2O4mm_a03	a03	137
ind_C2H5C2O4m_a03	a03	138
ind_NCO		139
ind_CH3COCOCO2H		140
ind_BZFUCO		141
ind_CO14O3CO2H		142
ind_CO2C4DIAL		143
ind_MALNHYOHCO		144
ind_C1ODC2O2C4OOH		145
ind_ISOPDOH		146
ind_C24O3CCO2H		147
ind_C4CO2DCO3H		148
ind_C5DIALCO		149
ind_MMALANHY		150

ind_LHC4ACCO2H		151
ind_PBZQOOH		152
ind_MCPDKETENE		153
ind_PTLQOOH		154
ind_TOLUENE		155
ind_C8BCCO		156
ind_C8BCOOH		157
ind_NORPINIC		158
ind_NSTYRENOOH		159
ind_PINIC		160
ind_CH3I		161
ind_HIO3		162
ind_HOETNHCHO		163
ind_DMCNH2		164
ind_HOC2H4CO2H		165
ind_AMPNNO2		166
ind_AMPO		167
ind_DEANCH2O2		168
ind_CHEXONE		169
ind_DEANCH2CHO		170
ind_DMSOOH		171
ind_DMSOHOO		172
ind_H2SO4_a01	a01	173
ind_H2NCHO_a01	a01	174
ind_HPMTF_a01	a01	175
ind_MALONAC_a01	a01	176
ind_GLUTARAC_a01	a01	177
ind_NH2CH2p_a01	a01	178
ind_H2SO4_a02	a02	179
ind_H2OH2O		180
ind_H2NCHO_a02	a02	181
ind_HPMTF_a02	a02	182
ind_MALONAC_a02	a02	183
ind_GLUTARAC_a02	a02	184
ind_NH2CH2p_a02	a02	185
ind_H2SO4_a03	a03	186
ind_H2NCHO_a03	a03	187
ind_HPMTF_a03	a03	188
ind_MALONAC_a03	a03	189
ind_GLUTARAC_a03	a03	190
ind_NH2CH2p_a03	a03	191
ind_NC3H7NO3		192
ind_ALOV		193
ind_ASOV		194
ind_C513CO		195
ind_MBOCOCO		196
ind_C4MCONO3OH		197
ind_BUT2OLO		198
ind_LISOPAB		199
ind_LISOPCD		200

a01, a02, a03: Aqueous phase species in Aitken(AI), Accumulation(AS) and Coarse(CS) modes. respectively.

Continued.

ind_C6125CO		201
ind_NO3CH2PAN		202
ind_C109CO		203
ind_ClNO2		204
ind_SO3		205
ind_MEABO		206
ind_TMAO		207
ind_NH4p_a01	a01	208
ind_ClOm_a01	a01	209
ind_FeOHp_a01	a01	210
ind_HOCH2CO2H_a01	a01	211
ind_IPROPOL		212
ind_MGLYOX_a01	a01	213
ind_ADIPAC_a01	a01	214
ind_CH3NH2CH2p_a01	a01	215
ind_NH3CH2CHOHp_a01	a01	216
ind_DMNHCH2p_a01	a01	217
ind_DENHp_a01	a01	218
ind_TENHp_a01	a01	219
ind_NH4p_a02	a02	220
ind_ClOm_a02	a02	221
ind_FeOHp_a02	a02	222
ind_HOCH2CO2H_a02	a02	223
ind_MGLYOX_a02	a02	224
ind_ADIPAC_a02	a02	225
ind_CH3NH2CH2p_a02	a02	226
ind_NH3CH2CHOHp_a02	a02	227
ind_DMNHCH2p_a02	a02	228
ind_DENHp_a02	a02	229
ind_TENHp_a02	a02	230
ind_NH4p_a03	a03	231
ind_ClOm_a03	a03	232
ind_FeOHp_a03	a03	233
ind_HOCH2CO2H_a03	a03	234
ind_MGLYOX_a03	a03	235
ind_ADIPAC_a03	a03	236
ind_CH3NH2CH2p_a03	a03	237
ind_NH3CH2CHOHp_a03	a03	238
ind_DMNHCH2p_a03	a03	239
ind_DENHp_a03	a03	240
ind_TENHp_a03	a03	241
ind_HOCH2OH		242
ind_ETHGLY		243
ind_C512OOH		244
ind_C514OOH		245
ind_CHOC3COOOH		246
ind_ISOPAOH		247
ind_ACCOMECO3H		248
ind_MMALNHYOOH		249
ind_NISOPOOH		250

ind_LMBOABNO3		251
ind_C614CO		252
ind_BZEMUCCO2H		253
ind_BZEMUCCO3H		254
ind_CATEC1OOH		255
ind_NPHEN1OOH		256
ind_C235C6CO3H		257
ind_C6H5CH2OOH		258
ind_C6H5CO3H		259
ind_MCATEC1OOH		260
ind_OXYL1OOH		261
ind_BUTENOL		262
ind_TLEMUCCO2H		263
ind_TLEMUCCO3H		264
ind_NCRES1OOH		265
ind_C721CO3H		266
ind_C812OOH		267
ind_C89OOH		268
ind_C312COCO3H		269
ind_C8BCNO3		270
ind_C811CO3H		271
ind_C85CO3H		272
ind_C97OOH		273
ind_HCOCH2CO2H		274
ind_NORPINENOL		275
ind_C96NO3		276
ind_MENTHEN6ONE		277
ind_PERPINONIC		278
ind_PINALOOH		279
ind_PINENOL		280
ind_HCOCH2CO3H		281
ind_MPROPENOL		282
ind_HNCHCH2OH		283
ind_H2NCH2CO3		284
ind_H2NCOCO3		285
ind_DMNCHOO2		286
ind_DMCOONH2		287
ind_MGLYOAC		288
ind_HOC2H4CO3H		289
ind_CH3SCHO		290
ind_HCl_a01	a01	291
ind_FeOH2Fepppp_a01	a01	292
ind_CH3NHCH2p_a01	a01	293
ind_DMNCH2p_a01	a01	294
ind_DENIMp_a01	a01	295
ind_HCl_a02	a02	296
ind_PROPACID		297
ind_EPXDLCO2H		298
ind_PROPENOL		299
ind_FeOH2Fepppp_a02	a02	300

a01, a02, a03: Aqueous phase species in Aitken(AI), Accumulation(AS) and Coarse(CS) modes. respectively.

Continued.

ind_EPXDLCO3H		301
ind_CH3NHCH2p_a02	a02	302
ind_DMNCH2p_a02	a02	303
ind_DENIMp_a02	a02	304
ind_HCl_a03	a03	305
ind_FeOH2Fepppp_a03	a03	306
ind_CH3NHCH2p_a03	a03	307
ind_DMNCH2p_a03	a03	308
ind_DENIMp_a03	a03	309
ind_NH2OH		310
ind_CN		311
ind_PHCOOH		312
ind_C8BC		313
ind_HOCH2CHNETOH		314
ind_TME		315
ind_FeClp_a01	a01	316
ind_H2NCOCH2OH_a01	a01	317
ind_CH3NHCHO_a01	a01	318
ind_NPROPOL		319
ind_ISOPBOH		320
ind_FeClp_a02	a02	321
ind_H2NCOCH2OH_a02	a02	322
ind_CH3NHCHO_a02	a02	323
ind_FeClp_a03	a03	324
ind_H2NCOCH2OH_a03	a03	325
ind_CH3NHCHO_a03	a03	326
ind_C2H5OH		327
ind_C2H6		328
ind_H		329
ind_TLFUOOH		330
ind_MACO3H		331
ind_C514NO3		332
ind_NC4OHCO3H		333
ind_NTLFUOOH		334
ind_LDISOPACO		335
ind_LHC4ACCO3H		336
ind_LIEPOX		337
ind_CO235C6OOH		338
ind_BZOBIPEROH		339
ind_C5CO2DCO3H		340
ind_MACROH		341
ind_C6H5OOH		342
ind_NBZQOOH		343
ind_C716OOH		344
ind_C721OOH		345
ind_C722OOH		346
ind_TLOBIPEROH		347
ind_C6H5CH2NO3		348
ind_NPTLQOOH		349
ind_C810OOH		350

ind_C813OOH		351
ind_C85OOH		352
ind_C86OOH		353
ind_C413COOOH		354
ind_C89CO2H		355
ind_C89CO3H		356
ind_C96OOH		357
ind_C511OOH		358
ind_C98OOH		359
ind_C44OOH		360
ind_C106OOH		361
ind_RO6R3O2		362
ind_RO6R1NO3		363
ind_ROO6R1NO3		364
ind_LAPINABNO3		365
ind_LNAPINABOOH		366
ind_IPRHOCO3H		367
ind_CH2NH		368
ind_C59OOH		369
ind_H2NCHO2CHO		370
ind_CH3CNH2MOH		371
ind_H2		372
ind_TMEO2		373
ind_TEAO		374
ind_DEANCH2COO2		375
ind_CO2H3CO2H		376
ind_DMSOOO		377
ind_NO4m_a01	a01	378
ind_GLYOX_a01	a01	379
ind_DMNCHO_a01	a01	380
ind_MMNp_a01	a01	381
ind_NH3CH2p_a01	a01	382
ind_BZFUOOH		383
ind_PR2O2HNO3		384
ind_NO4m_a02	a02	385
ind_GLYOX_a02	a02	386
ind_DMNCHO_a02	a02	387
ind_MMNp_a02	a02	388
ind_NH3CH2p_a02	a02	389
ind_MALANHYOOH		390
ind_HCOCOHCO3H		391
ind_NO4m_a03	a03	392
ind_GLYOX_a03	a03	393
ind_MECOACEOOH		394
ind_DMNCHO_a03	a03	395
ind_MMNp_a03	a03	396
ind_NH3CH2p_a03	a03	397
ind_IC3H7NO3		398
ind_IC4H9NO3		399
ind_NHOH		400

a01, a02, a03: Aqueous phase species in Aitken(AI), Accumulation(AS) and Coarse(CS) modes. respectively.

Continued.

ind_CH3CO3H		401
ind_HOCH2CH2O		402
ind_LTMB		403
ind_PINONIC		404
ind_DMSOH		405
ind_NH3_a01	a01	406
ind_MENp_a01	a01	407
ind_NH3_a02	a02	408
ind_MENp_a02	a02	409
ind_NH3_a03	a03	410
ind_MENp_a03	a03	411
ind_BZEMUCPAN		412
ind_C5CO2DBPAN		413
ind_C5CO2OHPAN		414
ind_DNPHENOOH		415
ind_NCATECOOH		416
ind_NNCATECOOH		417
ind_NPHENOOH		418
ind_ACCOMEPAN		419
ind_C6COOHCO3H		420
ind_TLEMUCCO		421
ind_C4CO2DBPAN		422
ind_C7PAN3		423
ind_C6CO2OHPAN		424
ind_C5COO2NO2		425
ind_DNCRESOOH		426
ind_MNCATECOOH		427
ind_MNNCATCOOH		428
ind_HCOCOHPAN		429
ind_TLEMUCPAN		430
ind_CHOC3COPAN		431
ind_DB1NO3		432
ind_STYRENOOH		433
ind_C810NO3		434
ind_C89NO3		435
ind_C1OOHC3O2C4OD		436
ind_C811PAN		437
ind_MACO2H		438
ind_C5COOHCO3H		439
ind_BPINAOOH		440
ind_C109OOH		441
ind_C513OOH		442
ind_C5PAN9		443
ind_C106NO3		444
ind_C10PAN2		445
ind_PINALNO3		446
ind_LAPINABOOH		447
ind_LNBPINABOOH		448
ind_CH3SO3H		449
ind_MMNNO2		450

ind_HNCO		451
ind_DMAO2		452
ind_C615CO2OOH		453
ind_HOOCH2CO3H		454
ind_DMS_a01	a01	455
ind_PERIBUACID		456
ind_IC3H7OOH		457
ind_FeHO2pp_a01	a01	458
ind_LZCPANC23DBCOD		459
ind_C2O4mm_a01	a01	460
ind_DMAp_a01	a01	461
ind_TMAp_a01	a01	462
ind_DEAp_a01	a01	463
ind_NC3H7OOH		464
ind_TEAp_a01	a01	465
ind_C2H5NO3		466
ind_EPXDLPAN		467
ind_DMS_a02	a02	468
ind_C614OOH		469
ind_C5DIALOOH		470
ind_FeHO2pp_a02	a02	471
ind_IBUTOLBOOH		472
ind_BENZENE		473
ind_C2O4mm_a02	a02	474
ind_DMAp_a02	a02	475
ind_TMAp_a02	a02	476
ind_DEAp_a02	a02	477
ind_C3DIALOOH		478
ind_TEAp_a02	a02	479
ind_NC4OHCPAN		480
ind_BZBIPEROOH		481
ind_DMS_a03	a03	482
ind_BZEMUCCO		483
ind_PERPROACID		484
ind_FeHO2pp_a03	a03	485
ind_C3PAN1		486
ind_IC4H9OOH		487
ind_C3PAN2		488
ind_C2O4mm_a03	a03	489
ind_DMAp_a03	a03	490
ind_BUT2OLNO3		491
ind_C312COPAN		492
ind_TMAp_a03	a03	493
ind_C4PAN5		494
ind_DEAp_a03	a03	495
ind_IBUTOLBNO3		496
ind_TEAp_a03	a03	497
ind_MALDIALPAN		498
ind_C2H5OOH		499
ind_C811O2		500

a01, a02, a03: Aqueous phase species in Aitken(AI), Accumulation(AS) and Coarse(CS) modes. respectively.

Continued.

ind_EBENZ		501
ind_NCATECHOL		502
ind_LXYL		503
ind_CH3COCO3H		504
ind_BPINANO3		505
ind_LISOPEFO		506
ind_LHAROM		507
ind_INO2		508
ind_N2O4		509
ind_MMAO2		510
ind_H2NCH2CHO		511
ind_DMCNH2CO3		512
ind_ClOHm_a01	a01	513
ind_FeSO4p_a01	a01	514
ind_MEANNO_a01	a01	515
ind_ROO6R3O2		516
ind_CRESOL		517
ind_ClOHm_a02	a02	518
ind_FeSO4p_a02	a02	519
ind_MEANNO_a02	a02	520
ind_BIACETOH		521
ind_ClOHm_a03	a03	522
ind_FeSO4p_a03	a03	523
ind_MEANNO_a03	a03	524
ind_IPRHOCO2H		525
ind_C2H2		526
ind_C721PAN		527
ind_ISOPBNO3		528
ind_C89PAN		529
ind_C9PAN2		530
ind_NDNPHENOOH		531
ind_PIPN		532
ind_HOCH2CO3H		533
ind_MEABO2		534
ind_TC4H9NO3		535
ind_DEAO2		536
ind_CH3CHCO		537
ind_DMCNH2CHO		538
ind_CHEXO2		539
ind_NBZFUOOH		540
ind_HOOCH2SO		541
ind_HOOCH2S		542
ind_HYPROPO2H		543
ind_NDNCRESOOH		544
ind_FeOHHO2p_a01	a01	545
ind_LNISOOH		546
ind_TC4H9OOH		547
ind_PBZN		548
ind_HCOCOOm_a01	a01	549
ind_CH3COCOOm_a01	a01	550

ind_TLEMUCNO3		551
ind_CRESOOH		552
ind_FeOHHO2p_a02	a02	553
ind_C5DICAROOH		554
ind_HCOCOOm_a02	a02	555
ind_CH3COCOOm_a02	a02	556
ind_LBUT1ENNO3		557
ind_LC4H9NO3		558
ind_FeOHHO2p_a03	a03	559
ind_IC4H9O2		560
ind_PROPOLNO3		561
ind_LBUT1ENOOH		562
ind_HCOCOOm_a03	a03	563
ind_PHENOOH		564
ind_CH3COCOOm_a03	a03	565
ind_C614NO3		566
ind_BZBIPERNO3		567
ind_CH3CO2H		568
ind_OHMENTHEN6ONEO2		569
ind_LISOPACO		570
ind_PBZQONE		571
ind_NBZFUONE		572
ind_LME3FURANO2		573
ind_HOOCH2CO2H		574
ind_DMSOHO		575
ind_CO2_a01	a01	576
ind_MSIA_a01	a01	577
ind_OXALAC_a01	a01	578
ind_HOCH2CHO_a01	a01	579
ind_C812O2		580
ind_SUCCAC_a01	a01	581
ind_MMAp_a01	a01	582
ind_MEAp_a01	a01	583
ind_TMNp_a01	a01	584
ind_CO2_a02	a02	585
ind_C44O2		586
ind_MSIA_a02	a02	587
ind_OXALAC_a02	a02	588
ind_HOCH2CHO_a02	a02	589
ind_SUCCAC_a02	a02	590
ind_MMAp_a02	a02	591
ind_MEAp_a02	a02	592
ind_TMNp_a02	a02	593
ind_MBOACO		594
ind_CO2_a03	a03	595
ind_MSIA_a03	a03	596
ind_OXALAC_a03	a03	597
ind_HOCH2CHO_a03	a03	598
ind_C97O2		599
ind_SUCCAC_a03	a03	600

a01, a02, a03: Aqueous phase species in Aitken(AI), Accumulation(AS) and Coarse(CS) modes. respectively.

Continued.

ind_MMAp_a03	a03	601
ind_MEAp_a03	a03	602
ind_TMNp_a03	a03	603
ind_NCRESOOH		604
ind_TMAO2		605
ind_C54CO		606
ind_HOCH2COCH2OOH		607
ind_CO2H3CO3H		608
ind_BUT2OLOOH		609
ind_FeOH2p_a01	a01	610
ind_C5CO14OOH		611
ind_MALANHY		612
ind_BIACETOOH		613
ind_PPN		614
ind_HYETHO2H		615
ind_DB2OOH		616
ind_FeOH2p_a02	a02	617
ind_C2H5O2NO2		618
ind_MALDALCO3H		619
ind_MALDIALOOH		620
ind_FeOH2p_a03	a03	621
ind_MC3ODBCO2H		622
ind_ETHOHNO3		623
ind_CH3O2NO2		624
ind_HOCH2O2NO2		625
ind_MPAN		626
ind_LC578OOH		627
ind_H2NCOCHO		628
ind_TEA		629
ind_C813O2		630
ind_CH3OH_a01	a01	631
ind_LC4H9OOH		632
ind_HSO4m_a01	a01	633
ind_FeSO3p_a01	a01	634
ind_TC4H9O2		635
ind_C6H5CH2O2		636
ind_CH3OH_a02	a02	637
ind_HSO4m_a02	a02	638
ind_FeSO3p_a02	a02	639
ind_NCCH2O2		640
ind_CO235C6O2		641
ind_ISOPDNO3		642
ind_C511O2		643
ind_CH3OH_a03	a03	644
ind_PTLQONE		645
ind_HSO4m_a03	a03	646
ind_Cl2		647
ind_FeSO3p_a03	a03	648
ind_BZEMUCOOH		649
ind_TLEMUCOOH		650

ind_C98O2		651
ind_CH3COCH2O2NO2		652
ind_BZEMUCNO3		653
ind_NH2O		654
ind_C512O2		655
ind_N2O3		656
ind_HOCl		657
ind_DMSO2OO		658
ind_HPMTF		659
ind_DEAN_a01	a01	660
ind_HC2O4m_a01	a01	661
ind_C6CO4DB		662
ind_HMAC		663
ind_MACRO		664
ind_HVMK		665
ind_ICl		666
ind_DEAN_a02	a02	667
ind_HC2O4m_a02	a02	668
ind_DEAN_a03	a03	669
ind_HC2O4m_a03	a03	670
ind_RO6R1O2		671
ind_CH2OOA		672
ind_MEK		673
ind_C1OOHC2OOHC4OD		674
ind_HOCHCHO		675
ind_PAN		676
ind_HI		677
ind_NC4MDCO2H		678
ind_LNMBOABOOH		679
ind_NC4DCO2H		680
ind_CH3NH		681
ind_PHAN		682
ind_LMBOABOOH		683
ind_AMP		684
ind_AMPN		685
ind_CH3SOO2		686
ind_CH3SO4		687
ind_DMSO_a01	a01	688
ind_HCOOm_a01	a01	689
ind_FeCl2p_a01	a01	690
ind_DB1OOH		691
ind_NISOPO2		692
ind_HCOCO2CH3CHO		693
ind_C614O2		694
ind_C106O2		695
ind_DMSO_a02	a02	696
ind_HCOOm_a02	a02	697
ind_FeCl2p_a02	a02	698
ind_HOCOC4DIAL		699
ind_LMEKOOH		700

a01, a02, a03: Aqueous phase species in Aitken(AI), Accumulation(AS) and Coarse(CS) modes. respectively.

Continued.

ind_C513O2		701
ind_C721CHO		702
ind_NOPINONE		703
ind_DMSO_a03	a03	704
ind_HCOOm_a03	a03	705
ind_C716O2		706
ind_FeCl2p_a03	a03	707
ind_C1ODC2O2C4OD		708
ind_TOL1O		709
ind_MACRNO3		710
ind_CH3ONO		711
ind_CHOC3COO2		712
ind_LC5PAN1719		713
ind_HCOCOCH2OOH		714
ind_I2_a01	a01	715
ind_CO235C6CHO		716
ind_NO3CH2CO3		717
ind_BZFUO2		718
ind_C85O2		719
ind_MEANNO2		720
ind_CH3COCHCO		721
ind_PRONO3BO2		722
ind_I2_a02	a02	723
ind_C7CO4DB		724
ind_C32OH13CO		725
ind_I2_a03	a03	726
ind_TLBIPEROOH		727
ind_PBZQO2		728
ind_C514O2		729
ind_NTLFUO2		730
ind_CH4		731
ind_NBZFUO2		732
ind_TLFUO2		733
ind_CH2CHOH		734
ind_MACO2		735
ind_MNCATECH		736
ind_HOC6H4NO2		737
ind_C4CODIAL		738
ind_NH2CH2CHOH_a01	a01	739
ind_NC3H7O2		740
ind_NH2CH2CHOH_a02	a02	741
ind_NCRES1O		742
ind_CATECHOL		743
ind_NH2CH2CHOH_a03	a03	744
ind_NPHEN1O		745
ind_LISOPACNO3O2		746
ind_TLBIPERNO3		747
ind_NO_a01	a01	748
ind_STYRENO2		749
ind_NPHENO2		750

ind_MGLYOAC_a01	a01	751
ind_C8BCO2		752
ind_NSTYRENO2		753
ind_NO_a02	a02	754
ind_C59O2		755
ind_DNPHENO2		756
ind_IBUTOLBO2		757
ind_C721O2		758
ind_NO_a03	a03	759
ind_CH2NCH3		760
ind_C810O2		761
ind_HOCH2COCHO		762
ind_DNCRESO2		763
ind_CH3CHOHOOH		764
ind_HCOCO3H		765
ind_HNO4_a01	a01	766
ind_IC3H7O2		767
ind_C1ODC3O2C4OOH		768
ind_LNAPINABO2		769
ind_CO14O3CHO		770
ind_LHMVKABOOH		771
ind_TENp_a01	a01	772
ind_HNO4_a02	a02	773
ind_CRESO2		774
ind_PTLQO2		775
ind_HO12CO3C4		776
ind_NCRESO2		777
ind_C6CO2OHCO3		778
ind_NPTLQO2		779
ind_C85CO3		780
ind_MCATECHOL		781
ind_MBO		782
ind_TENp_a02	a02	783
ind_HNO4_a03	a03	784
ind_LMEKNO3		785
ind_MEPROPENE		786
ind_TENp_a03	a03	787
ind_HCO3m_a02	a02	788
ind_CH3CN		789
ind_HCO3m_a03	a03	790
ind_BUT1ENE		791
ind_LNISO3		792
ind_C5CO14OH		793
ind_NBZQO2		794
ind_HNCO_a01	a01	795
ind_NDNPHENO2		796
ind_NDNCRESO2		797
ind_LAPINABO2		798
ind_TEAO2		799
ind_HOOCH2SCO		800

a01, a02, a03: Aqueous phase species in Aitken(AI), Accumulation(AS) and Coarse(CS) modes. respectively.

Continued.

ind_C5DICARBO2		801
ind_HOC2H4CO3		802
ind_MVKNO3		803
ind_DEA		804
ind_C1OOHC2O2C4OD		805
ind_MALDIALO2		806
ind_C5CO2DBCO3		807
ind_CH2CO		808
ind_FeClpp_a01	a01	809
ind_SABINENE		810
ind_HOCH2OOH		811
ind_HNO3_a01	a01	812
ind_DMNCH2_a01	a01	813
ind_MNCATECO2		814
ind_NCATECO2		815
ind_BENZAL		816
ind_MNNCATECO2		817
ind_DENp_a01	a01	818
ind_HNO3_a02	a02	819
ind_SO2_a02	a02	820
ind_FeClpp_a02	a02	821
ind_NNCATECO2		822
ind_CO235C5CHO		823
ind_DMNCH2_a02	a02	824
ind_MCATEC1O2		825
ind_OXYL1O2		826
ind_DENp_a02	a02	827
ind_MACROOH		828
ind_HNO3_a03	a03	829
ind_SO2_a03	a03	830
ind_HYPERACET		831
ind_DEANNO2		832
ind_FeClpp_a03	a03	833
ind_ME3FURAN		834
ind_SO2_a01	a01	835
ind_DMNCH2_a03	a03	836
ind_IPRCO3		837
ind_ACCOMECHO		838
ind_C312COCO3		839
ind_HCOCH2CHO		840
ind_DENp_a03	a03	841
ind_NH2		842
ind_HNO		843
ind_CH3NO3		844
ind_C4CO2DBCO3		845
ind_HCN		846
ind_CATEC1O2		847
ind_NC4OHCO3		848
ind_C5CO2OHCO3		849
ind_ALCOCH2OOH		850

ind_LC4H9O2		851
ind_PINALO2		852
ind_C33CO		853
ind_DENCH2CHOH_a01	a01	854
ind_BPINENE		855
ind_LNBPINABO2		856
ind_CO2C3CHO		857
ind_CO23C4CHO		858
ind_C109O2		859
ind_DENCH2CHOH_a02	a02	860
ind_LBUT1ENO2		861
ind_DENCH2CHOH_a03	a03	862
ind_TLEPOXMUC		863
ind_NOA		864
ind_CH3SOH		865
ind_BPINAO2		866
ind_CH3O2_a01	a01	867
ind_HCOOH_a02	a02	868
ind_CH3O2_a02	a02	869
ind_C5DIALO2		870
ind_LZCO3C23DBCOD		871
ind_CH3NHCH2_a01	a01	872
ind_CH3NHCH2_a02	a02	873
ind_STYRENE		874
ind_PHENOL		875
ind_BZBIPERO2		876
ind_MALDALCO2H		877
ind_C6H5O2		878
ind_C6H5CO3		879
ind_HCOOH_a03	a03	880
ind_CH3O2_a03	a03	881
ind_NDELA		882
ind_C721CO3		883
ind_DMA		884
ind_CH3NHCH2_a03	a03	885
ind_MMALANHYO2		886
ind_C615CO2O2		887
ind_CH3COCO3		888
ind_CATEC1O		889
ind_CO3m_a01	a01	890
ind_C5134CO2OH		891
ind_HOI		892
ind_CH3COCHO2CHO		893
ind_HCOCCH3CO		894
ind_IO2m_a02	a02	895
ind_NCRES1O2		896
ind_CO23C4CO3		897
ind_IO2m_a01	a01	898
ind_NPHEN1O2		899
ind_IO2m_a03	a03	900

a01, a02, a03: Aqueous phase species in Aitken(AI), Accumulation(AS) and Coarse(CS) modes. respectively.

Continued.

ind_C89O2		901
ind_LMBOABO2		902
ind_IBUTALOH		903
ind_IPRCHO		904
ind_LC578O2		905
ind_LNMBOABO2		906
ind_NOPINDO2		907
ind_MEAN		908
ind_BZEPOXMUC		909
ind_EPXC4DIAL		910
ind_TLBIPERO2		911
ind_APINENE		912
ind_ROO6R1O2		913
ind_CAMPHENE		914
ind_HYPROPO2		915
ind_CARENE		916
ind_CH2OHSO3m_a01	a01	917
ind_TLEMUCCO3		918
ind_BZEMUCCO3		919
ind_H2SO4		920
ind_CH3SOO		921
ind_PHENO2		922
ind_IBUTDIAL		923
ind_LISOPEFO2		924
ind_BZEMUCO2		925
ind_HOCH2COCH2O2		926
ind_C3DIALO2		927
ind_HCOCOHCO3		928
ind_TMA		929
ind_MECOACETO2		930
ind_TBUT2ENE		931
ind_HOCH2CO		932
ind_CBUT2ENE		933
ind_CH3OH		934
ind_CH3CHOHO2		935
ind_CH2OHSO3m_a02	a02	936
ind_CO235C6CO3		937
ind_LMEKO2		938
ind_CH2OHSO3m_a03	a03	939
ind_HCOC5		940
ind_BZFUONE		941
ind_DMNNO2		942
ind_C722O2		943
ind_EPXDLCO3		944
ind_HCOCO		945
ind_HNCO_a02	a02	946
ind_HCOCO2H_a02	a02	947
ind_C2H5CO3		948
ind_C96CO3		949
ind_MALANHYO2		950

ind_HCOCO2H_a03	a03	951
ind_ACCOMECO3		952
ind_HCOCO2H_a01	a01	953
ind_BIACETO2		954
ind_CO23C3CHO		955
ind_CH3S		956
ind_NH2CH2_a02	a02	957
ind_NH2CH2_a03	a03	958
ind_NH2CH2_a01	a01	959
ind_TLEMUCO2		960
ind_N2O5		961
ind_TOL1OHNO2		962
ind_DNCRES		963
ind_MGLYOAC_a02	a02	964
ind_MCATEC1O		965
ind_NDMA		966
ind_C6H5O		967
ind_DNPHEN		968
ind_EZCHOCCH3CHO2		969
ind_OIO		970
ind_C1ODC2OOHC4OD		971
ind_SO5m_a02	a02	972
ind_DMNp_a02	a02	973
ind_HSO5m_a01	a01	974
ind_MACO3		975
ind_SO5m_a03	a03	976
ind_DMNp_a01	a01	977
ind_TLFUONE		978
ind_MEA		979
ind_DMNp_a03	a03	980
ind_HOCH2O2		981
ind_C2H5O2		982
ind_BUT2OLO2		983
ind_NO3CH2CHO		984
ind_C811CO3		985
ind_INO3		986
ind_C3H7CHO		987
ind_C2H5CHO		988
ind_CH3COCH3		989
ind_CO2H3CO3		990
ind_MALDIALCO3		991
ind_CH3SO3		992
ind_O1D		993
ind_CHOC3COCO3		994
ind_C5H8		995
ind_SO5m_a01	a01	996
ind_HOOCH2CHO		997
ind_MMA		998
ind_HSO5m_a03	a03	999
ind_HSO5m_a02	a02	1000

a01, a02, a03: Aqueous phase species in Aitken(AI), Accumulation(AS) and Coarse(CS) modes. Respectively.

Continued.

ind_NORPINAL		1001
ind_ISOPBDNO3O2		1002
ind_C5CO14O2		1003
ind_DMSOO		1004
ind_CH3SO		1005
ind_NC4CHO		1006
ind_HOOCH2CO3		1007
ind_CO13C4CHO		1008
ind_HCOCH2CO3		1009
ind_MALDIAL		1010
ind_MMNNO2_a02	a02	1011
ind_HNCO_a03	a03	1012
ind_ISOPBOOH		1013
ind_MVK		1014
ind_HCOOH_a01	a01	1015
ind_DB2O2		1016
ind_EZCH3CO2CHCHO		1017
ind_ICl_a01	a01	1018
ind_IPRHOCO3		1019
ind_CH3CO3		1020
ind_LDISOPACO2		1021
ind_MGLYOAC_a03	a03	1022
ind_NOPINOO		1023
ind_APINAOO		1024
ind_CH2O2H2_a02	a02	1025
ind_CH2O2H2_a03	a03	1026
ind_LHC4ACCO3		1027
ind_MACRO2		1028
ind_C5DICARB		1029
ind_HCOCO3		1030
ind_NO3_a03	a03	1031
ind_NO3_a02	a02	1032
ind_NO3_a01	a01	1033
ind_MACR		1034
ind_APINBOO		1035
ind_CH3COCO2H		1036
ind_ClNO3		1037
ind_C2H4		1038
ind_CH2O2H2_a01	a01	1039
ind_C86O2		1040
ind_CH3OOH		1041
ind_CHOCOCH2O2		1042
ind_MEANNO2_a03	a03	1043
ind_ISOPDOOH		1044
ind_MBOOO		1045
ind_LISOPACO2		1046
ind_ACETOL		1047
ind_C3H6		1048
ind_Im_a02	a02	1049
ind_Im_a03	a03	1050

ind_ISOPDO2		1051
ind_C89CO3		1052
ind_C96O2		1053
ind_CH3COCH2O2		1054
ind_LISOPACNO3		1055
ind_DB1O2		1056
ind_HOETNETOH		1057
ind_H2NCHO		1058
ind_MMNNO2_a03	a03	1059
ind_LHC4ACCHO		1060
ind_H2O2		1061
ind_LHMVKABO2		1062
ind_CO2H3CHO		1063
ind_PINAL		1064
ind_HOCH2CO3		1065
ind_CH3SO2		1066
ind_FeOHpp_a01	a01	1067
ind_FeOHpp_a03	a03	1068
ind_FeOHpp_a02	a02	1069
ind_DMNCHO		1070
ind_HCOCH2O2		1071
ind_DB1O		1072
ind_CH3		1073
ind_CH3NCH3		1074
ind_Cl2_a01	a01	1075
ind_ISOPBO2		1076
ind_LISOPACOOH		1077
ind_LZCODC23DBCOOH		1078
ind_C4MDIAL		1079
ind_LZCO3HC23DBCOD		1080
ind_CH3CO		1081
ind_CH3CHO		1082
ind_HOCH2CH2O2		1083
ind_Cl2m_a03	a03	1084
ind_NO2m_a01	a01	1085
ind_NO2m_a02	a02	1086
ind_MEANNO2_a02	a02	1087
ind_FeOpp_a02	a02	1088
ind_FeOpp_a03	a03	1089
ind_FeOpp_a01	a01	1090
ind_H2NCOCH2OH		1091
ind_MMNNO2_a01	a01	1092
ind_DMSO		1093
ind_HONO		1094
ind_O3P		1095
ind_CH2OO		1096
ind_DEANNO2_a02	a02	1097
ind_HOCH2CO2H		1098
ind_TEA_a02	a02	1099
ind_MEANNO2_a01	a01	1100

a01, a02, a03: Aqueous phase species in Aitken(AI), Accumulation(AS) and Coarse(CS) modes. Respectively.

Continued.

ind_HOI_a03	a03	1101
ind_HCl		1102
ind_HCO3m_a01	a01	1103
ind_CO3m_a02	a02	1104
ind_Im_a01	a01	1105
ind_Cl_a02	a02	1106
ind_Feppp_a01	a01	1107
ind_SO4m_a03	a03	1108
ind_SO3m_a01	a01	1109
ind_DMNNO2_a03	a03	1110
ind_SO4m_a01	a01	1111
ind_Fepp_a01	a01	1112
ind_CO3m_a03	a03	1113
ind_MEANNO		1114
ind_HCHO_a01	a01	1115
ind_DEA_a03	a03	1116
ind_ClO		1117
ind_SO3mm_a02	a02	1118
ind_MGLYOX		1119
ind_NDMA_a03	a03	1120
ind_TMA_a03	a03	1121
ind_CH3OOH_a01	a01	1122
ind_SO3m_a03	a03	1123
ind_Feppp_a03	a03	1124
ind_Feppp_a02	a02	1125
ind_MEA_a01	a01	1126
ind_Cl_a01	a01	1127
ind_Fepp_a03	a03	1128
ind_Cl_a03	a03	1129
ind_SO3mm_a03	a03	1130
ind_DMS		1131
ind_DEANNO2_a03	a03	1132
ind_SO3m_a02	a02	1133
ind_Fepp_a02	a02	1134
ind_SO4m_a02	a02	1135
ind_CH3SOOH		1136
ind_NH3		1137
ind_HCOCO2H		1138
ind_HNO3		1139
ind_TEA_a01	a01	1140
ind_BLOV		1141
ind_BSOV		1142
ind_TMA_a02	a02	1143
ind_HOI_a02	a02	1144
ind_Cl2m_a02	a02	1145
ind_CH3O		1146
ind_TEA_a03	a03	1147
ind_NDELA_a03	a03	1148
ind_GLYOX		1149
ind_DMNNO2_a02	a02	1150

ind_CH3NHCHO		1151
ind_TMA_a01	a01	1152
ind_HNO4		1153
ind_MMA_a01	a01	1154
ind_HOCl_a01	a01	1155
ind_DEANNO2_a01	a01	1156
ind_MEA_a03	a03	1157
ind_MEA_a02	a02	1158
ind_HCHO_a03	a03	1159
ind_HOCH2CHO		1160
ind_OHm_a03	a03	1161
ind_SO4mm_a03	a03	1162
ind_DMNNO2_a01	a01	1163
ind_MMA_a02	a02	1164
ind_MMA_a03	a03	1165
ind_HCHO_a02	a02	1166
ind_DMA_a03	a03	1167
ind_OHm_a02	a02	1168
ind_SO4mm_a02	a02	1169
ind_SO4mm_a01	a01	1170
ind_NO3m_a03	a03	1171
ind_OHm_a01	a01	1172
ind_IO		1173
ind_N2O4_a02	a02	1174
ind_N2O4_a03	a03	1175
ind_N2O4_a01	a01	1176
ind_N2O3_a03	a03	1177
ind_NDELA_a01	a01	1178
ind_N2O3_a01	a01	1179
ind_DMA_a01	a01	1180
ind_DEA_a01	a01	1181
ind_NDMA_a01	a01	1182
ind_SO3mm_a01	a01	1183
ind_NO3m_a02	a02	1184
ind_HONO_a02	a02	1185
ind_H2O2_a02	a02	1186
ind_I2		1187
ind_I		1188
ind_H2O2_a01	a01	1189
ind_HSO3m_a03	a03	1190
ind_OH		1191
ind_Hp_a01	a01	1192
ind_NO		1193
ind_NO2		1194
ind_NO3		1195
ind_HOI_a01	a01	1196
ind_OH_a03	a03	1197
ind_HO2_a01	a01	1198
ind_HO2		1199
ind_O2_a01	a01	1200

a01, a02, a03: Aqueous phase species in Aitken(AI), Accumulation(AS) and Coarse(CS) modes. Respectively.

Continued.

ind_O2_a02	a02	1201
ind_Cl		1202
ind_HSO3m_a02	a02	1203
ind_NO2_a03	a03	1204
ind_O2_a03	a03	1205
ind_ICl_a03	a03	1206
ind_N2O3_a02	a02	1207
ind_Clm_a03	a03	1208
ind_CH3O2		1209
ind_O2m_a02	a02	1210
ind_O3_a02	a02	1211
ind_HO2_a02	a02	1212
ind_CO		1213
ind_HCHO		1214
ind_HCOOH		1215
ind_NO2_a02	a02	1216
ind_HOCl_a03	a03	1217
ind_CH3OOH_a03	a03	1218
ind_Hp_a02	a02	1219
ind_DMA_a02	a02	1220
ind_Cl2_a02	a02	1221
ind_O3_a01	a01	1222
ind_OH_a01	a01	1223
ind_HONO_a01	a01	1224
ind_CH3OOH_a02	a02	1225
ind_NDMA_a02	a02	1226
ind_HO2_a03	a03	1227
ind_Cl2m_a01	a01	1228
ind_NO3m_a01	a01	1229
ind_NDELA_a02	a02	1230
ind_ICl_a02	a02	1231
ind_DEA_a02	a02	1232
ind_H2O2_a03	a03	1233
ind_Cl2_a03	a03	1234
ind_OH_a02	a02	1235
ind_HSO3m_a01	a01	1236
ind_Hp_a03	a03	1237
ind_O3		1238
ind_Clm_a01	a01	1239
ind_O3_a03	a03	1240
ind_O2m_a01	a01	1241
ind_HOCl_a02	a02	1242
ind_H2O		1243
ind_Clm_a02	a02	1244
ind_HONO_a03	a03	1245
ind_O2m_a03	a03	1246
ind_NO2_a01	a01	1247
ind_SO2		1248
ind_NO2m_a03	a03	1249

a01, a02, a03: Aqueous phase species in Aitken(AI), Accumulation(AS) and Coarse(CS) modes. respectively.

8 Appendix B: The Chemical Mechanism of MAFOR v2.2.0

Download as separate PDF document: meccanism_mafor_v2.2.0.pdf.

The Chemical Mechanism of MAFOR v2.2

KPP version: `2.2.3_rs3`

MECCA version: `4.0`

Date: November 30, 2024

Batch file: `mafor.bat`

Integrator: `rosenbrock_posdef`

Gas equation file: `gas.eqn`

Replacement file: `maforchem`

Selected reactions:
"`Tr && (G || Aa) && !Br && !Hg`"

Number of aerosol phases: 3

Number of species in selected mechanism:

Gas phase:	782
Aqueous phase:	465
All species:	1247

Number of reactions in selected mechanism:

Gas phase (Gnnn):	1873
Aqueous phase (Annn):	714
Henry (Hnnn):	378
Photolysis (Jnnn):	356
Aqueous phase photolysis (PHnnn):	39
Heterogeneous (HETnnn):	0
Equilibria (EQnn):	300
Isotope exchange (IEXnnn):	0
Tagging equations (TAGnnn):	0
Dummy (Dnn):	3
All equations:	3663

9 Appendix C: List of Error Messages

Error Message	Type of Error	Required Action
Fortran runtime error: File {*filename*} does not exist	Input error	Make sure that the input file {filename} is included in the same directory as the MAFOR executable
(unit = {*unit*}, file = {*filename*}) Fortran runtime error: End of file	Input error	Make sure that all required values are entered in input file {filename}
Note: The following floating-point exceptions are signalling: IEEE_INVALID_FLAG IEEE_DENORMAL	Compiler warning	This message occurs after completion of the run and is a known issue with the gfortran compilation. Please ignore.
Note: The following floating-point exceptions are signalling: IEEE_INVALID_FLAG IEEE_DIVIDE_BY_ZERO IEEE_OVERFLOW_FLAG IEEE_UNDERFLOW_FLAG IEEE_DENORMAL	Compiler warning	This message occurs after completion of the run and is a known issue with the gfortran compilation. Please ignore.
File {filename} cannot be opened !	Input error	Make sure that the input file {filename} is included in the same directory as the MAFOR executable
STOP: RH<0.991 in ingeod.dat	Input, Warning	Input file ingeod.dat: check that RH is not smaller than 0.991 for Cloud 1 run
STOP: RH>1.1 in ingeod.dat	Input error	Input file ingeod.dat: RH cannot be greater than 1.10
STOP: initial SO3 too high (must be <= 5.0e11 cm^-3)	Input error	Input file inchem.dat: KPP_SO3 cannot be greater or equal 5.0E11
STOP: allowed range of hvap1 in organic.dat is 10-200 kJ/mol	Input error	Input file organic.dat: values for the enthalpy of vaporization of organic vapors has to be in the range of 10 to 200 kJ/mol
sum of OC molar fractions >1.0 in organic.dat	Input error	Input file organic.dat: mole fractions gamma-oc must not exceed 1.0 per mode
STOP: molar yield > 1.0 in incham.dat	Input error	Input file incham.dat: the sum of ya_soan1 and ya_soan2 must not exceed 1.0
STOP: amine number must be <6 in incham.dat	Input error	Input file incham.dat: select an amine with number 1, ..., 5

Continued.

Error Message	Type of Error	Required Action
STOP: chamber volume must be >0 m3 incham.dat	Input error	Input file incham.dat: the chamber volume must not be zero
STOP: negative input value in monitor.dat	Input error	Input file monitor.dat: Replace negative values by zero
STOP SIGMA too small in inaero.dat. Mode: x	Input error	Input file inaero.dat: increase value of SIGMA for mode x. Typically betwee 1.1 and 2.2
STOP SIGMA >2.2 not accepted in inaero.dat. Mode: x	Input error	Input file inaero.dat: value of SIGMA for mode x must not exceed 2.2
STOP GMD too small in inaero.dat. Mode: x	Input error	Input file inaero.dat: value of GMD for mode x has to be increased
Type 2: dil2_c has to be between 0 and -2	Input error	Input file dispers.dat: value of dil2_c for Type 2 plume dispersion has to lie between 0 and -2
Type 3: tau_d has to be greater than 0	Input error	Input file dispers.dat: value of tau_d for Type 3 plume dispersion has to be greater than 0
STOP: V_updraft must be < 0.5 m/s in dispers.dat	Input error	Input file dispers.dat: value of vupdra has to be less than 0.5
'before kpp:', c, t, cair 'after kpp:', c, t, cair	Chemistry warning or error	Problem in KPP for concentration c of a species at model time t. Make sure that inchem.dat contains reasonable concentration values. Immediately report problem
WARNING: negative N before Nucl.: m,I,N	Aerosol dynamics warning	Negative number concentration N in mode m, bin i. The model run continu Most often changing input in inaero.dat for nucleation mode solves this problem, otherwise ignore
EMERGENCY STOP: i=1 vpt(i) >= vpt(i+1)	Severe error	Most likely connected to the condensation of water. Immediately report problem
EMERGENCY STOP: i=imax vpt(i) >= vpt(i+1)	Severe error	Most likely connected to the condensation of water. Immediately report problem
EMERGENCY STOP: 1<i<imax vpt(i) >= vpt(i+1)	Severe error	Most likely connected to the condensation of water. Immediately report problem

Please report any error messages that are not included in this list.